Carla Mayara Costa Rodrigues

Licenciada

Development of a Mathematical model to predict sedimentation rates

Dissertação para obtenção do Grau de Mestre em
Engenharia Química e Bioquímica

Orientador: Leandro Rafael de Almeida Parada, Researcher em Química, GEO- Grounding Engineering Operations

Coorientadores: Telma Godinho Barroso, Doutora, GEO- Grounding Engineering Operations

Ana Isabel Nobre Martins Aguiar de Oliveira Ricardo, Professora catedrática, FCT/UNL

Júri:

Presidente: Rui Manuel Freitas Oliveira, Doutor, Professor Associado com Agregação, FCT/UNL

Arguente(s): Mário Fernando José Eusébio, Doutor, Professor Auxiliar, FCT/UNL

Vogal(ais): Leandro Rafael de Almeida Parada, Researcher em Química, GEO- Ground Engineering Operations

FACULDADE DE CIÊNCIAS E TECNOLOGIA
UNIVERSIDADE NOVA DE LISBOA

Novembro, 2020

Development of a mathematical model to predict sedimentation rates

“The greatest glory in living lies not in never falling, but in rising every time we fall.”

-Nelson Mandela

Agradecimentos

E assim termina uma das fases mais importantes e marcantes da minha vida. De uma forma ou de outra, os meses passados a realizar este projeto resumem bem os 5 anos de faculdade. Foi um caminho cheio de altos e baixos e com adicionais obstáculos para ultrapassar tendo em conta a fase que o mundo enfrenta atualmente. No entanto, em meio a tantas adversidades, contei sempre com o suporte de um grupo de pessoas sem as quais isto não seria possível.

Em primeiro lugar queria agradecer ao meu querido orientador Eng.Leandro Parada por todo o seu apoio, ajuda e motivação desde o primeiro dia. Nada disto teria sido possível sem a sua disponibilidade constante e as suas palavras de incentivo e encorajamento que me ajudaram a sempre seguir em frente e não perder o foco.

À Dra. Telma Barroso um especial agradecimento por toda a sua boa disposição e otimismo. A sua sabedoria, os seus valiosos conselhos e a sua vontade de fazer ciência tornaram este caminho extremamente enriquecedor.

Queria igualmente agradecer à Stéphanie Leal e ao Jorge Capitão-mor, que estiveram presentes nesta jornada e que sempre mostraram toda a prontidão e vontade de ajudar em especial com as suas opiniões e ideias.

À minha família, mãe, pai, padrasto e irmão, um simples obrigado não chega por tudo o que fizeram por mim e por todo o apoio e incentivo. Os valores e a educação que me passaram fizeram, de mim quem sou hoje e contribuem todos os dias para o meu sucesso.

À família que eu escolhi, os meus queridos amigos, os que a faculdade me deu e os que fui encontrando ao longo da vida, agradeço a todos pela amizade, o companheirismo e todos os momentos vividos ao longo deste caminho.

Por fim, mas não menos importante por isso, ao meu querido namorado, Pedro Furtado, um agradecimento especial. Agradeço o amor, o carinho, a força e a motivação incessante todos os dias ao longo deste caminho. A sua paciência, o seu bom humor e o seu companheirismo fizeram com que tudo isto fosse possível. Muito obrigada meu amor.

Obrigada nunca será suficiente para exprimir todo o meu agradecimento.

Abstract

In this project it was developed a mathematical model to predict sedimentation rates of suspended soil for a period of 24h. The final goal is the development of a mathematical model considering different polymers and concentrations (between 0 and 1 $g.L^{-1}$) in aqueous medium with a pH between 5 and 12,5, using different soil types (clay, sand and a mixture of clay and sand) at concentration ranging from 25 to 200 $g.L^{-1}$.

The first step consisted in performing a series of laboratorial experiments gradually combining the goal variables. In these experiments, values of initial and final density were measured, as well as Brookfield and Marsh viscosity, electrical conductivity and pH. After collecting these data, it was organised in a data base to be introduced in the R software.

With the R software a set of equations, combining the study variables, were built in function of initial and final density. Sedimentation rate was later calculated through the difference between initial and final density. The model obtained was validated once it achieved an average sedimentation rate error ≤15%. Once a set of equations (for initial and for final density) considering certain goal variables were validated, another variable was introduced into the model until it considers all the conditions set in the goal.

At the end, it was achieved a mathematical model composed of two equations, one in function of initial density and the other in function of final density. Through these equations it is possible to predict sedimentation rates for a 24h period, considering polymer concentration (between 0 and 1 $g.L^{-1}$), pH (between 5 and 12,5), clay concentration (between 25 and 200 $g.L^{-1}$), and polymers with different anionic percentages (between 0 and 100%) and molecular weight (between 5 and 40 MDa). To achieve this, the fixed variables were soil type (clay), volume of deionized water (4L), bucket diameter (280 mm) and mixing time (150 min).

The final model presented an average error for sedimentation rate of 18%, with a standard deviation of 15%.

Resumo

Neste projeto foi desenvolvido um modelo matemático capaz de prever taxas de sedimentação de solo em suspensão por um período de 24h. O objetivo final é o desenvolvimento de um modelo matemático considerando diferentes polímeros e concentrações de polímero (entre 0 e 1 $g.L^{-1}$) em meio aquoso com pH entre 5 e 12,5, utilizando diferentes tipos de solo (argila, areia e uma mistura de argila e areia) em concentrações de solo que variam de 25 a 200 $g.L^{-1}$.

A primeira etapa consistiu em realizar uma série de ensaios laboratoriais combinando gradativamente as variáveis de objetivo. Nestes ensaios foram medidos os valores de densidade inicial e final, bem como a viscosidade de Brookfield e de Marsh, condutividade elétrica e pH. Após a recolha desses dados, os mesmos foram organizados em um banco de dados para serem introduzidos no software R.

Com o software R um conjunto de equações, combinando as variáveis de estudo, foram estabelecidas em função da densidade inicial e final. A taxa de sedimentação foi posteriormente calculada pela diferença entre a densidade inicial e final. O modelo obtido foi validado uma vez atingido um erro de taxa de sedimentação média ≤15%. Uma vez validado um conjunto de equações (para densidade inicial e final) considerando determinadas variáveis objetivo, outra variável foi introduzida no modelo até que este considere todas as condições estabelecidas no objetivo.

No final, foi obtido um modelo matemático composto por duas equações, uma em função da densidade inicial e outra em função da densidade final. Por meio dessas equações é possível prever taxas de sedimentação para um período de 24h, considerando um modelo matemático composto por duas equações, uma em função da densidade inicial e outra em função da densidade final. Por meio dessas equações é possível prever taxas de sedimentação para um período de 24h, considerando a concentração de polímero (entre 0 e 1 $g.L^{-1}$), pH (entre 5 e 12,5), concentração de argila (entre 25 e 200 $g.L^{-1}$), e polímeros com diferentes percentagens aniónicas (entre 0 e 100%) e peso molecular (entre 5 e 40 MDa). Para isto, as variáveis fixas foram o tipo de solo (argila), volume de água desionizada (4L), diâmetro do balde (280 mm) e tempo de mistura (150 min).

O modelo final apresentou um erro médio para a taxa de sedimentação de 18%, com desvio padrão de 15%.

Contents

List of Equations

List of Figures

List of Tables

List of Appendix

Abbreviations

APS- anionic polysaccharide

ºC- degree Celsius

Df- Final density

Di- Initial density

FV- Flocculation value

GG- guar gum

HA- humic acid

HCl- hydroxide chloride

HEC- hydroxyethyl cellulose

HPAM- hydrolysed polyacrylamide

MW- molecular weight

η- viscosity of the suspension

ηc- viscosity of the fluid phase

Φ- solid volume fraction

Φm- maximum possible solid volume fraction

PAA- polyacrylic acid

PAM- polyacrylamide

PDADMAC- polydiallyldimethylammonium chloride

PEG- polyethylene glycol

PZNPC- point of zero net proton charge

Rpm- rotations per minute

SR- stability ratio

S(l/s)- spreading coefficient

γsl- solid liquid interface tension

γsv- solid vapor interface tension

γlv- liquid vapor interface tension

Symbology

Φ- Solid volume fraction

η- Viscosity

ξ- Volume ratio

γ- Particle size ratio

λ- Crowding factor

ρ- Density

g- Gravity acceleration constant

ϵ- Voidance

1. Goals

The aim of this project is to develop a mathematical model able to predict sedimentation rates for at least 24 hours, considering pH range between 5 and 12,5. It is expected to use sand with particle size up to 3mm, clay and a mix of both, as well as polymer or polymer and additive combination with concentration rates from 0.4 $g.l^{-1}$ to 1 $g.l^{-1}$.

2. Introduction

Achieving a mathematical model able to predict sedimentation rates arise to fulfil both a researching environment and a construction field necessity. Based on the characteristics of a polymer and the soil where the construction will take place, it might be possible to predict density values through time and therefore, sedimentation rates. With the generated knowledge it is possible to infer about a polymer efficiency regarding the field and operational conditions, while still in a researching phase, allowing an accurate polymer selection. On the other hand, when applying the model to the construction field, it comes with great advantage to know in advance the behaviour of the interaction between the polymer and the soil over time. With this knowledge it is possible to develop a prediction of the hydrostatic pressure towards the pile and therefore, conclude about the stability of the pile. Thus, it is required a preliminary research regarding chemical and physical principles of suspension and their interactions with polymeric stabilization fluids, as well as mathematical equations able to predict it.

2.1 Suspension mechanisms

Suspension can be defined as a heterogeneous mixture of two or more unlike substances that contains particles larger than 1 μm [1]. The Oxford Dictionary of Chemistry (2008) defines suspension as the state in which small, insoluble particles are evenly distributed within a fluid, and the particles are carried upwards when turbulence outstrips the force of gravity [2]. Other authors also refer that the particles are suspended throughout the solution in bulk and can be easily seen by naked eyes, since the solute does not dissolve in the solution [3]. However, some say that the word suspension is used when the particles are large enough to settle, leading do sedimentation, otherwise, the mixture is named a colloid [4]. Colloids can exist has a dispersion of one substance in another (smoke particles in air) or as single materials (cell membrane) [5]. In suspensions, the suspending fluid may be simple, like a Newtonian fluid, or more complex, such as a polymeric fluid. There are some factors that must be considered in the preparation and achievement of a suspension [6]. These include favourable wetting conditions, the absence of strongly bound aggregates, fluid motions in the mixing cell, that will submerge the particles, and shear to aid in disaggregation. The dispersion method can be implemented through the application of high shear forces, to break up aggregates of particles. To obtain a reasonably stable suspension, some stabilizing (peptizing) electrolyte or surfactant may have to be present as well.

Therefore, when mixed with particles that could have different shapes, sizes, size distributions and properties, the resulting suspensions could be quite complex due to the interactions between the fluid and the particles and the interactions between the particles themselves [7]. These forces can be defined as: hydrodynamic interactions, non-hydrodynamic interactions.

Hydrodynamic interactions result from the relative motion of the suspending medium with respect to the particles, being responsible for the migration of particles and structure breakdown [8]. On

the other hand, non-hydrodynamic interactions consist of the Brownian forces, responsible for the motion and diffusion of the particles, and forces arising from physical and chemical interactions, driven by forces such as the van der Waals and electrostatic forces. These low-range attractive forces promote flock building. However, the forces could also be repulsive enough, causing the particles to distribute in the suspension. Generally, in order to achieve a good dispersion of particles in liquids, two methods can be applied: Addition of a dispersing agent and the use of physical dispersing methods. Dispersing agents can produce a strong repulsive force and/or reduce the van der Waals attractive force between the interacting particles, allowing them to stay dispersed in the suspension medium. Physical means is usually required to make particles separated and suspended in liquids. This can be achieved through ultrasonic treatment, violent mechanic agitation, high frequency vibration and ejecting. Despite of the wide application of physical dispersing methods in practice, the principal shortcoming of physical methods is the reversibility of the process. Figure 1 represents a combination of these two suspensions inducing mechanisms [9][10].

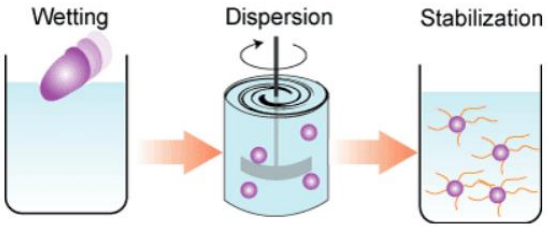

Figure 2.1- Mechanism in the dispersion process [10]

However, particles dispersed in a suspension will have the tendency to settle over time. The main driving forces for this phenomenon are gravity and centrifugal acceleration. According to a study from Goro Imai (1981) [11], for a dilute clay-water mixture, the sedimentation process comprises 3 stages. The first stage of particle settling takes places with flocculation, which is, basically the agglomeration of small particles into bigger ones. This can be enhanced by electrostatic interaction between particles and, also between the suspended particles and the surfactant or polymeric stabilizing agent. In the second stage flocs gradually settle and form a layer of sediment, which undergoes consolidation and reduction of water content. In the third stage all the sediment thus formed undergoes self-weight consolidation and finally approaches an equilibrium stage. When particles with higher density than the medium are obtained, settling occurs, leading to sedimentation. For larger particles (from 2 to 10mm), such as sand, the first stage of the process does not occur the same way. Gravity effect will lead to immediate particle deposition. The speed at which this occurs will depend mostly on the fluid rheological properties (viscosity), as well as on the particle size and density [12][13].

Being our goal in this project to have particles totally suspended in the medium, the manipulation of the mechanism in order to promote and keep the particles in suspension, possess a significant impact on the process efficiency.

2.2 Dispersion Vs Flocculation

Depending on the process or product required, to promote suspension or sedimentation, it may be desirable to resort to one of this two phenomena. According to IUPAC, dispersion consists in a “material comprising more than one phase where at least one of the phases consists of finely divided phase domains, dispersed throughout a continuous phase”[14], and flocculation can be defined as “something which leads to aggregates that are loose or open. Usually is derived from a mixing stage which increases the particle size from sub-microscopic microfloc to visible suspended particles. Microfloc particles collide, causing them to bond to produce larger, visible flocs called pinflocs [15][16]. To help floc size building, inorganic polymers or inorganic salts (coagulants) are usually added. By being oppositely charged, when compared with the suspended solids, it helps to build, bridge and strengthening the floc, adding weight and increasing settling rate. Once the floc has reached its optimum size and strength, sedimentation occurs [15][17][18].

Therefore, in order to promote dispersion, as suspension is the goal of our project, we must consider that factors such as pH [19] , electric charges [20], viscosity, density[21][22] [23], mixing speed and time [24] play a huge roll. Dispersion agents (both chemical and physical) alter fluid and material characteristics such as aggregation, conductivity, shape and size, as well as the balance between repulsive and attractive forces acting simultaneously among the suspended particles [25] and contributing to keep the particles in suspension.

In 1967, a study was published by A. P. Edwards et al [26] where dispersion of soil particles is achieved by subjecting an aqueous suspension of soil sample (10 g soil, 25 ml water) to sonic vibration at 13 to 15^{o}C using a Raytheon (9 Kc, 50 W) vibrator. Studies using soils of widely different textures and organic matter contents showed that the dispersion caused by sonic vibration for 30 min, was similar to that obtained by chemical methods currently used for dispersion of soils, and could keep a stable suspension up until 9 days, as it is possible to observe from the data in Table 2.1. This mechanism permits dispersion of soil particles without dissolution of more than trace amounts of organic or inorganic material and does not significantly affect the pH or conductivity of the soil suspension.

Table 2.1- Stability of suspensions obtained by sonic vibration of soil [26]: [2] vibrated suspension was diluted before standing, [3] vibrated suspension was not diluted before standing

Soil Nº	Time between vibration and analysis of suspension	Particle-size analysis of vibrated suspension		
		Sand	Silt	Clay
	days	%	%	%
7	0	25,0	45,1	29,9
	2^2	25,2	45,0	29,8
	2^3	25,1	45,3	29,6
	9^2	25,3	45,0	29,7
	9^3	25,2	45,0	29,8
9	0	50,4	27,7	21,9
	2^2	50,5	27,5	22,0
	2^3	50,3	27,9	21,8
	9^2	50,7	27,6	21,7
	9^3	50,6	27,6	21,8

In 1979, H. Arora at al. [27] performed an experiment that showed that with the increase of salt concentration in the solution it tends do coagulate, on the other hand, in the presence of low salt concentration, the diffuse double- layer repulsion prevents particle association and a stable suspension is obtained.

In Colloids Surfaces A: Physicochem. Eng. Aspects 125 (1997) 95-107 [28], concentrated dispersion properties where analysed with different pH and ionic strength conditions, as well as viscosity and stability where also evaluated under different solution conditions. As it is demonstrated in Figure 2.2, for several alumina concentrated dispersions, viscosity was maximal at pH values around PZNPC (point of zero net proton charge) (pH 8,8) and decreased away from this point. This is the result of increasing particle aggregation near PZNPC where surface charge is low and repulsive forces are minimum, resulting in decreasing interparticle space.

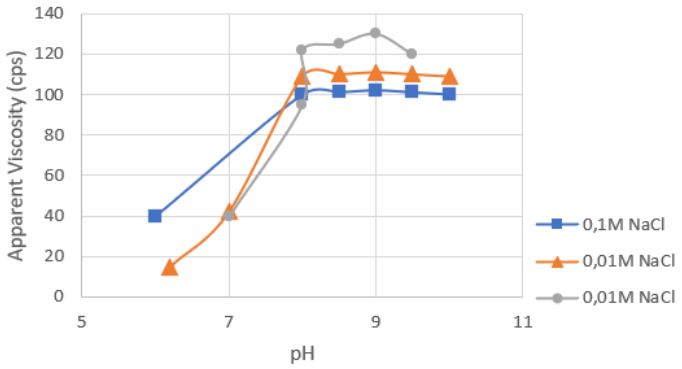

Figure 2.2- Effect of pH and ionic strength on viscosity of 15 wt% alumina suspensions. (adapted from [24])

In 1998, S. Shimabayashi et al [29]. studied the dispersion of particles in liquid environments, analysing the elementary processes behind this phenomenon. The authors define wetting of particles by liquid as well as particles dispersing and homogenization in liquid, as the two basic principles for particle dispersion. As a first step to produce a stable solid particle dispersion in liquid, particles must be wetted initially by the liquid. Spreading coefficient $S_{L/S}$ can be used to evaluate whether or not the liquid will wet a solid surface and spread over the surface. This coefficient can be defined by the following Equation 2.1:

$$S_{L/S}=Y_{S/V}\text{-}(Y_{S/L}+Y_{L/V})=Y_{L/V}(\text{Cos}\sigma\text{-}1)$$

Equation 2.1- Spreading coefficient.

Where γ_{sl}, γ_{lv}, γ_{sv} are solid-liquid, liquid-vapor, and solid-vapor interface tensions, respectively; θ is the contact angle of solid surface with liquid, if existing. A positive value of $S_{L/S}$ indicates that the liquid will spread over the solid surface, completely wet the solid surface. Once the particles are immersed in liquid, they are subjected to actions of various forces, e.g. hydrodynamic force, particle-liquid interaction forces, inter- particle interaction forces, and other physical field forces. The dispersion-aggregation states of particles in suspension totally depend on the mutual correlation of these interactions, among them the inter-particle interaction forces are the most important factors controlling particle dispersion. Therefore, the second necessary condition of particle dispersion is the surface force principle. The total surface forces between particles must sufficiently repulsive, so that the particles cannot come into direct contact and cannot be involved into aggregation.

In 2005, Shainberg et al. [25] studied the interaction between soil solution and soil clay to understand the phenomena of clay dispersion and flocculation. It was possible to corroborate that the dispersion and flocculation of clays depends on the mineralogy of the clay and are affected by the composition of exchangeable ions, salt concentration, pH level, presence of peptizing agents and also the application of a stirring mechanism. For instance, sodium montmorillonite had a FV (flocculation value) of 12 mmolc.l^{-1} NaCl, while calcium montmorillonite had a FV of 0,25 mmolc.l^{-1} $CaCl_2$. However, the sodium montmorillonite FV value was pH dependent. It was possible to verify that sodium montmorillonite FV was pH dependent, having a value of 12,6 mmolc.l^{-1} at pH's 7; 10 and 13, but a value of 44 mmolc.l^{-1} at pH's 5; 7,5; 8,5 and 9,8. The salt concentration influence was measured based on the sodium adsorption ratio (SAR). It was determined that a SAR of 20 (molc.m^{-3})$^{1/2}$ allowed an FV of 6 mmolc.l^{-1}, while a SAR of 60 (molc.m-3)1/2 allowed an FV of 11,5 mmolc.l^{-1}. The peptizing agents influence also proved to be significant. Without any agent, the FV for NaCl was 12 mmolc.l^{-1}. After adding 0,01 mmolc.l^{-1} of peptizing agent, this value raised to 20 mmolc.l^{-1}.

To promote coagulation, some Industries use combinations of oppositely charged polyelectrolytes [30]. Experiment with natural wastewater from gravel pits showed that the addition of polycation (PDADMAC) followed by the polyanion (poly(acrylamide-co-sodium acrylate) proved to be an

effective method, since a combination of patching and bridging is obtained [31]. With a clay concentration of 10 $g.l^{-1}$, the initial turbidity was at 80%, after letting the suspension settle for 30 minutes. The addition of PDADMAC (0,16 mg of polycation per 1 g of clay), made cause the residual turbidity to decrease to 5%. However, the restabilisation (increasing of turbidity) occurs very rapidly. In order to spread the “flocculation window”, high molecular weight polyanion was added to the mixture, reducing turbidity to 1%. The charge effect was considered a factor of outstanding importance on this phenomenon. Therefore, the optimal charge ratio for the best turbidity removal and settling time was found to be [-]/[+]=0,2. This means that a small amount of polyanions (1 anionic charge per 5 cationic charges) is required to promote the bridging between particles and, consequently flocculation.

Stirring speed has also proved to be an important factor. It promotes a uniform dispersion of the reagent, the destabilization of the colloid micelles and the formation of small aggregates. The growth of the aggregates towards larger and heavier flocs, which are then removed by precipitation, is achieved by slow agitation that enhances the movement of the aggregates and their attenuation in small distances [32]. In 2005, Katerine Borja et al [33]. studied mechanical methods to promote dispersion in soil particles. Four methodologies using chemical dispersions: ($(NaPO_3)6$ + Na_2CO_3), (NaOH) 1M, ($Na_4P_2O_7$) 0.1M pH 10, and CH3COONa 1M, and two methodologies of mechanical dispersion were evaluated: a slow one at 60 rpm for 6 hours and another at 4000 rpm for 15 minutes. The results were analysed using a correlation test and contrasts. It was verified that the highest content of clay in the soil samples was found when using the 60rpm agitation methodology, due to greater dispersion of the granulometric fractions. Likewise, when comparing the different methods of chemical dispersion, it was determined that NaOH had the highest dispersing ability and sodium acetate presented a low efficiency in the separation of soil particles.

2.3 Variables that affect suspension

Suspension is a phenomenon that is highly depended on a series of variables. The study of this variables has been a concern for different authors for several years. There’s studies approaching pH values of flooded soils, in terms of redox-potential, to show its effect on soil suspension [34], others analysing the effect of viscosity [35] and several studies on the field of particle granulometry[36], electric conductivity[37][38] and rheology[39]. These, among other variables such as magnetic and mineralogic properties [40][41] , have been analysed over the years in order to understand what influences particle suspension, a phenomenon of great interest in different fields of study.

2.3.1 Fluid Rheology

The understanding of fluid rheology has proven to be out of extremely importance for the study of particle suspension under different conditions [42][43]. Rheology is defined as the study of flow behaviour and it is normally applied to fluids or materials that exhibit a time-dependent response to stress [44][45].

Different types of flow behaviour can occur. The simplest is Newtonian behaviour, with a linear relationship between stress and strain rate. Also, many fluids show plastic behaviour, in which flow only initiates above some level of stress (called the yield stress), and once flow initiates the relationship between stress and strain rate is linear. Another common behaviour is pseudoplastic (or shear thinning), in which viscosity decreases as strain rate increases [45][46].

According to the "Handbook of analytical techniques in concrete science technology" [44], there are two key factors that affect the suspension of solid particles rheological behaviour. These are the volume fraction of solid particles in the suspension, and the extent to which the particles are agglomerated or flocculated. Increasing the solids volume fraction (Φ) causes a significant increase in the viscosity of the suspension (η). The effect of solids volume fraction on viscosity can be fully described with the following Equation 2.2, proposed by Krieger and Dougherty, which is extensively used in suspensions:

$$\eta = \eta c * [1 - \frac{\Phi}{\Phi m}]^{-(\eta)*\Phi m}$$

Equation 2.2- Relationship between volume fraction (Φ) and viscosity (η) [37]

Being ηc the viscosity of the fluid phase and Φm the maximum possible volume fraction for the assemblage of particles, which has a maximum value of 65% for randomly close-packed spheres. $-(\eta) * \Phi m$ is the limit of the function when Φm tends to 0.

Regarding to the extent to which particles are flocculated or dispersed, flocculated particles either form discrete aggregates or a gel. The forces are often weak and easily broken by shear, so enough stress can be applied to cause disruption of the flocculated network such that the suspension begins to flow. The stress at which such a breakdown occurs is called the yield stress. Thus, flocculation produces plastic behaviour with the yield stress reflecting the forces holding particles together[44].

In 1971, investigators from the University of Utah, Salt Lake City, USA, [47], studied the dependence of the viscosities of highly concentrated suspensions on solids concentrations and particle size distributions, in order to understand the rheology of concentrated suspensions. They conclude that relative viscosities of the monodispersed systems investigated where independent of the particle size and temperature, being a function only of solids concentrations. Above 50 vol% solids, the viscosity of monodispersed systems increases much more rapidly with increase in solids concentrations than at the less concentrated range, as we can observe in Figure 2.3.

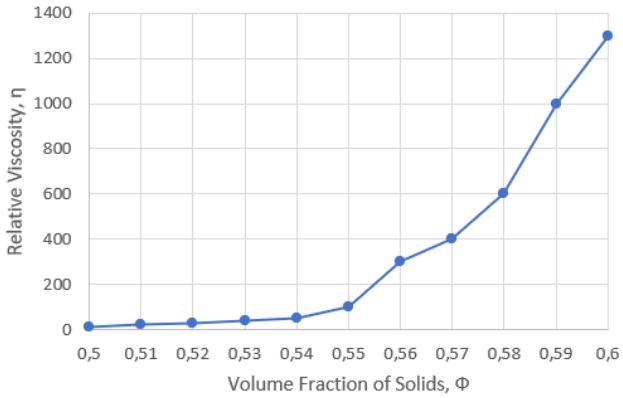

Figure 2.3- Viscosity of monodispersed systems and comparison of equations (adapted from [43])

The lower the viscosity by diluting a suspension, the higher the transportability, but a fewer number of particles can be processed. On the other hand, increasing the particle concentration would increase particle-particle interactions and viscosity thus, transportability would reduce which could result in less process yield [48].

The effect of pH on rheological properties has also been a field of study, with different authors dedicating time to investigate this correlation [49][50][51]. M. Benna et al. [50] studied the effect of pH on the rheological behaviour of three purified sodium bentonite suspensions. It was possible to realize that depending on pH value, the shear stress value will change. The study demonstrated that at high basic and high acidic pH values, the static yield stress is greater than steady shear stress. However, for pH closer to the natural values (between 8 and 10), values of yield stress are a prolongation of shear stress values.

Other properties such as chemical composition, particle density, and size and shape of suspended particles also play an important role in fluids rheological behaviour[52][48][53].

For example, experiments performed by P. Del Gaudio et al. [54] show that crystal size has a strong effect on values of Newtonian viscosity and the inset of non-Newtonian behaviour of suspensions. A shear thinning behaviour ($n<1$) is observed in suspensions with crystals size <125 μm at Φ (volume fraction) larger than about 0,1. Suspensions with crystals size >125 μm exhibit shear thinning at $\Phi > 0,2$. The deviation from Newtonian behaviour is more pronounced with finer crystal sizes. These experiments are in accordance with sand-water suspensions.

2.3.2 Fluid Viscosity

Fluid viscosity is one of the most important variables to consider when studying what influences suspension.

In 1951, M. Mooney [55], investigator for the General Laboratories of the United States Rubber Company, studied the viscosity of a concentrated suspension of spherical particles, presenting the Crowding Theory of Viscosity. According to this theory, the interaction between the spheres in a suspension is primarily the simple geometric crowding action, referring to the first order interactions between particles in a suspension, which is the basis of the theory. The mutual disturbance of flow lines around two near particles is therefore a matter of secondary importance. Substantiating this theory, it was developed an equation for the relative viscosity of a monodisperse suspension of spheres [Equation 2.3]:

$$\ln\frac{\eta}{\eta 0} = \frac{2.5\emptyset}{1 - \lambda 1\emptyset'}$$

Equation 2.3- Viscosity in function of volume fraction

Here, Φ corresponds to the first solid volume fraction, Φ' is the second solid volume fraction, η is the suspension's viscosity and η0 refers to viscosity of the fluid. λ corresponds to the crowding factor. It is an adjustable parameter, whose value may change according to the data available. In this paper, the author resorted to other researcher's data do validate the equation developed. H. Eillers [56] published a series of viscosity measurements on Concentrated emulsions of a bituminous material of high softening point. With this data it was obtained a value for λ of 0,75.

In 2001, researchers from School of Aeronautical and Mechanical Engineering, University of Salford, [57], went a step further by developing a semi-analytical method for the viscosity of bidisperse suspensions. According to this model, at high solid volume fraction, Φ>0,40, both γ (particle size ratio) and ξ (volume ratio of large particles to total particles) significantly influences viscosity, causing it to increase, as it is possible to notice from Otherwise, the suspension is composed of clusters of particles and demonstrates predominantly liquid like behaviour.

Table 2.2. Otherwise, the suspension is composed of clusters of particles and demonstrates predominantly liquid like behaviour.

Table 2.2- Mean diameters of Aerosil 200 aggregations determined by DLS

Suspension	Mean diameter (nm)
0,01M	
pH 2	422 ± 2
pH 4	626 ± 29
pH 9	390 ± 3
pH 12	385 ± 3
0,001M	
pH 4	380 ± 13
Water	
pH 4	249 ± 7

On the other side, to understand how particles sediment in viscous fluids, A. V. Bazilevsky et al.[58] (2009) proceeded to do experiments measuring the settling velocity of single particles in several viscous and viscoelastic fluids on a wide range of variation of the Couette flow shear rate. The results for the polymeric non-Newtonian fluids GG and PAA demonstrate the increase of the sedimentation velocity with increase in the shear rate, similar to the case of single particles (c = 0). Thus, the results show that in a non-Newtonian fluid the sedimentation velocity first increases with the concentration and then decreases. This behaviour differs from the behaviour of Newtonian suspensions, in which the sedimentation velocity always decreases with increase in the particle concentration [59].

In 2010, N. M. Kovalchuk et al. [60], considered that colloidal interactions between particles composing a suspension have a considerable influence on the suspension viscosity behaviour. If interactions between particles are strong enough, the solid volume fraction is large and external forces provoking the breakage of bonds between particles are absent or small enough, then gel like structures possessing viscoelastic properties are formed. The higher the shear rate, the higher the solid fraction leading to gelation [61][62].

2.3.3 pH

The effect of pH changing in different suspension, has been an important factor to many researchers [63][64][65].

Experiments by F. Rey et al. [22] in soil fulvic acid showed that viscosity is minimum at pH=6 and decreases when the ionic strength increases. This last can be explained with the coiling of fulvic

acid molecules due to repulsions by the counterions or neutralization by the added salt. On the other hand, pH effect can be explained with the fact that at the lowest pH values, the particles remain uncharged and electrostatic repulsions are weak. Also, the particles present a higher association due to the possible formation of hydrogen bonds, van der Waals forces, and other weak forces. [66]

A study developed by Shukun Chen et al.[67] (2007) determined the effect of pH and salt on rheological properties of aerosil suspensions. In this study, it was possible to notice that zeta potential is useful to evaluate the electrical double layer repulsive forces between particles in suspension. This property is deeply influenced by ionic strength and pH that, consequently, affect particle interactions and the rheological properties of suspensions. Experiments proved that the isoelectric point is found around pH 4 (Figure 2.4).

At this pH, the particle charge density and the magnitude of the zeta potential are low. The consequence is that suspensions become unstable and flocculation is expected to occur.

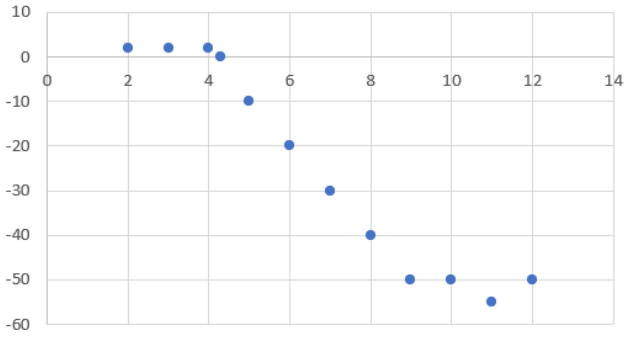

Figure 2.4- Zeta potential profiles for Aerosil 200 suspensions in water (Adapted from [63])

With pH increase, the association of the particles is destroyed due to the increase in electrostatic repulsions that are greater than the weak forces and the aggregates break up because any sort of rearrangement disperses the fully ionized molecules to form small particles.[68]

When studying the clay dispersion from sodic soils, M. Chorom et al. [19] obtained a positive relationship between pH and the percentage of dispersible clay, noticing that the pH affected clay dispersion by changing the net charge on clay particles. It was possible to conclude that as the pH decreases bellow 6, the soils develop positive charge so that the net negative charge decreases. When the pH increases above 6, negative charge increases.

Depending on clay mineralogy and oxide contents, soils may exhibit a net negative or positive charge at high or low pH respectively. The results on soil clays demonstrated that clay dispersion and flocculation is dependent on net particle charge and pH. The net negative charge on clay systems is influenced by pH. In general, it was found that soil clays have higher flocculation values than the values reported for pure clay minerals at comparable pH values. For example, pure

kaolinite had a maximum flocculation value of 5 mmol.l^{-1}, while kaolinitic soil clay had a maximum value of 120 mmol.l^{-1}, at pH 7.

For instance, some studies concluded that adsorption of simple organic molecules onto clay particles increases their negative charge which is also influenced by pH.[69]

The sedimentation behaviour of particles in suspension can also be induced by pH change [70] [71]. I. E. Melton et al. [70] studied sediment volumes of suspensions of aqueous kaolinite as a function of pH and NaCl concentration. The study demonstrated that the highest value of pH at which the sediment volume could be observed in these suspensions, in the absence of added electrolyte, was 7,3. Above this value the suspensions deflocculated. However, after the addition of NaCl, sedimentation occurred at high pH.

Tseng and Wu [72] observed in their experiments that suspensions with high solid concentration, and pH=11, flocculate, leading to a high rate of sedimentation (Φ- 0,15 leads to suspension height of 10 cm, while for Φ-0,05 leads to a sedimentation heigh of 6 cm). On the other hand, at pH 2 the suspension presented a better dispersion stability (Φ- 0,15 leads to suspension height of 5 cm, while for Φ-0,05 leads to a sedimentation heigh of 2 cm). Rheology of the pH 2 suspensions shows in parallel a shear-thinning flow followed then by a shear-thickening flow character at high shear rates. Contrarily, the particles in pH 11 tend to aggregate at the beginning of the sedimentation. The gravitation force eventually prevails over the particle interaction, accelerating the settling of the aggregate clusters at the initial stage of the settling.

As we will discuss in the next chapter, pH possesses a significant influence in the electric charges present in a suspension [73][74], as some species ionize well at certain pH, which possesses a direct result in the suspension ability of a mixture.

2.3.4 Electric Charge

Since early times, the effect of charges has been an important factor to consider relatively to suspension, in particular in the soil science field.[34][75][20]

In 1954, R. K. Schofield et al [30] studied flocculation and dispersion in a kaolinite suspension due to attraction/repulsion of oppositely charged crystal faces. The chloride adsorption exhibited by kaolinite provides the clue to the nature of the inter-particle forces. Before addition of NaOH, pure Na-kaolinite exhibits strong flocculation in salt-free suspension. The flocculation is evidently due to electrostatic attraction between positive edges and negative cleavage-faces of adjacent kaolinite crystals. On the other hand, when NaOH is added, hydrons are lost from the edge-faces by proton transfer, the number of positive charges decreases, and consequently, the positive adsorption is reduced. Chloride adsorption becomes zero when there is an exact balance between attraction and repulsion, and eventually changes over to negative. It is near this point that dispersion occurs.

In 2016, P. Rengasamy et al. [76], in order to correlate exchangeable cations with clay dispersion, defined net dispersive charge as the difference between the dispersive charge, calculated from

the concentration of exchangeable cations measured at a given soil pH, and their dispersive powers. The net dispersive charge of a soil determines the clay dispersion, which occurs when the net dispersive charge is positive. 96 different soil samples collected and prepared by adding 20g of soil into 100ml of distilled water. The degree of swelling and dispersion of clay is determined by the reaction of polar water molecules with the charge on soil particles which is mostly negative. Therefore, clay dispersion is influenced by cations and can be defined has followed in Equation 2.4:

$$Dispersion\ Charge = [Ca] + 1.7[Mg] + 35[K] + 45[Na]$$

Equation 2.4- Dispersion Charge [72]

The dominant clay minerals in these samples are illite and kaolinite, and the samples have small organic carbon contents. The soil is alkaline; pH ranges from 7.25 to 9.83, and the average is 8.99. The correlation coefficient between % dispersed clay and dispersive charge is strong and positive, which supports the concept that the dispersive charge derived from exchangeable cations, weighted by their dispersive powers, is responsible for the amount of clay dispersed.

2.3.5 Additives: Types and Nature

It is common the use of additives in order to promote suspension in different industries, such as wastewater treatment and engineering [77][78][79].

One of these additives is soil humic acid. This is an organic polyanion that, within a certain concentration range, is able to act as a dispersing agent. An article from S.A.Visser et al.[80] (1988) evaluated the dispersive capacity of this substance, comparing it with other dispersive agents used in the industry. The soil sample used, had a pH of 6,7 and was mostly composed of sand (>50 µm) (37,3%), clay (2 µm) (37,4%) and fine silt (2-20 µm) (20,9%). Results presented in Figure 2.5 showed that the dispersive effect was particularly evident at humic acid concentrations of around 40 mg.l^{-1}, at higher concentrations the action was less effective.

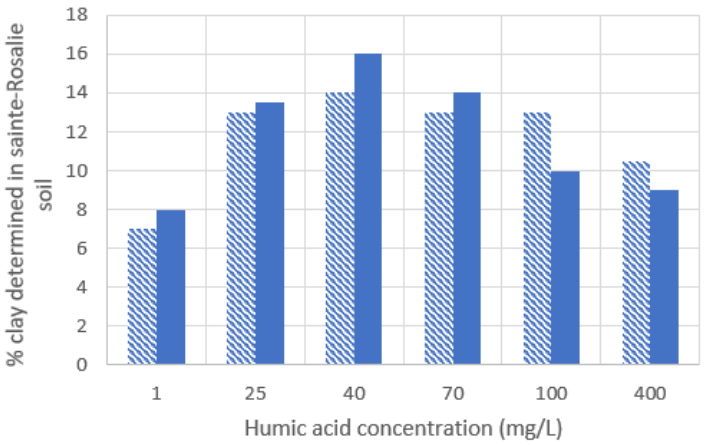

Figure 2.5- Distribution of clay soil samples obtained by using humic acid at different concentrations as dispersant. (Adapted from [76])

At 40 $mg.l^{-1}$ this additive was 20 and 30% less effective than the commonly used hexametaphosphate at 0,4%. further in this project, we will discuss the application of this additive as a dispersive agent.

Polysaccharide also act as effective dispersive agents, especially in soil particles since the adsorption of complexing organic acids increase the negative charge on clays [80]. In 2002 J. Tarchitzky et al.[81] studied the effect of polysaccharides on sodium montmorillonite characteristics such as flocculation/dispersion and rheological properties. Flocculation values (FV) increased with increasing concentrations of the anionic polysaccharide polygalacturonic acid (PGA). The pattern was similar at pH 4 and 8, a relatively sharp increase in FV with small additions of PGA up to a concentration of 10 $mg.l^{-1}$. For pH 4, the FV obtained was 136 $mmol.l^{-1}$ and at pH 8 that value increased for 160 $mmol.l^{-1}$. However, by increasing pH to 10, at the same polysaccharide concentration, the FV value dropped significantly to 24,2 $mmol.l^{-1}$. Therefore, this additive may be used as an effective deflocculant at higher pH values.

Sodium hexametaphosphate has also proven to be effective in soil dispersion and is widely used for agricultural soils. A.M. Wintermyer et al. (1955) [82] analysed this salt as a dispersive agent. It was tested, among other dispersive agents, with a broad selection of soil. Results showed that sodium hexametaphosphate (0,4 N) was highly and about equally effective for all of the experimental soils. For clay soils in particular, this polymer allowed a dispersion percentage of 63% in bentonite (clay mineral montmorillonite) and 35% in kaolinite. This result was obtained using 140ml of sodium hexametaphosphate from a solution of 0,4N.

Lime and gypsum are other additives commonly used in soil deposits dispersion. In 2010, researchers from the University of Khartoum [83] studied the effects of lime and gypsum additives on the dispersive behaviour of two river Nile deposits. The natural materials presented in the river deposit are a Nile silt (ML), found in the flood plain of the river, and low plastic sandy clay (CL) found in the upper terraces of the Nile. As it is possible to notice from Table 2.3 addition of small quantities (2 and 4 %) of hydrated lime to the soil samples significantly affected the gradation and the clay content of the tested materials by reducing their fines content whereas their clay dropped to traces. The addition of lime rendered the two materials to be non-plastic. The addition of gypsum (by 2 and 4 %) did not affect the gradation or the clay content of CL material, which implies that the soil sample did not experience aggregation formation upon gypsum addition. As for the ML sample, the addition of gypsum significantly reduced the clay fraction. The addition of gypsum considerably reduced the plasticity of CL material, but the reduction in the plasticity indices of the ML samples was less significant.

Table 2.3- Summary of fines content of tested soil samples [79]

Material source	Soil property	Natural material samples	Treated material samples			
			Lime added		Gypsum added	
			2%	4%	2%	4%
Area 1, Silty clay (CL)	FC %	57	63	48	55	60
	CC %	11	7	1	10	11
	LL %	44	39	42	34	36
	PI %	18	NP	NP	7	7
Area 2, Silty soil (ML)	FC %	73	62	62	72	70
	CC %	14	7	6	0	0
	LL %	37	36	37	33	36
	PI %	11	NP	NP	7	7

Being NP- non processed, FC- fine contents, CC- cay contents, LL- liquid limits, PI- plasticity index, the pinhole dispersion tests performed showed that, for the CL and ML soil materials, the addition of lime and gypsum resulted in significant improvements in their dispersive behaviour such that the treated samples became non-dispersive (Table 2.4). The chemical and double hydrometer results indicated an improvement in the dispersion behaviour in the two samples upon gypsum treatment.

Table 2.4- Summary of soil dispersion evaluation based on various test results [79] D = Dispersive, ID = Intermediate dispersion, NA = Not appropriate

Material type	Dispersion test method	Natural material samples	Treated material samples			
			Lime added		Gypsum added	
			2%	4%	2%	4%
CL Soil sample	Double hydrometer	D	NA	NA	ID	ID
	Pinhole	D1	ND1	ND1	ND2	ND1
	Chemical analysis	D	D	D	D	ND1
ML Soil sample	Double hydrometer	ID	NA	NA	NA	NA
	Pinhole	D2	ND1	ND1	ND1	ND1
	Chemical analysis	D	D	D	ID	ND

2.4 Suspension Methods

2.4.1 Construction Engineering

In Civil Engineering, when building a structure, a foundation is imperative in order to keep its stability since it can be used to transfer superstructure loads to stronger soil layers deep underground [84]. There are different foundations types depending on the soil characteristics and the building structure. However, during the foundation development process there is the issue of losing slurry through coarse, unconsolidated formations. If the level of the slurry drops below the required level to maintain adequate hydrostatic head pressure, the shaft can collapse [85].

Therefore, the industry resources to drilling fluids (suspensions of solids in an aqueous or invert-emulsion suspending medium) to maintain pile stability (borehole in case of petroleum holes). To achieve this a barrier must be placed between the drilling fluid or slurry and the formation and a positive pressure must be applied evenly against the filter cake or polymer gel membrane. This is accomplished by hydrostatic head pressure when the hole is kept full of slurry [85].

A paper from Robert D. Carico [86], presented a study evaluating the suspension ability of some polymer fluids, relating this ability to a low shear rate viscosity measurement of the flow. According to the test performed, PS-7, an experimental biopolymer, presented the best suspension ability. For sand in the 10-20 mesh range (0,84 to 2mm), a viscosity of approximately 500 cP, had the best results, with a shear rate of 8 sec^{-1}. The total sedimentation for this polymer, was achieved passed 12 minutes.

In 2007, Ahmadi Tehrani [87] studied the behaviour of suspensions and emulsions in drilling fluids. The rheology of drilling fluids affects many aspects of their performance and is critical to the safe and successful execution of a well. Drilling hydraulics, hole cleaning and barite sag are areas where rheology plays a dominant role. Drilling fluids rheology depends on the concentration of the various phases and on the interactions of different components. Low-shear rheology and presence of a structure play an important role in solids suspension. The more common types of organoclays (modified bentonite and hectorite) showed evidence of two Newtonian regimes, at very low and at high shear rates.

For fluid OB2 the first Newtonian regime occurred at shear rates below $0.0005s^{-1}$, while the second regime emerged above $100s^{-1}$. In the intermediate region the fluid exhibited evidence of several structural changes. For most of these fluids the quasi-Newtonian region occurred in the $0.01 – 1s^{-1}$ shear-rate range. The structural changes are likely to be due to a strong interaction between the organoclay particles and emulsion droplets. Fluid OA2, with needle-shaped organoattapulgite, and P5/1, with polymeric additive, show much weaker structural changes.

Shu-qing Hao (2011) [88] developed a study to optimize drilling fluids to improve borehole stability in natural gas hydrate (NGH) frozen ground. The experiment tested 4 different additives and each at 3 different concentrations. The main drill fluid ingredients investigated to influence borehole stability under low temperature conditions were HEC (hydroxyethyl cellulose), PEG (polyethylene

glycol), NaCl (sodium chloride), and KCl (potassium chloride). Low temperature rheology behaviour and API filtration tests show that the optimum fluid formula is:

$$HEC(0.5\%) + PEG(5\%) + NaCl(20\%) + KCl(5\%)$$

The following drill fluid factors need to be considered in respect to borehold stability: temperature gradient, relative density and filtration and caking.

The polymer HEC has the biggest influence in PV (plastic viscosity), η_m (marsh funnel viscosity), YP (yield point). To meet the drilling requirements of low YP and higher PV, the optimum HEC concentration is between 2-5 $g.l^{-1}$. KCl, the main additive, has a strong borehole instability inhibit effect, 50 $g.l^{-1}$ was the optimum concentration. The function of NaCl is to improve low temperature behaviour, influencing the fluid density and improving stability. 300 $g.l^{-1}$ is the best concentration found. The polymer PEG has the function to maintain low-temperature resistance and inhibit flocculation. The best results were obtained at a polymer concentration of 50 $ml.l^{-1}$.

2.4.2 Domestic effluents treatment

Rapid urbanisation and population growth have contributed for an accelerated pollution in the water environment. Being a limited but crucial resource, it has become important the development of methods and technologies for the treatment of these wastewaters [89][90].

It exists a multitude of processes for treatment of wastewater such as physicochemical and biological treatments [91][92]. Each treatment method has its advantages and disadvantages. Coagulation-flocculation is one of the most popular unit operations in water treatment, is a frequently applied process in the primary stage of wastewater treatment. It is based on the addition of chemical products which destabilize and flocculate dispersed solid particles and form separable clusters of flocks [93]. Therefore, the understanding of this process may provide information about how to promote dispersion in suspended particles.

In 2001, L. Semerjian et al.[94] proceeded to do a review of high pH–magnesium coagulation–flocculation processes in wastewater treatment. Magnesium ions proved to be efficient in terms of turbidity, TSS (total suspended solids) (91%), colour, COD (72%), nutrients and metal removal.

A study from 2014, by Omar Assobhei et el.[95] evaluated the coagulation-flocculation capacity of Moroccan clays in domestic wastewaters. The clay that presented the best results was perlite. At a dosage of 25 $mg.l^{-1}$ it allowed a reduction of COD in 66,8% and in TSS of 97,4%.

This is a field of constant interest, therefore many researchers invested time and resources investigating optimization techniques to improve the knowledge and methods already existent [96][97].

2.4.3 Wastewater treatment in Natural Dimension Stone cutting

Natural Dimension Stone (NDS) cutting and polishing is an industry that generates large amounts of wastewater rich in suspended stone material. Cutting a marble block, for instance, generates

a part of 30-40% in weight of the block as fine powder [98]. Thus, it is of extremely importance, to study and understand methods available to treat these wastewaters.

Coagulation-flocculation is widely used to remove the colloidal matter and nutrients present in wastewater [99]. In 2009, Bahri Ersoy et al.[100] studied coagulation/flocculation methods for turbidity removal from wastewaters of natural stones processing. It was possible to verify that flocculation and coagulation plus flocculation provided superior purification rates. The lowest residual turbidity values were obtained with 1.3 mg/L polymer dosage (optimum dosage) and 20 $mg.l^{-1}$ $FeCl_3N_6H_2O$ + 1,3 $mg.l^{-1}$ polymer dosages, which gave a residual turbidity of 12 and 5 NTU, respectively. Also, the suspension pH directly affected the coagulation conditions of NSPW (natural stone processing wastewater). The coagulating powers of all the coagulants tested increased with decreasing pH. As a result, the lowest residual turgidities were obtained at pH 6. Therefore, we may infer that with increasing pH dispersion will be induced in the suspension.

Being pH an important factor for turbidity removal and settling rate improvement in NSS, in 2005 Bahri Ersoy [98] proceeded to a deeper study on this subject. Marble, travertine and pure calcite samples were analysed. Marble and travertine isoelectric point was not found, this means that electrostatic forces play an important role in polymer-marble and polymer-travertine interactions. In marble suspensions, anionic polymer gave the best flocculation results for both turbidity and settling rate. For travertine 28% anionic charge polymer (with a concentration of 357 g/ton) gave the best settling rate while a polymer with 34% anionic charge (at a concentration of 47 g/ton) gave the best turbidity reduction. High pH suspension provides the best settling rate and increases the supernatant turbidity. Therefore, pH 11 was the optimum value for all suspensions to flocculate.

On the other hand, a more recent study, by Zeki Karaca et al.[101] stablished the connection between mineral content and flocculant characteristics, such as charge and concentration, for slurry wastewater recycling at marble processing plants. In recent studies, anionic flocculants have been found to be suitable for the treatment of waste from carbonate stone plants, such as marble plants, and cationic flocculants have been found to be suitable for the treatment of wastewater from granite plants [102]. In this study it was able to realize that DM (dolomite marble) grains are more sensitive to anionic flocculants than CM (calcite marble) grains; turbidity increases with changes in the natural pH and also, CM grains are more sensitive to pH changes in basic media, while DM grains are more sensitive to pH changes in acidic media. Another factor to consider is mixing speed.

Other authors developed similar studies for these topics, reaching similar conclusions[103][104][105].

2.4.4 Agriculture Soils

Agricultural soils require a series of conditions to optimize its potential at the same time that preserves the environment.

In 2012, Bruno T. Ribeiro et al.[106] studied Aggregate breakdown and dispersion of soil samples amended with sugarcane vinasse by using ultrasonic energy. Vinasse is an important by-product of sugarcane industries, intensively applied to soils in Brazil as liquid fertilizer. Samples of two Oxisols and one Ultisol were used in this study. After incubation, aggregates were submitted to levels of ultrasonic energy, and the particle size distribution (53 to 2,000 µm, 2 to 53 µm, and < 2 µm fractions) was quantified. Soils showed an aggregate-hierarchy resulting in a stepwise breakdown under ultrasonic agitation. In Figure 2.6 represented SDCC (soil-dispersion characteristic curve) (A), represented by clay size fraction (< 2 µm), the ADCC (aggregate - disruption characteristic curve) (B), represented by sand size fraction (53 to 2,000 µm), and the RADC (realising of aggregate and dispersion curve) (C), represented by silt size fraction (2 to 53 µm) for samples of the three soils.

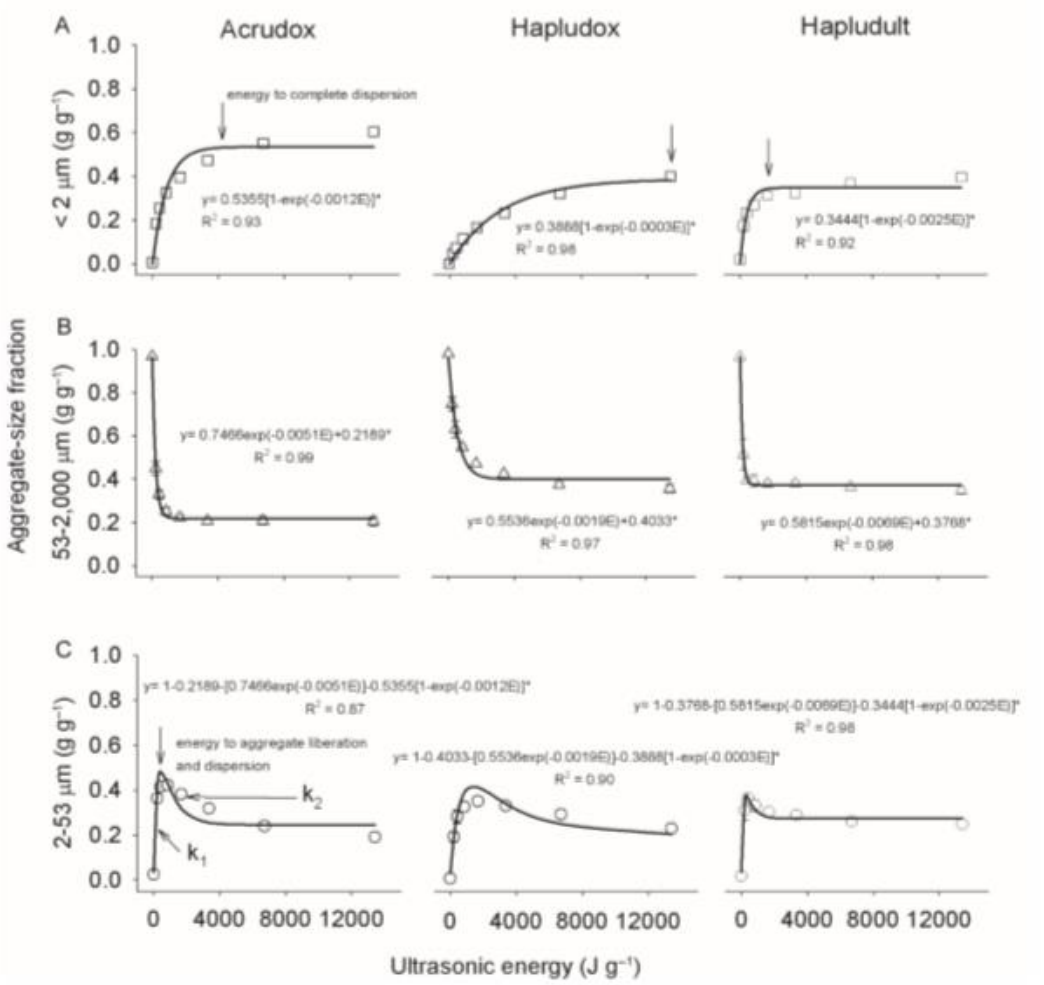

Figure 2.6- Soil dispersion characteristic curve – SDCC (A), aggregate disruption characteristic curve – ADCC (B) and releasing of aggregate and dispersion curve – RADC (C) of 1-2 mm aggregates from the Acrudox, Hapludox and Hapludult. [101]

As the < 2 µm fraction increased (Figure 1A), the 53 to 2,000 µm fraction decreased (Figure 1B), reaching respectively the clay and sand contents of the soils. Based on SDCC, the Hapludult

needed less ultrasonic energy to complete dispersion. These differences are closely related to the factors that affect the soil aggregation, such as soil texture, organic matter and oxide content.

Ellen R. Graber et al. (2014) developed a research on soil stabilization in semiarid and arid land agriculture. In this paper, it was considered the potential of four types of soil amendments, namely gypsum, organic polymers, organic matter waste materials, and fly ash, as soil stabilizers.

Synthetic organic polymer addition to soil surface aggregates leads to their stabilization, improved bonding between adjacent aggregates, and clay flocculation (it is considered that high molecular weight polymer $2*10^7$Da- with a concentration of 10 - 40 $kg.ha^{-1}$ have a better effect). Organic matter, also used for promoting aggregate stabilization, enhances soil microbial activity that transforms the newly added organic matter into polysaccharides and long chain aliphatic compounds capable of binding and stabilizing aggregates. Fly ash additives can improve soil physical characteristics including texture, structure, water holding capacity, hydraulic properties, and aeration. It was seen that the addition of 250 $Mg.ha^{-1}$ to the upper layer of a sandy soil increased by 6% the content of water retained by the soil at soft tensions (from −0.05 to −1.0 bar). However, fly ash has a number of inherent qualities that under certain circumstances may limit its usefulness for soil stabilization, and which may even result in increased erosion and soil loss.

2.4.5 Triggers that affect flocculation/dispersion systems

By analysing the methods and technologies used to promote flocculation or dispersion in different systems and fields of study, we can gather a set of triggers that affect these phenomena. For instance, several examples showed that low pH values increase flocculation while high pH values induce dispersion [100]. It was also able to verify that the addition of an anionic polymer in a negatively charged marble/travertine suspension induces flocculation, since strong marble/travertine-polymer electrostatic interactions are present, on other side, the addition of cationic polymer induces flocculation in granite plants (positively charged)[98]. However, other polymers, such as PEG inhibits flocculation, allowing particles to stay dispersed in the suspension. Mixing speed also plays an important role [107]. While alone, rapid mixing speed induced dispersion in a suspension, if combined with a polymer that enhances flocs strength, it induces a better flocculation and improves settling rates. On the other hand, slower mixing speeds induces particle breakdown and dispersion.

2.5 Suspension applied to Drilling fluids

According to “Oilfield Glossary”[108], a drilling fluid is an integral part of rotary drilling and it serves to carry cuttings from the bit and are added to the wellbore to facilitate the drilling process by suspending cuttings. Hole conditions may dictate other necessary functions for the fluid such as controlling pressure, stabilizing exposed rock, providing buoyancy, cooling and lubricating [109]. It has proven to be a useful mechanism for several industries, from petroleum industry to civil engineering [110][111]. Thus, its study and the understanding of the presupposed mechanisms help developing and improving the technologies and products used.

2.5.1 Soil suspension mechanisms

Suspension is defined as a heterogeneous mixture of particles dissolved in a fluid. This phenomenon depends on series of interactions between the particles and the fluid. Therefore, we take in consideration the soil characteristics, the fluid properties and the mechanisms involve in the interaction between them, which can either be that can be physical or chemical.

2.5.1.1. Physical mechanisms

There are some physical mechanisms crucial in the understanding of soil suspension, such as viscosity, pH and particle size. These can help us learn how to work with different types of soils and fluids in order to promote suspension has we want it.

Viscosity is one of these properties as it directly influences the capacity of a particle to stay suspended or to sediment. Therefore, factors such as clay and salt concentration, type of exchangeable ions and suspension pH were found to significantly impact the viscosity of clay suspensions. In 2012 Louxiang Wang, et al. [112] studied the viscosity of mixed clay suspensions. In this research three types of clay, kaolinite, illite, and montmorillonite, were used. The addition of montmorillonite in a kaolinite clay suspension caused an increase in the suspension viscosity. This can be explained by the interference between particles, which becomes dominant at higher concentrations [113].

A similar effect was observed for illite clay suspensions. The addition of a small amount of montmorillonite (1–2 wt%) to an illite suspension of 45 wt% total solids significantly increased the slurry viscosity (from 20 mPa.s to approximately 30 mPa.s). These findings suggest that for a given water chemistry, the viscosity of clay suspensions is very sensitive to the amount and type of clays present in the suspension [114].

When studying viscosity and the main physical mechanisms associated to soils suspension, it is imperative to study fluid rheology and understand its assumptions and trigger. For this reason, many authors studied how to manipulate rheological properties[39][43]. pH has proven to have a great influence in fluid rheology. It alters the yield stress (the yield stress increases with a pH increase), it alters the ionic strength and, therefore, altering the clay-fluid attraction structure. Particle size also plays an important role in solid-liquid mixtures. Experiments where made that showed that, at constant volume fraction (Φ), finer suspensions display higher viscosities than coarser ones. Shear thinning (flow index $n < 1$) occurs at $\Phi > 0,1–0,2$ and is more pronounced in finer suspensions [54].

In 1995, T. Y. Chu et al. [115] performed experiments to determine the effect of a deflocculating agent on the specific gravity of the soil dispersed and, on the viscosity, and specific gravity of the suspending medium. After using as deflocculant 100 ml of 0.5N Sodium Metaphosphate B solution per litre of soil suspension, it was able to observe that the effect of this solution on the specific gravity of the soils tested is insignificant. However, considering a soil suspension containing silt-size and clay-size particles, it is possible to compare the viscosity of these solutions, compared with other liquid solutions.

Table 2.5- Comparison of viscosities of distilled water, distilled water with deflocculating agents and soil suspensions. [110]

Liquid		Viscosity ate 68 F. (centipoise)
A	Distilled water	1.004
B	(20 mL 3 deg Baume sodium silicate solution mixed with 961 mL distilled water)	1.018
C	(40 mL 0.5N sodium metaphosphate B solution mixed with 941 mL distilled water)	1.025
D	(100 mL 0.5mL sodium methaphosphate B solution mixed with 881 mL distilled water)	1.038
Soil suspension prepared from fraction finer than 0.001 mm in Sample 1 with the following suspending medium:		
Liquid A		1.026
Liquid B		1.031
Liquid C		1.056
Liquid D		1.097
Soil suspension prepared from fraction finer than 0.001 mm in Sample 6 with the following suspending medium:		
Liquid A		1.116
Liquid B		1.195
Liquid C		1.251
Liquid D		1.274

In 2009, an article published by J.L. Amoro´s et al.[116] presented the relationship between the viscosity of concentrated clay suspensions with solids volume fraction, shear stress, and deflocculant content, developing a functional relationship between these parameters based on Krieger equation (Equation 2.2). It was considered a high deflocculant content of Xs=0.53 and a low content of Xs=0.25 (being xs deflocculant/cay mass ratio). As it was experimentally demonstrated (**Erro! A origem da referência não foi encontrada.**), the shear rate at which curve viscosity minimises decreases as solids content rises and is practically independent of

deflocculant content. The minimum viscosity of each suspension has been related satisfactorily to suspension solids volume fraction by the Krieger equation (Equation 2.2), considering intrinsic viscosity to be independent of deflocculant content.

Another way to promote soil dispersion is through agitating the mixture [33][106]. Vibration is a method of dispersing soil particles yields stable suspensions and is effective in different types of soils. It permits the dispersion of soil particles without dissolution of more than trace amounts of organic or inorganic material and does not significantly affect the pH or conductivity of the soil suspension. Studies using a widely variety of soils showed that the dispersion caused by sonic vibration for 30 min, was similar to that obtained by chemical methods currently used for dispersion of soils [26].

2.5.1.2. Chemical mechanisms

When it comes to the chemical mechanisms associated to soil suspension, it is important to understand the relationship between pH and the electric charges in the mixture and, consequently, how these properties directly affect particle suspension.

There are mainly four types of soils, each with its characteristics [117][118]:

Sandy soils- Sandy soil is usually formed by the fragmentation of rocks like granite, limestone, and quartz. Its poor in nutrients and has a low water holding capacity. Sand particle size ranges from 0,05mm to 2,0mm. Sand has no charge, therefore it has no ability of changing ions even in suspension, being dispersion usually a function of concentration [119]. For instance, in water bodies, suspension occurs as a result of the moving water entraining loosely consolidated sediments, such as sand, and carrying them up into the water column. When the movement stops, the sediments eventually settle under the influence of gravity [120].

Slit soils- Composed with smaller particles compared to the sandy soil (from 0.002mm to 0.05mm) and is made up of rock and other mineral particles which are smaller than sand and larger than clay. It has a better water holding capacity than and is mainly found near rivers, lakes, and other water bodies.

Clay soil- it is the smallest particles amongst the other two types of soil, with diameters smaller than 0,002mm. The particles in this soil have a negative charge and are tightly packed together with each other with very little or no airspace. This soil has very good water storage qualities and making hard for moisture and air to penetrate it [121].

Loamy soil- It is a combination of sand, silt, and clay. It has the ability to retain moist and also has higher calcium and pH levels because of its inorganic origins.

Based on this, we can infer that, depending on the soil characteristic, the chemical interactions happening that induce suspension will be different.

On that note, we can come across a constant charge soil, or a pH dependent soil (variable charge). Permanent charge usually occurs with minerals such as montmorillonite and

vermiculite[75]. The constant surface charge for these minerals results from the substitution of ions with differing valence within the crystal units or from crystal imperfections, both of which almost universally creates negatively charged surfaces [122][123]. On the other hand, pH-dependence occurs on components such as organic matter, oxides, hydroxides, oxyhydroxides. Variable charge can result from either ion adsorption, or the dissociation of surface ionizable groups [124].

In 1976, M. D. Bolland et al.[125] measured the surface charge of kaolinite in aqueous suspension, in a pH range of 3-10. The positive charge was found to increase with decreasing pH (Figure 2.7). It occurred on the kaolinites at pH values as high as 9 and 10 and was particularly evident at high ionic strengths.

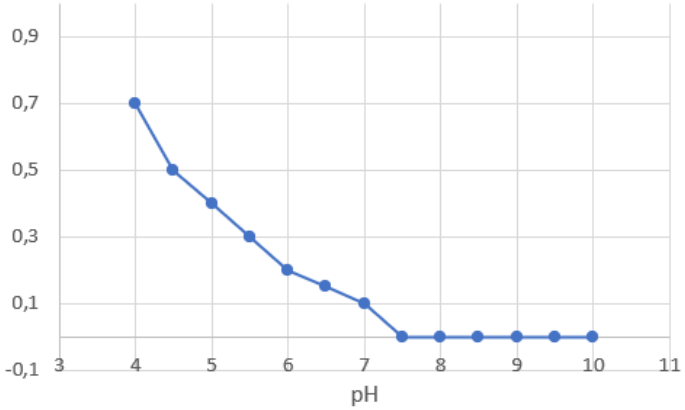

Figure 2.7- Positive surface charge (m-equiv/100g) on API-9 kolinite as a function of the equilibrium pH. (adapted from [119])

In 2006, Etelka Tombácz [126] compared surface charge heterogeneity of kaolinite in aqueous suspension with montmorillonite. The initial pH of suspensions and the net proton surface excess vs. pH functions shifted to the lower pH with increasing ionic strength indicating the presence of permanent charges in both cases, but these shifts were smaller for kaolinite, since it has a lower layer charge density. The pH-dependent charge formation was similar, positive charges formed only at pH below 6–6,5, considered as point of zero net proton charge (PZNPC) of kaolinite particles. So, oppositely charged surface parts on both clay particles are only below this pH. Large aggregates were able to form only below pH 7 in kaolinite suspensions. Similarly, to montmorillonite, heterocoagulation at pH 4 occurs only above a threshold electrolyte concentration, which was much smaller, only 1 mmol.l^{-1} NaCl for kaolinite, than that for montmorillonite due to the substantial difference in particle geometry. There was practically no difference in the critical coagulation concentration of kaolinite and montmorillonite (concentration 100 mmol.l^{-1} NaCl). Rheological measurements showed shear thinning flow character at and above pH 6,7 proving the existence of repulsive interaction between uniformly charged particles in 0,01 M NaCl for both clays.

In the same year, a study from Katsuhiko Itami and Hideaki Fujitani [20], correlated the electric charges with the dispersion/flocculation behaviour of different soils suspensions (montmorillonite, sericite, kaolinite, halloysite and allophane). The mixtures where obtained by mixing 0,2g of soil in 20 mL NaCl (5 $mmol.l^{-1}$). The charge characteristics of the clays were determined by the modified ion adsorption method using caesium as an index cation, in a pH range from 3 to 10. The experiments determined that montmorillonite is a clay mineral with large and constant charge. This means that it has structural charges, originated from isometric substitutions and do not vary with pH. Negative Cl- was not detected and dispersion was evenly high in al pH ranges. This indicates that montmorillonite is easily dispersed, even at low pH, as long as its negative charge is saturated with a hydrated monovalent cation.

On the other hand, sericite presented a charge highly pH depended (**Erro! A origem da referência não foi encontrada.**). This clay is considered to incorporate cations according to ambient solution condition, suggesting the variable charge characteristic. The dispersion behaviour of sericite was very sensitive, increasing abruptly above pH 6,5. Some author attributes this high dispersibility to the irregular surfaces, leading to bad contact between the edges and the faces [127].

2.5.2 Polymers

When it comes to soils suspension, polymers have been used from a long time due to its characteristics, versatility and availability [128][129].

In 1988, Awad M. Helalia et al.[130] compared 10 polyacrylamides (PAM) with different charges at 0,10, and 50 $mg.L^{-1}$ concentration with low electrolyte solution (1 $molc.m^{-3}$) at 0, 5, and 20 sodium absorption ratio (SAR) values for their ability to reduce dispersion of three soils. All compounds were effective in promoting clay flocculation at a concentration of 10 $mg.l^{-1}$. When compared at comparable charge, the PAM compounds were more effective than the guar compounds, which is consistent with their higher molecular weight. The order of effectiveness of the compounds was cationic > non-ionic > anionic. In this study it was evident that the effect of low electrolyte concentration was the prominent factor in dispersion.

Polyacrylamide (PAM) is one the most used polymers in soil stabilization. It is a long-chain synthetic polymer that binds clay particles together. This characteristic helps to control wind and water erosion, improve water infiltration and retention, improve soil aeration, and inhibit crusting or sealing. It is also used to treat pavement foundation in civil engineering since it allows lower deformations and a higher unconfined compressive strength (UCS) to the soil. Usually, PAM suspensions with the most desirable properties for Soil conditioning has a molecular weight of about 15-22 million a.u. (atomic units) and is about 20% anionic [131]. In 2002 by Charles A. Arnold et al. developed a PAM with the aim of obtaining a stable suspension for soil conditioning. It is a water-soluble suspension of polyacrylamide particles, with at least 2.5% by weight polyacrylamide, and a maximum of 15%. The aqueous medium includes a saturated solution of an ammoniated salt (ammonium sulfate, ammonium nitrate, urea, and thiourea), with an

approximate concentration of 0.90 $Kg.l^{-1}$. The suspension is stable for at least twelve hours without any visible settling or stratification.

The addition of PAM stabilizes existing aggregates and improves bonding between particles. This was evaluated in 2010 by A. I. Mamedov et al [132]. 16 soil samples (loam and clay) were tested by measuring aggregate sensitivity to slaking. To compare, some soils were treated with an anionic high-molecular-weight PAM and others were not. The index for aggregate susceptibility to slaking, termed stability ratio (SR), was obtained from quantifying differences in the water retention curves at a matric potential range of 0 to 5.0 $J.kg^{-1}$ for the treatments studied. For the untreated soils, the SR ranged widely from 0.24 to 0.80. The SR of PAM-treated aggregates exhibited a narrow range from 0.70 to 0.94 $J.kg^{-1}$. The efficiency of PAM in improving aggregate and structural stability relative to untreated soils ranged from 1.01 to 3.90 $J.kg^{-1}$. It was also possible to notice that the addition of PAM acts differently according to the soil mineralogy. The effectiveness of PAM in improving structure and aggregate stability is directly related to clay activity and to soil conditions affecting PAM adsorption (e.g., electrolyte resources, pH, and exchangeable cations) to the soil particles and inversely to the inherent aggregate stability. In this article, an anionic PAM of high-molecular-weight (~18×10^6 Da) and 30% hydrolysis with a concentration of 200 $mg.L^{-1}$ was used at pH 6.7. The efficacy of PAM in improving aggregate stability was therefore proposed to be inversely related to the inherent stability of the aggregates, and directly linked to soil conditions affecting PAM adsorption to the soil.

Aqueous based drilling fluids are usually composed of a water-soluble polymer that imparts desirable performance characteristics to the final drilling fluid. Arvind D. Patel (1991) [133] developed a polymer that exhibits superior tolerance to divalent cations, salts, solids and elevated temperatures when added to aqueous drilling fluids. The drilling fluid in this experiment comprises an aqueous continuous phase, a water-soluble polymer, a weighting agent and a gelling agent. The polymer additive of this invention remains relatively unaffected by pH levels in the drilling fluid ranging from 7 to as high as 12, being the preferred range from 7,5 to 9, and has a molecular weight between $2\text{-}7*10^6$ Da. It has been found that the copolymer additives of this invention should comprise between about 70% by weight of AMPS (2-acrylamide-2-methyl propane sulfonic acid), about 5% by weight of N,N-dimethylacrylamide and 25% by weight acrylamide.

In order to understand and evaluate the effect of the electric field associated with the basal and edge surfaces of the clay minerals on the adsorption of anionic polymers, in 2003 Hadar Heller et al.[134] used two negatively charged polymers, PAM90 and ACC86 (a co-polymer of polyacrylamide), of the same molecular weight (26105 $g.mol^{-1}$) but with different degrees of hydrolysis (90 and 20%, respectively). The effect of pH (6, 10), NaCl concentration (0, 10 $mmol_C.l^{-1}$) and clay particle size on PAM90 were also evaluated. As it possible to notice from **Erro! A origem da referência não foi encontrada.** the results showed that the adsorption of PAM90 polymer per unit weight of pyrophyllite increased as the particle size of the clay decreased and the adsorption of PAM90 polymer by pyrophyllite was much greater than that by Na-montmorillonite. This means that pyrophyllite has a better chance to form flocs and separate from

the suspension with the addition of PAM90 when compared with montmorillonite. However, affinity of both clays for ACC86 was about the same. Whereas the affinity of Na-montmorillonite for ACC86 was greater than for PAM90, the opposite was observed for pyrophyllite. These results were attributed to the repulsive forces which develop between the negatively charged, extended-chain polymer and the extended negative electric field associated with the basal surfaces, around the Na-montmorillonite platelets.

The molecular weight (MW) of PAM is an important factor to consider when evaluating this polymer suspension capacity. Heller and Keren (2002)[128], reported that the higher the MW of PAM, the more effective its ability to stabilize flocs of clay in a free electrolyte clay suspension. However, PAM of low to moderate MW will be more effective than PAM of high MW in penetrating into aggregates and contributing to their stabilization. In 2007, A. I. Mamedov et al.[135] studied this relationship by using two anionic polymers, a high-MW (12×10^6 Da) and a medium-MW (2 × 105 Da) PAM, deionized water (electrical conductivity of 0.004 dS/m) or a 15 $mmol.l^{-1}$ gypsum solution, on the stability of aggregates from four soils, varying in clay content. The soils used where loam, sandy clay, clay-y (from the region of Yagur, richer in sand and silt) and clay-E (from the region of Eilon, richer in clay). The results indicated that, to enhance aggregates' resistance to slaking, it is enough to stabilize the exterior surfaces of the aggregates with PAM. Because most of the PAM added to the aggregates was adsorbed on the exterior surfaces of the aggregates, the small fraction of the PAM that entered the aggregates' pores, had no significant impact on aggregate stability. Treating aggregates with PAM, irrespective of its MW, improved their stability in comparison to that of untreated aggregates. Therefore, no specific PAM could have been singled out as preferable between the two PAM polymers tested, as the effects of the PAM varied among the soils tested and depended on initial aggregate size and solution ionic strength. For instance, for both loam and sandy soils, both polymers had similar results, reaching a soil Stability Ratio (SR) of 0,4 SR and 0,7 SR, respectively. This unity indicates stable aggregates that resisted slaking by fast wetting. A value of zero SR indicates that fast wetting destroyed the aggregates to the extent that all pores that drain at the matric range applied no longer exist. For clay Y, as well as for clay E, the medium molecular weight polymer presented a slightly better stability ratio (0.9 SR) compared with the high molecular PM (0.8 SR).

Haihong Li (2008) [136] analysed the effect of charge density and molecular weight (MW) of partially hydrolysed polyacrylamide (HPAM) polymers in processing low-grade oil sand ores. It was found that HPAM polymers with a low MW acted as dispersants in the bitumen extraction process, resulting in low bitumen recovery and slow tailings settling. In contrast, the use of HPAM polymers with a high MW improved both bitumen recovery and tailings settling. To achieve high bitumen recovery and fast tailings settling, a HPAM polymer must have a low to medium charge density (~30%) and a high MW (17,5 million Daltons). Therefore, for our goal, apparently, high molecular weight partially hydrolysed polyacrylamide does not appear to be the most indicated to promote suspension. However, in this article they are using oil sand ores, which has different properties from clay and sandy soil.

However, the industry keeps developing new synthetic polymers, able to satisfy a wider range of needs with the best quality and effectiveness possible.

In 2014, [138] a new material was developed to be used in firefighting. It comprises a mineral inorganic gel, and an organic polymer and it improves the quality of sand injection and reduces water wastage. The material in discussion can steadily suspend sand, through the addition of a small amount of colloid yielding steady sand-suspended slurry. The dispersion effect of the sand suspended colloid is demonstrated by the incorporation of the electrostatic effect by the double-electric layer and the steric hindrance effect on the sand particle, ensuring system stability and the suspension of the sand particles. With a colloid concentration of 0,4%, and a pH range between 5,8 and 7,5, the sand particles (with a grain size of 0,5mm) remain in suspension up to 5 days. The organic polymer used is a polysaccharide biopolymer (comprising in its structure mannuronic acid and guluronic acid).

Organic polymers have gained attention as suspension/sedimentation agents duo to its great industrial potential [139]. In 1993 Baohua Gu et al. [129] studied the influences of three organic polyanions (a soil humic acid, a soil polysaccharide, and a commercial anionic polysaccharide) and hydroxy-Al polycations (Al-p) on soil clay dispersion and aggregation. It was found that the organic polyanions, especially humic acid, were not flocculating agents, but were effective dispersing agents for the Na-clays and Na-soils. It was possible to observe that none of the negatively charged organic polymers caused the flocculation of soil suspensions. On the other hand, they resulted in generally more stabilized colloidal suspensions (relative clay dispersion > 1). Similarly, addition of these polyanions to illite and montmorillonite suspensions increased clay dispersion in general, except for the montmorillonite suspensions treated with the anionic polysaccharide. The anionic polysaccharide caused a partial flocculation of the montmorillonite suspensions, which reached a minimum at about 10 $g.m^{-3}$ polysaccharide addition. Further addition of the polysaccharide increased montmorillonite dispersion.

The fact that none of the three organic polyanions caused a complete flocculation of the Na-soil or clay suspensions may well indicate that these polyanions were unable to form bridges between clay particles and to form aggregates. On the other hand, the possible adsorption of these polyanions onto edge sites of clay particles could have increased the surface negative charge on soil or clay colloids, and therefore created an electrostatic repulsion, acting as effective dispersants.

Some other biopolymers used are proteins, nucleic acids, and polysaccharides. They behave in a similar way to synthetic polymers, however they are more environmentally friendly and sustainable [140].

Therefore, as we can see, there is a large variety of polymers that can be used with the purpose of suspending soil particles. The best choice will depend mostly on the soil characteristics as well as the operation conditions.

2.6 Suspension from a modelling point of view

From decades, it has been of interest to find mathematical models to describe dispersion and sedimentation of particles in suspensions[141][141], [142].

According to Coulson and Richardson [143], the sedimentation velocity of particles tends to decrease steadily as the concentration of the suspension is increased. Several attempts have been made to predict the apparent settling velocity of a concentrated suspension. In 1926, Robinson [144] suggested a modification of Stokes' law and used the density (ρc) and viscosity (μc) of the suspension in place of the properties of the fluid to give:

$$uc = \frac{K''d\text{^}2(\rho s - \rho c)g}{\mu c}$$

Equation 2.5-Apparent settling velocity of a concentrated suspension [153]

where K'' is a constant.

The effective buoyancy force (is readily calculated since:

$$(\rho s - \rho c) = \rho s - [\rho s(1 - e) + \rho e] = e(\rho s - \rho)$$

Equation 2.6- Effective buoyancy force [134]

Where e is the voidage (free space, in total fraction of volume, available for the flow of fluids) of the suspension. Buoyancy arises from the fact that fluid pressure increases with depth and from the fact that the increased pressure is exerted in all directions so that there is an unbalanced upward force on the bottom of a submerged particle.

In 1988, V. L. Lopes et al.[145] published a study where a physically based, mathematical model of small watershed sedimentation is described. For this it was considered an unsteady and spatially varying sedimentation process on overland flow areas and in small, concentrated flow. The rate of sediment deposition (downward sediment flux) is proportional to the local mean sediment concentration and to an effective particle fall velocity (Vs). The deposition rate in kilograms per second per metre of channel width can be computed as:

$$d = \in * Tw * Vs * C$$

Equation 2.7- Deposition rate [135]

In which Tw is the flow top width (m), and ϵ is a dimensionless coefficient depending on the soil and fluid properties. Other authors have later resourced to this model to evaluate erosion patterns and suspended sediments behaviour [146][147].

Chongyoup Kim (2004) [148] developed a mathematical model to describe the migration of particles under the influence of inertia and particle-particle interaction. It was considered spherical

particles of radius *a* suspended in a Newtonian fluid, between two parallel and infinite plane walls. It was also assumed that the particles were large enough to neglect the influence of Brownian motion.

They started from defining the mass flux due to inertia between two plates, being ρ the particles density, Φ the solid fraction and U_{IM} migration velocity.

$$N_{IM} = \rho \Phi U_{IM}$$

Equation 2.8- Mass flux due to inertia [138]

The particle flux due to particle-particle interaction (N_{PP}) was also determined through the addition of concentration gradient (N_C) and viscosity gradient ($N\eta$):

$$N_{PP} = N_C + N_\eta$$

Equation 2.9- Particle flux due to particle-particle interaction [138]

Thus, by non-dimensionalizing the governing equations the dimensionless shear rate (β) equation is obtained, being *s* the dimensionless distance from the wall:

$$\beta(s) = -\frac{2}{\mu(\Phi)}(2s - 1)$$

Equation 2.10- Dimensionless shear rate [138]

By the practical application of these equations it was possible to observe that once particles are concentrated at a certain position, particle-particle interaction tend to spread them out. Therefore, in the migration of particles in suspension, inertia, as well as particle-particle interaction should be taking properly into account regardless of particle loading.

Hajir Kourki (2011) [149] studied the effect of polymer concentration on particle-particle interaction and particles and, therefore, how that influences sedimentation velocity. The results showed that at low particles concentrations, addition of small amounts of polymer in the solution would decrease particle-particle interactions. At low particle concentration, effect of particle-particle interactions on sedimentation velocity is negligible, so sedimentation velocity in these concentrations is a function of particle-matrix interaction and hydrodynamic motion of particles. Stokes equation can be used to define this motion:

$$V_h = \frac{d^2}{18\mu_m}(\rho_s - \rho_m)g$$

Equation 2.11- Hydrodynamic motion of a particle [139]

Here, d is the particle diameter, μ_m is the media viscosity, ρ_s corresponds to the particle density and ρ_m the media density. Therefore, only particle–particle interactions are influenced by

changing in particle concentration, causing variation in sedimentation velocity, so the difference between sedimentation velocity and low concentration sedimentation velocity (v_0) is just a function of particle–particle interaction. Dimensionless velocity that is a function of particle–particle interaction at different particle concentration can be defined as follows:

$$l_{pp}(\Phi) = \frac{V_0 - V(\Phi)}{V_0}$$

Equation 2.12- Sedimentation velocity [139]

Where V is the sedimentation velocity, V_0 is the velocity at low concentrations, and l_{pp} is the dimensionless sedimentation velocity that is a result of only particle–particle interactions.

The effects of electrolyte concentration and pH on the sedimentation rate and particle association has been studies on coagulated suspension of sodium montmorillonite [150]. The results indicated that the effect of pH (between 4 and 9.5) on the ultimate sediment height was considerable at low ionic strength and almost negligible at high ionic strength with 0.25–0.5 M NaCl as an inflection range. Increasing salt concentration accelerated the maximum sedimentation rate. This can be explained by increasing salt concentration decreases the repulsive electrostatic effect. According to this, maximum velocity as a function of solid concentration can be described according to the Michaels and Bolger method:

$$Q^{1/4.65} = V_s^{\frac{1}{4.65}}(1 - \alpha\Phi_p)$$

Equation 2.13- Maximum sedimentation velocity [140]

Where p denotes the volume fraction primary particles, Q is the velocity of the boundary, V_S is the terminal velocity of floc and Φ_p is the volume fraction of primary particles. α corresponds to the increment ratio of effective volume fraction and is obtained from the slope of the maximum velocity as a function of solid concentration.

In order to develop a new mathematical model to achieve our goal, a series of programs and software's were analysed.

Copasi is a free software for simulation and analysis of biochemical networks and their dynamics[151]. The models here developed are based on reactions that convert a set of species into another set of species. The program automatically converts reactions network to a set of differential equations or to a system of stochastic reaction events. It allows:

- An optimization of arbitrary components, using a range of diverse algorithms.
- Parameter estimation, which can be done over several different experiments simultaneously, including mixtures of steady-state and time course experiments.

- Local sensitivity analysis
- Time scale separation analysis, this allows definition of fast and slow components of the model, in a time-dependent way.

Despite the many characteristics and advantages of this program, it may be too orientated to biochemical processes therefore it might present us with some limitations for its application on our project along the way.

The next program considered is Arena, a business process simulation software that allows the user to analyse and make decisions on how to improve processes [152].

It evaluates potential alternatives to determine the best approach to optimizing performance based on key metrics such as costs, throughput, cycle times, equipment utilization and resource availability. Therefore, it reduces risks and uncertainty through rigorous simulation and testing of process changes before committing significant capital or resource expenditures.

However, as it is possible to notice, this software targets directly business process in order to optimize them. Thus, it will most likely present some limitations when applied to our goal.

Another option analysed was Excel. This is a platform with a wide variety of features that makes it a simple but extremely functional tool for data organization, mathematical models development, problem formulation, among others [153]. It is already largely used for academic purposes and several authors have used this program to develop mathematical models in different fields [154][155].

Compared with other platforms evaluated, the most evident limitation that this program contains is the limited (even though large) number of rows (1,048,576) and columns (16,384). However, its simplicity and wide variety of tools makes of this an option with great potential.

R-framework is a program developed in R which is a language and environment for statistical computing and graphics [156]. R provides a wide variety of statistical and graphical techniques and is highly extensible. It includes:

- Effective data handling and storage facility.
- A suite of operators for calculations on arrays, in particular matrices.
- A large, coherent, integrated collection of intermediate tools for data analysis.
- Graphical facilities for data analyses and display.
- A programming language which includes conditionals, loops, user-defined recursive functions and input and output facilities.

For this reason, being such an open platform, this software seems to be a good option to develop our mathematical model.

Matlab is a widely used platform that combines a desktop environment tuned for iterative analysis and design processes with a programming language that expresses matrix and array mathematics directly [157]. It allows the user creating scripts that combine code, output, and

formatted text. All these tools grant the user access and pre-process data, build machine learning and predictive models, and deploy models to enterprise IT systems.

The predictive analytics that this platform allows us, as well as the possibility to explore a wide variety of modelling approaches, makes of Matlab a useful and efficient tool to achieve our goal in this project.

Our final alternative is Statistica, a data visualization and analysis program [158]. Its analysis capabilities cover thousands of algorithms, functions, tests, and methods ranging from the simple table to advance non-linear modeling, through generalized linear models to the series of temporal methods. Therefore, it presents as a viable option for our goal, however it is not clear if the program allows us to develop our own model our if we can only adjust our data to the predefined models.

2.7 Strategy

In order to decide the procedure to achieve the goal of this project a strategy was developed combining the variables that are part of the project goal, and information found in the state-of-the-art research.

Therefore, the strategy formulated and used consisted in using a 4L aqueous suspension medium composed of water and 8 different polymers (varying in anionicity and molecular weight) or a combination of polymer and additives, considering different polymer concentrations and different solution pH. Clay, with a grain size between 0.5 and 2 µ, sand or a mixture of clay and sand, at different concentrations, will be considered.

The sedimentation rate will be calculated considering the difference between the initial density and the density passed 24h.

Control points of the experiment include varying the pH between 5 and 12,5, polymer concentration between 0 $g.L^{-1}$ and 1 $g.L^{-1}$, as well as a soil concentration of 25 $g.L^{-1}$; 100 $g.L^{-1}$ and 200$g.L^{-1}$.The mixing time will vary between 30 minutes and 210 minutes at a speed of 250rpm.

Through all this, operation conditions such as pH, polymer and soil concentration, anionicity and molecular weight, will be combined in a data processing software in order to develop the mathematical model.

3. Protocols

3.1 Execution protocols

3.1.1 Mixing time as function of Column diameter

This protocol was executed to correlate the relationship between mixing time and the column diameter. The following diagram represents the series of steps executed in the development of the experiments:

1º Filling the reactor with 4L of water;

2º adjusting the pH with a NaOH or HCl according to the need;

3º Adding the polymer and letting agitate for 1h;

4º Retrieve a sample with a cup and proceed to the characterization tests;

5º Transfer the polymeric solution to a bucket and add the soil;

6º After mixing the soil with the polymeric solution, retrieve a sample and proceed to the characterization tests;

7º Divide the mixture through 3 beakers;

8º Proceed to measure the solutions density for 3h with 5 minutes break.

For this experiment, a reactor filled with 4L of deionized water was maintained in a cool bath, with a temperature of 22ºC. Mixing was achieved through air flow. The solution pH was adjusted to a value of 12,5 using 40mL of a 2.5M solution of NaOH. Next, 4g of the selected polymer (7156) was dissolved in it for 1h.

Passed the dissolving time, a sample was collected to characterize the solution according to the protocols to Brookfield viscosity, Marsh viscosity, electric conductivity, pH and register of density. After the measurements, the solution was transferred to a bucket whose diameter is specified in Table 3.1. An agitator was used to mix the solution previously prepared. The agitation was at a speed of 300rpm and 400g of clay was added to the solution. The mixture was maintained in agitation accordingly to Table 3.1. Passed that time, the solutions density was measured accordingly to the protocol “register of density” (chapter 3.2.6) and a sample was collected to characterize accordingly to the characterization protocols Brookfield viscosity (chapter 3.2.1), Marsh viscosity (chapter 3.2.2), electric conductivity (chapter 3.2.3), and pH (chapter 3.2.4). A separated beaker was used in the determination of the solutions density through time, accordingly to protocol ‘register of density’ (chapter 3.2.5). Three to four 1L beakers were filled with the prepared mixture. After 24h, the sedimentation rate was calculated. The characterization protocols were executed once again: Brookfield viscosity (chapter 3.2.1), Marsh viscosity (chapter 3.2.2), electric conductivity (chapter 3.2.3), pH (chapter 3.2.4) and final density (chapter 3.2.6).

Table 3.1- Runs and respective mixing time and bucket diameter

Run	Time (min)	Diameter (mm)
1	45	280
2	45	190
3	90	280
4	90	190
5	150	280
6	150	190
10	210	280

3.1.2 Polymer concentration as function of pH

This protocol was executed to correlate the relationship between polymer concentration and the solutions pH. For this, a reactor filled with 4L of deionized water and it was maintained in a cool bath, with a temperature of 22ºC. Mixing was achieved through air flow. The solution pH was adjusted to a value accordingly to Table 3.2 using a 2.5M solution of NaOH. The polymer (7156) concentration is selected accordingly to Table 3.2 and it was dissolved in the deionized water for 1h.

Passed the 1h dissolving time, a sample was collected to characterize the solution according to the protocols to Brookfield viscosity, Marsh viscosity, electric conductivity, pH and 26 register of density. After the measurements, transfer the solution inside a bucket whose diameter is specified in table. An agitator was used to mix the solution previously prepared. The agitation was turned on at a speed of 300rpm and 400g of clay was added to the solution. The solution was maintained in agitation for 150 minutes. Passed that time, the solutions density was measured accordingly to the protocol “register of density” (chapter 3.2.6) and a sample was collected to characterize accordingly to the characterization protocols Brookfield viscosity (chapter 3.2.1), Marsh viscosity (chapter 3.2.2), electric conductivity (chapter 3.2.3), and pH (chapter 3.2.4). A separated beaker was used in the determination of the solutions density through time, accordingly to protocol ‘register of density’ (chapter 3.2.5). Three to four 1L beakers were filled with the prepared mixture. After 24h, the sedimentation rate was calculated. The characterization protocols were executed once again: Brookfield viscosity (chapter 3.2.1), Marsh viscosity (chapter 3.2.2), electric conductivity (chapter 3.2.3), pH (chapter 3.2.4) and final density (chapter 3.2.6).

Table 3.2-Runs and respective polymer concentration and pH

Run	Polymer concentration ($g.L^{-1}$)	pH
7	0,4	12,5
8	0,6	12,5
9	0,8	12,5
5	1	12,5

11	1	5
12	1	10
13	1	7
14	1	11,5
33	0,8	11,5
35	0,6	10
36	0,4	7
37	0,8	7

3.1.3 Polymer concentration as function of Soil concentration

This protocol was executed to correlate the relationship between polymer concentration and soil concentration. For this, a reactor filled with 4L of deionized water and it was maintained in a cool bath, with a temperature of 22ºC. Mixing was achieved through air flow. The solution pH was adjusted to 12,5 using 40mL of a 2.5M solution of NaOH. The polymer (7156) concentration is selected accordingly to table and it was dissolved in the deionized water for 1h.

Passed the 1h dissolving time, collect a sample to characterize the solution according to the protocols to Brookfield viscosity, Marsh viscosity, electric conductivity, pH and register of density. After the measurements, transfer the solution inside a bucket whose diameter is specified in Table 3.3. An agitator was used to mix the solution previously prepared. The agitation speed was at 300rpm while the clay was being added to the solution. The mixture was maintained in agitation for 150 minutes. Passed that time, the solutions density was measured accordingly to the protocol "register of density" (chapter 3.2.6) and a sample was collected to characterize accordingly to the characterization protocols Brookfield viscosity (chapter 3.2.1), Marsh viscosity (chapter 3.2.2), electric conductivity (chapter 3.2.3), and pH (chapter 3.2.4). A separated beaker was used in the determination of the solutions density through time, accordingly to protocol 'register of density' (chapter 3.2.5). Three to four 1L beakers were filled with the prepared mixture. After 24h, the sedimentation rate was calculated. The characterization protocols were executed once again: Brookfield viscosity (chapter 3.2.1), Marsh viscosity (chapter 3.2.2), electric conductivity (chapter 3.2.3), pH (chapter 3.2.4) and final density (chapter 3.2.6).

Table 3.3- Runs and respective polymer and soil concentration

Run	Polymer concentration ($g.L^{-1}$)	Soil concentration ($g.L^{-1}$)
5	1	100
15	1	5
16	1	10
17	1	50
18	1	200
19	1	400
20	1	100

3.1.4 Polymer as function of additive

This protocol was executed to correlate the relationship between polymer and additive types. For this, a reactor was filled with 4L of deionized water and it was maintained in a cool bath, with a temperature of 22ºC. Mixing was achieved through air flow. The solution pH was adjusted to 12.5 using 40mL of a 2.5M solution of NaOH. 1g.L^{-1} of polymer was dissolved in the deionized water for 1h. Passed the 1h dissolving time, a sample was collected to characterize the solution according to the protocols to Brookfield viscosity (chapter 3.2.1), Marsh viscosity (chapter 3.2.2), electric conductivity (chapter 3.2.3), pH (chapter 3.2.4) and register of density (chapter 3.2.6). After the measurements, the solution was transferred to transfer to a bucket with a 280mm diameter. After 10minutes of mixing the additive was added accordingly to Table 3.4. An agitator was used to mix the solution previously prepared. The agitation speed must be at 300rpm while the clay is added to the solution. The mixture was maintained in agitation for 150 minutes. Passed that time, the solutions density was measured accordingly to the protocol "register of density" (chapter 3.2.6) and a sample was collected to characterize accordingly to the characterization protocols Brookfield viscosity (chapter 3.2.1), Marsh viscosity (chapter 3.2.2), electric conductivity (chapter 3.2.3), and pH (chapter 3.2.4). A separated beaker was used in the determination of the solutions density through time, accordingly to protocol 'register of density' (chapter 3.2.5). Three to four 1L beakers were filled with the prepared mixture. After 24h, the sedimentation rate was calculated. The characterization protocols were executed once again: Brookfield viscosity (chapter 3.2.1), Marsh viscosity (chapter 3.2.2), electric conductivity (chapter 3.2.3), pH (chapter 3.2.4) and final density (chapter 3.2.6).

Table 3.4- Runs and respective polymer concentration and additive type and concentration

Run	Polymer concentration (g.L^{-1})	Additive (name)	Additive concentration (mL.L^{-1})
28	1	Alfabond	1,4
29	1	HY5040	0,8
30	1	Alfabond	1,4
31	1	HY5040	0,8
32	1	HY168	0,8

3.2 Characterisation protocols

3.2.1 Determination of Brookfield viscosity

The determination of Brookfield viscosity was obtained is a viscometer model DV2T. To use it, turn on the device and proceed to calibration step- confirm that the viscometer is levelled using the bubble level on the front of the instrument. AUTO ZERO the instrument with no spindle attached (the auto zero will automatically appear after turning equipment on and before main menu appear). In main menu set spindle, speed, and endpoint. Select spindle LV-01 (or other) and speed 10rpm and choose multipoint averaging (last entry of main menu) selecting 5 seconds to data interval and 5 minutes to averaging duration. Measure around 50 mL of the suspension solution and pour it into the measuring vessel. Immerse the spindle into the sample. Attach the

spindle to the viscometer. The spindle should not touch the bottom or sides of the container and should be centred. After all assembling done, press Run to start viscosity analysis. At the end of time analysis, display will show analysis data.

3.2.2 Determination of Marsh cone viscosity

The determination of Marsh viscosity was obtained using a Marsh cone, as in the figure. To use it, spill the polymeric and soil suspension into the Marsh cone. Immediately start measuring the time that a quart of gallon of the polymeric solution takes to flow between the cone and the cup of the Marsh funnel.

Figure 3.1- Marsh funnel

3.2.3 Determination of the electrical conductivity of a polymeric suspension

To determine the electrical conductivity, calibrate the conductivity meter according to the manufacturer's instruction using the KCl reference solution to obtain the cell constant. Rinse the cell thoroughly. Measure the electrical conductivity of the 3M KCl at the same temperature as the soil suspensions. Rinse the conductivity cell with the soil suspension. Refill the conductivity cell without disturbing the settled soil. Record the value indicated on the conductivity meter. Rinse the cell with deionized water between samples.

3.2.4 Determination of the pH of a polymeric suspension

To determine the pH of a polymeric suspension, turn the pH meter on by pressing the "power" button. Rinse the pH electrode with distilled water. Dip the pH electrode into a testing solution or suspension. Wait 5 minutes and record the value indicated on the pH meter screen. Rinse the cell with deionized water between samples.

3.2.5 Determination of the total density of the mixture

Turn on the scale and proceed to calibration step- confirm that the scale is at 0.00Kg. Weight the empty container that will be used for the experiment. Note the value presented in the scale screen. Add the mixture to the container. Wight the container filed with the mixture. Note the value presented in the scale screen. Proceed to calculate the mixture's density, knowing that $\rho = \frac{m}{V}$.

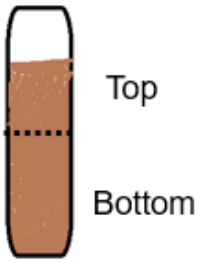

Figure 3.2- Representation of a beaker filled with the polymer and clay mixture, being brown the representation of the mixture and white the empty space on the beaker

3.2.6 Determination of the density of the mixture

To determine the density of the mixture, a density meter model “Mettler Toledo™ Densito™ 30PX”. Pour a sample of the polymeric soil solution to a testing cup. Turn the density meter on. Adjust the sampling speed to avoid the formation of air bubbles. Dip the tube directly into the sample previously collected. Collect the results present in the meter screen.

3.2.7 Calculation of the equation trough R Software

The first step consisted in opening the R software. This will have four windows that should look like this:

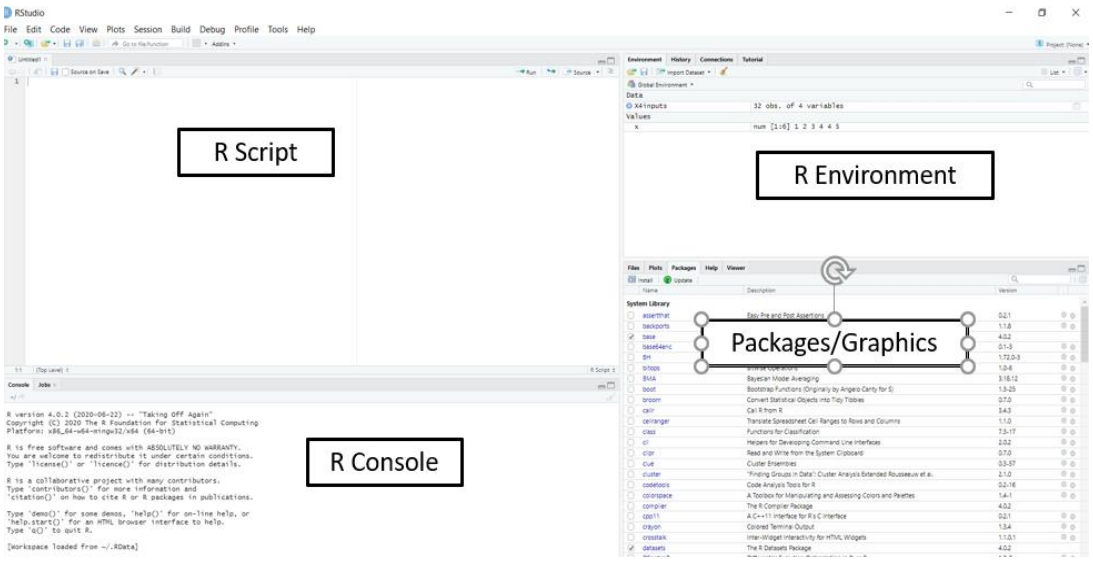

Figure 3.3- Overview of the R software script

After that, import a database with the information to work with from excel to the R environment.

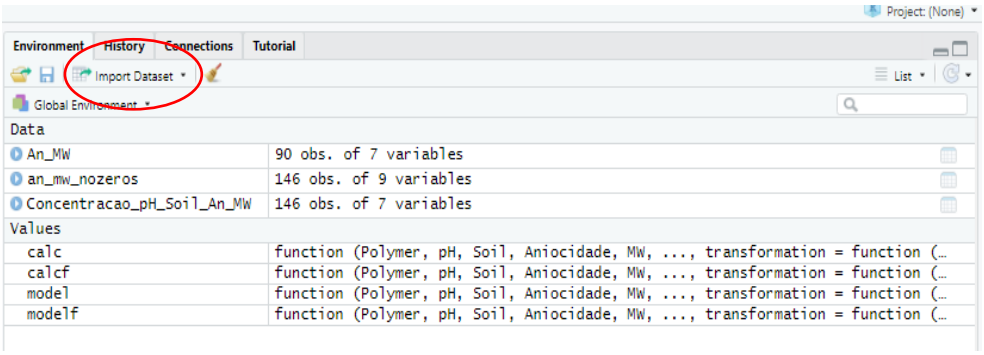

Figure 3.4- Importing a data base into R software

After selecting in ‘import database’, select ‘From excel’.

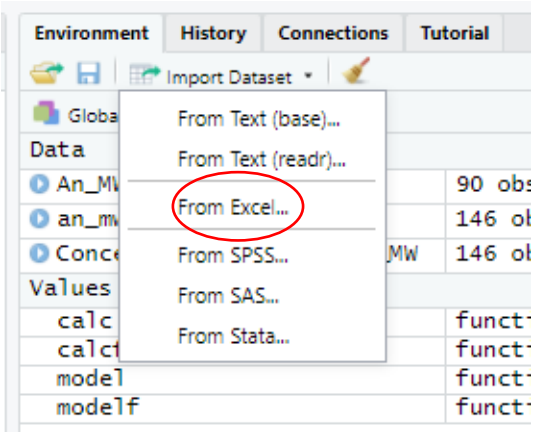

Figure 3.5- Importing a data from excel into R software

After clicking the option ‘From Excel’, select the button ‘Browse’ to choose a data base to work with and then click in ‘import’ to import the data base.

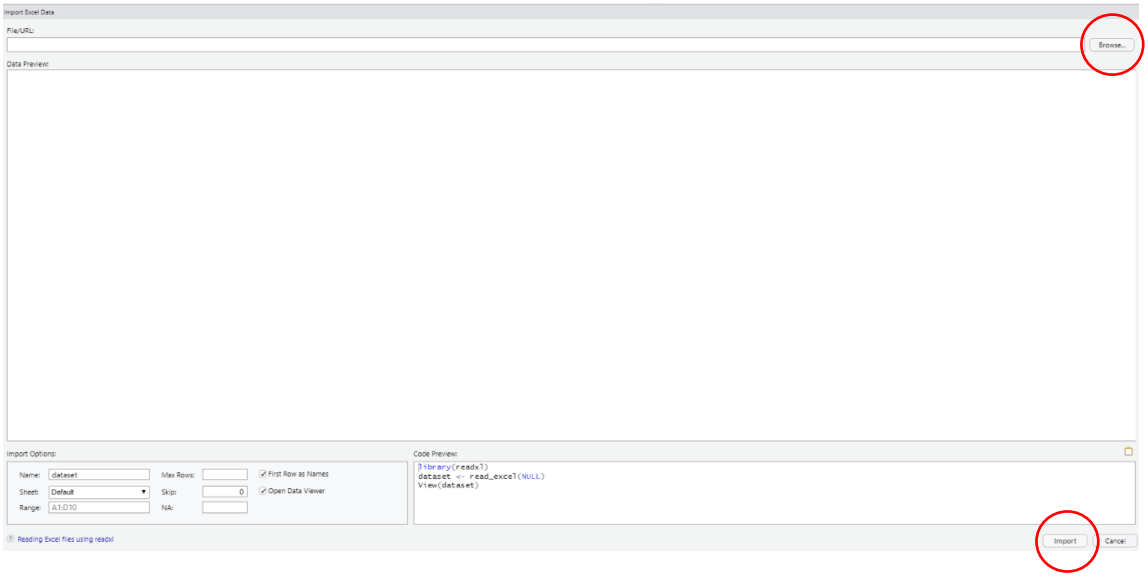

Figure 3.6- Final step to import a data base

After selecting the data base to work with, this will be stored in the environment window of the R software and it will be available for consultation in the top left window, next to the scripts.

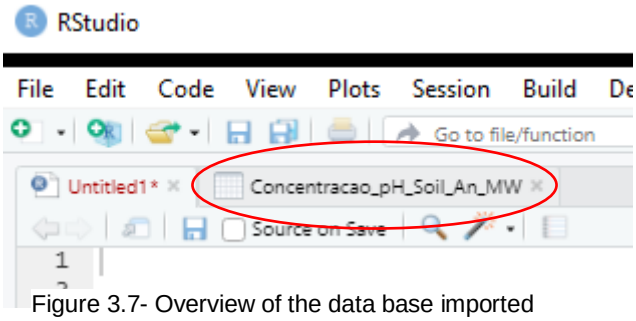

Figure 3.7- Overview of the data base imported

Since the functions in R work through a series of packages, it is a necessary to install the required packages to do the data modeling. In this case, the main packages are “mosaic”, “mosaicData”, “mosaicCore” and “ggplot2”.

To import and install the packages, go to the right bottom corner of the R studio environment and select the file ‘Packages’. Once here, just the select the desired packages and they will be installed.

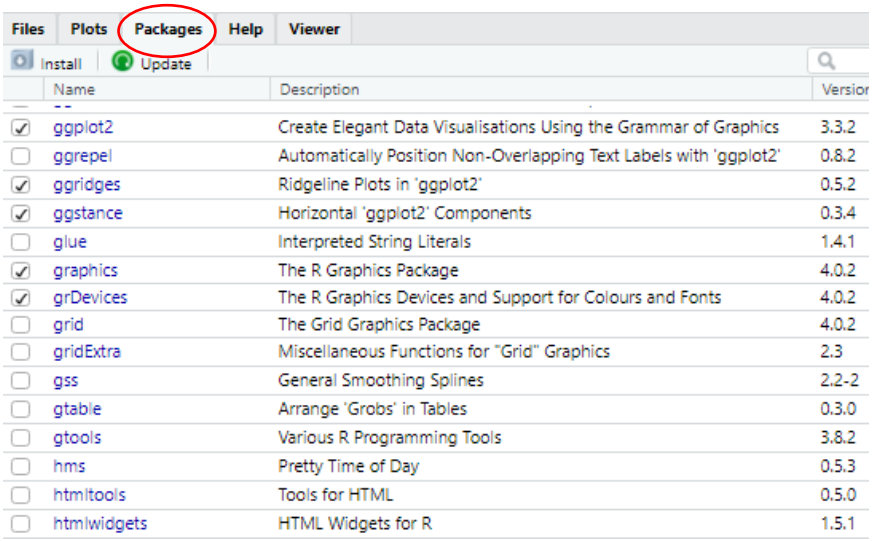

Figure 3.8- Selecting and importing packages

In order to achieve the mathematical model, open a new script in the top left corner of the R studio.

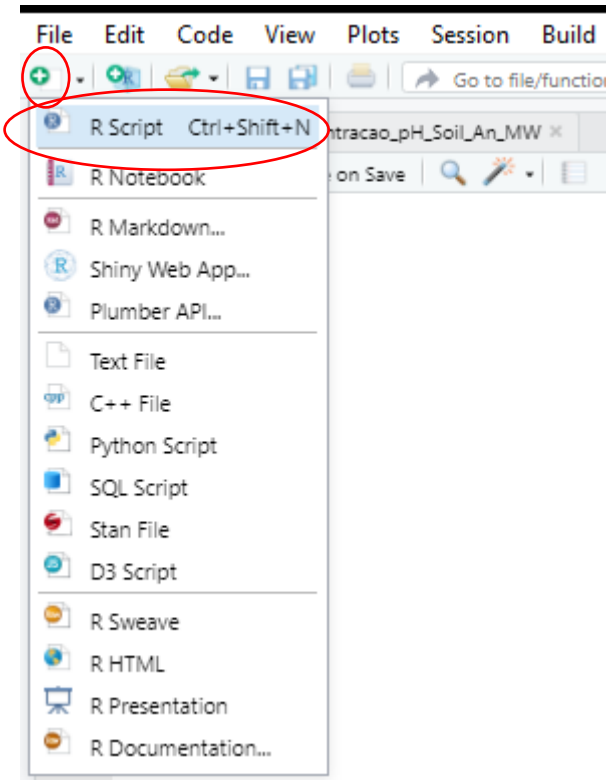

Figure 3.9- Opening a new R script

After opening the scrip, it is now possible to start writing the equation. To build the model/equation the first steps consists in naming it. After that, use the function ‘fitModel’ and then build the desired model inside it by introducing any equation desired. At the end of the equation introduce the command ‘data=’ to indicate the data base that is being used.

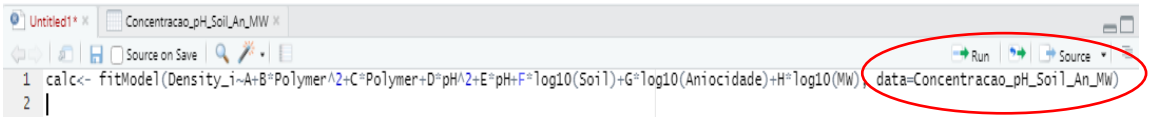

Figure 3.10- Building an equation in function of the information present in the data base

To activate the equation to the console, at the end of the equation press ‘Ctrl+enter’.

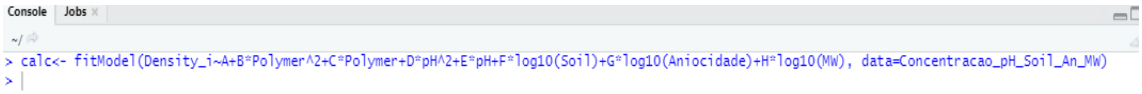

Figure 3.11- View of the console

To calculate the coefficients that compose the model use the function ‘coef’, (ex:coef(calc)) in the script. The results of the actions executed in the script will be exposed in the console, located in the left bottom corner of the R script.

4. Discussion of Results

4.1 Variables correlations

The goal of this project is to develop a mathematical model capable to predict suspensions sedimentation rates for at least 24h. In order to achieve this goal, the first step of the strategy consisted in establishing a series of criteria to optimize the experiments carried out and to understand how each variable affects the system, promoting and maintaining suspension. Therefore, the objective for this first step is to achieve a sedimentation rate less or equal to 1,7 g.h/L, a gradient value ≤30% and a density conservation ≥ 12%.

Equation 4.1- Calculation of sedimentation rate

$$Sed.Rate = \frac{Initial\ Density - Final\ Demsity_{24h}}{24h} * 1000 \frac{cm^3}{L}$$

Equation 4.2- Calculation of the gradient percentage

$$Gradient = 1 - \frac{Final\ Density_{top\ of\ column} - Density\ of\ polymer}{Final\ Density_{bottom\ of\ column} - Density\ of\ polymer}$$

Equation 4.3- Density conservation percentage

$$Density\ conservation = \frac{Final\ Density_{top\ of\ column} - Density\ of\ polymer}{Initial\ Density - Density\ of\ polymer} * 100\%$$

The gradient value represents the amount of clay that was lost throughout the column, since it is calculated based on the difference between the top and bottom of the column (as represented in chapter 3.2.5). The density conservation percentage represents the density preserved in the suspension for the 24h period, in a quantitative way while the sedimentation rate translates the amount of soil sedimented per hour and litter. The value established was calculated considering that 40% of the material in suspension sediments passed 24h.

Density values were registered every 5 minutes for the first hour, after stopping agitation, and then for every 30 minutes for the next two hours. In this phase, values of pH, electrical conductivity, Marsh and Brookfield viscosity were registered as well. Passed 24 hours the final density value, as well as the other output values (pH, electrical conductivity, Marsh and Brookfield viscosity) were also registered.

4.1.1 Mixing time in function of Column diameter

In this chapter it was performed a series of tests between the mixing time of the solution and the column diameter. The goal is to reach the criteria established of a sedimentation rate less or equal to 1,7 $g.h^{-1}$. This protocol 3.1.1 was performed at a fixed solution pH (12,5) with a PolyMud

concentration of 1 $g.L^{-1}$, in a 4L reactor, using 400g of clay. In order to decide what run is best compared to the others, some criteria where established. The gradient value must be ≤30%, density conservation ≥ 12% and sedimentation value ≤ 1,7 g.h/L.

Table 4.1- Outputs achieved in each run

Run	Mixing time (min)	Bucket diameter (mm)	Gradient (%)	Density Conservation (%)	Sedimentation rate (g.h/L)
1	45	280	27	10	1,53
2	45	190	31	20	0,6
3	90	280	64	28	0,58
4	90	190	24	31	0,47
5	150	280	27	16	1,33
6	150	190	40	19	0,97
10	210	280	31	31	0,7

In Table 4.1 are represented the output values for each run performed. As explicit in the table, run 4 presents a gradient of 24%, a density conservation of 31% and a sedimentation rate of 0,47 g.h/L. Run 5 presents a gradient of 27%, a density conservation of 16% and a sedimentation rate of 1,33 g.h/L. Run 10 presents a gradient of 31%, a density conservation of 31% and a sedimentation rate of 0,7%. Considering the limits previously established (gradient ≤30%, density conservation ≥ 12% and sedimentation rate ≤ 1,7 g.h/L) it is possible to notice that these runs demonstrate the best results for the combination of outputs considered. However, run 10 presented a gradient percentage slightly higher than the limit considered (31%, being the limit 30%). Therefore, to determine the run with the values closer to the criteria, a graphical comparison was executed.

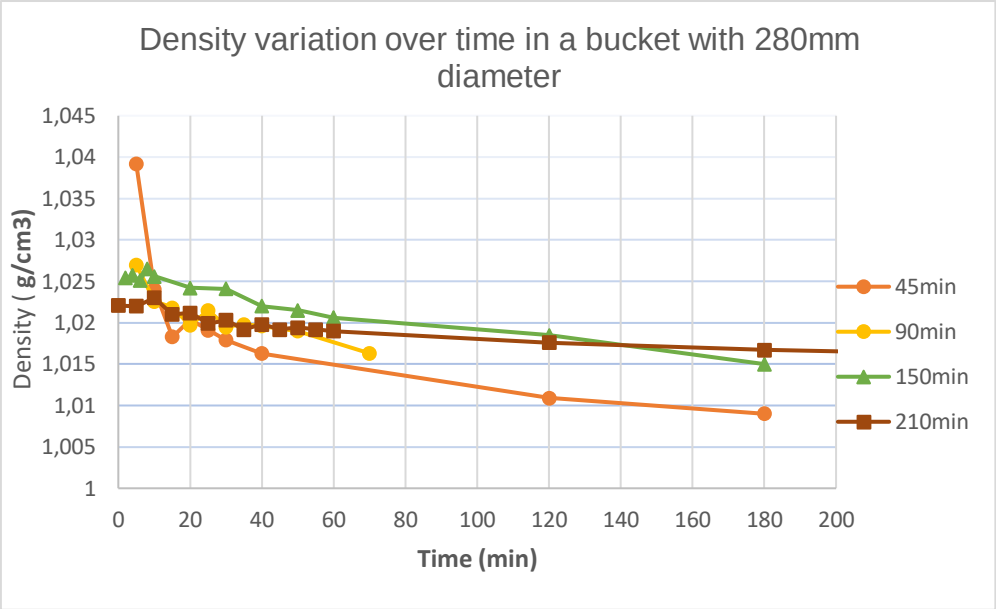

Figure 4.1- Density variation over time in the 280mm diameter bucket

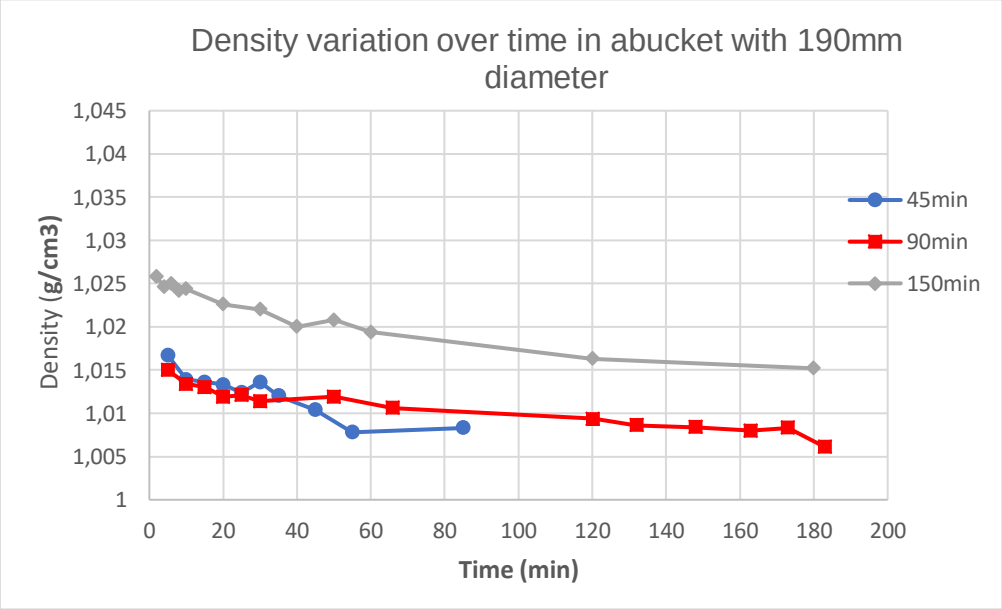

Figure 4.2- Density variation over time for the 190mm diameter bucket

In Figure 4.1 and Figure 4.2 it is represented the density variation over time, obtained after altering the bucket diameter (280 and 190mm respectively) and the mixing time (45min, 90min, 150min and 210min).

As it is possible to notice from the graphic in Figure 4.1, the run 5 presents the best results regarding to the loss of density over time, maintaining approximately 99,33% of its density in a 2 hour period. With this result we can better optimize the operation conditions to use in the next experiments. These will be performed using a 280mm diameter bucket and considering a mixing time of 150 minutes. Even though run 10 presents a similar curve, it is possible to notice that it

starts with a lower value for initial density (1,023 +/- 0,001 g/cm^3 comparing to 1,025 +/- 0,001 g/cm^3 obtained in run 5), meaning a lower capacity to set soil in suspension. On the other hand, from Figure 4.2, it is possible to notice that the best results occur in run 6, with a similar density preservation (99,07%) for a 2 hour period, considering a bucket diameter of 190mm and a mixing time of 150 minutes. When comparing these two runs, despite the similar behaviour of both curves, it is clear that run 5 presents a better column homogeneity (gradient of 27% oppositely to 40% in run 6), possible meaning that the density of the column remains relatively constant over time. This result might be due to a smaller ratio paddle diameter/bucket diameter, resulting in more space for the mixture to incorporate and disperse.

According to G. Dungan, 2018 [85], when building a foundation it is important to maintain the stability in the column up until it is filled with cement. Therefore, it is required to maintain the density value at a certain point (between 1 and 1,06 g/cm^3) and preserve that value for a certain period of time, which can be up to 24 hours. Thus, since run 5 presents a difference of densities of 16% and a gradient of 27%, it goes accordingly to what is presented in the bibliography.

One reason that might be behind these results is the fact that, whit a larger bucket diameter, the ratio between paddle size and bucket diameter is smaller, representing more space available for the mixture to disperse and for the soil particles absorb into the polymer. Thus, less soil sediments allowing the mixture's density to remain more homogeneous over time.

Hence, even though the results obtained go along with the criteria established and the concepts described in the bibliography, it is still required that the sedimentation rate does not reach a value higher than 1,7 g.h/L. This value was established as a way to guarantee minimum soil sedimentation, in order to maintain the density value in the column (between 1 and 1,06 g/cm^3) and consequently maintain the hydrostatic pressure in the column. However, run 5 presented a gradient value of 27%, a density conservation of 16% and a sedimentation rate of 1,3 g.h^{-1}. Therefore, in order to reduce the sedimentation rate and also investigate the influence of other variables in this value, other combinations of variables were studied.

4.1.2 Polymer concentration in function of pH

In this chapter protocol 3.1.2, was executed. It consisted in a series of experiments combining the polymer concentration (varying from 0 to 1 g.L^{-1}) and the pH (between 0 and 12,5) of the solutions in order to achieve a sedimentation rate less or equal to 1.7 g.h^{-1}. For the execution of this protocol it was considered a 4L mixture with a mixing time of 150min in a 280mm diameter bucket, using different concentrations of the polymer 7156 (from 0 to 1 g.L^{-1}) 400g of clay. In order to decide what run is best compared to the others, some criteria where established. The gradient value must be ≤30%, density conservation ≥ 12% and sedimentation rate value ≥ 1,7 g.h/L.

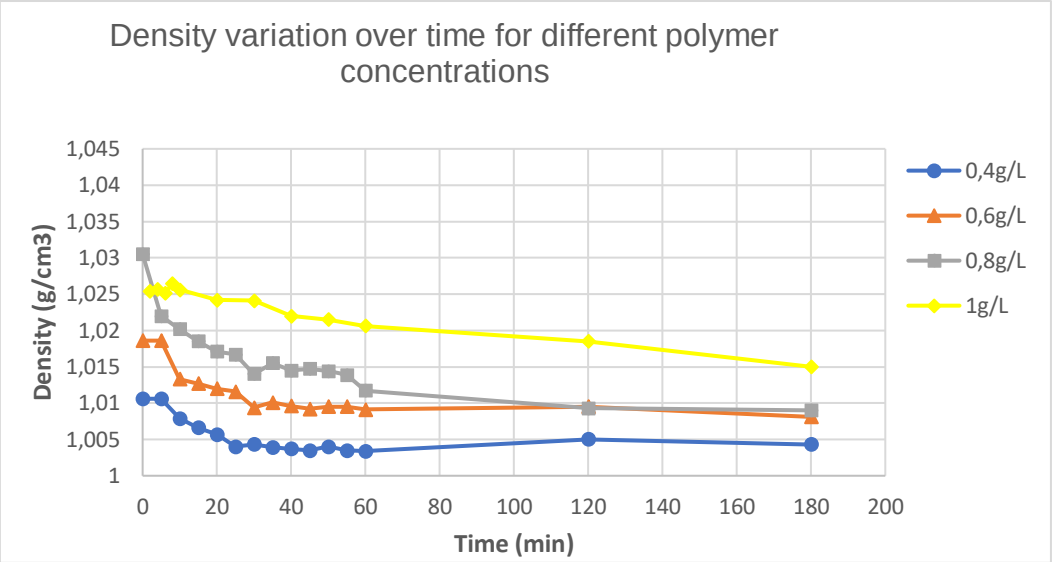

Figure 4.3- Density variation over time for different polymer concentrations considering a pH of 12,5 and a mixing time of 150 minutes.

In Figure 4.3 is represented the density tendency over time considering different polymer concentrations at 12,5 pH level.

These runs were performed to determine the best polymer concentration to use in the following experiments at different pH's. As it is represented in Figure 4.3, run 5, which was executed using 1 $g.L^{-1}$ of polymer, starts at a density value of 1,025 +/- 0,001 g/cm^3 and, passed 3h, the density registered was 1,015 +/- 0,001 g/cm^3. This value is clearly higher than the rest of the experiments since they all present a density value inferior to 1,01 g/cm^3 passed 3h. It is noticeable that the curves have a similar behaviour over time, however in run 5 the mixture is more capable of conserving its density throughout the time break considered.

However, knowing that a mixing time of 150 minutes presented the best results so far, a mixing time of 210 minutes was tested to understand its effect on the criteria established. The tendency observed so far (from chapter 3.1.1) is that the longer the mixing time is, better are the results, for this reason a mixing time of 210 minutes was tested.

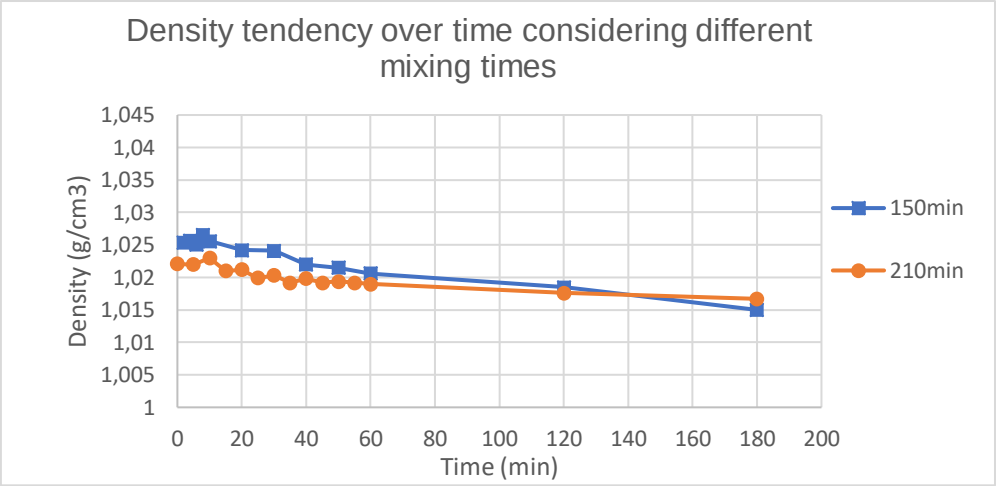

Figure 4.4- Density tendency over time considering different mixing times.

The results obtained passed 24h are represented in the following table.

Table 4.2- Density values obtained passed 24h

Run	Density (+/- 0,001 g/cm^3)	Mixing time (min)
5	1,0045	150
10	1,0053	210

As it is possible to notice from Figure 4.4 both run 5 and 10 have a very similar behaviour. However, it is visible that run 5 starts with a density value slightly superior to run 10 (1,025 +/- 0,001 g/cm^3 compared to 1,022 +/- 0,001 g/cm^3). Yet, throughout the experiment time the density values for run 10 surpasses the ones of run 5, as it represented in Table 4.2 (1,0167 +/- 0,001 g/cm^3 compared to 1,0150 +/-0,001 g/cm^3), meaning a better hold capacity and density preservation over time. To decide which of the runs provides the best results it was performed the analysis of the outputs results (gradient, density conservation and sedimentation rate) for each run.

Table 4.3- Outputs achieved in each run

Run	Mixing time (min)	Gradient (%)	Density Conservation (%)	Sedimentation rate (g.h/L)
5	150	27	16	1,33
10	210	31	31	0,7

The output values obtained, present in Table 4.3, are in agreement with the tendency observed in the graphic. It is possible to notice that run 10, executed at a 210 minute mixing time, presents a gradient and a density conservation percentage of 31% and a sedimentation rate of 0,7 g.h/L.

on the other hand, run 5, executed at a mixing time of 150 minutes, presents a gradient of 27%, a density conservation percentage of 16% and a sedimentation rate of 1,33 g.h/L. Despite the gradient value obtained in run 10 being slightly higher than the value obtained for run 5, both the density conservation value (31%) and the sedimentation rate (0,7 g.h/L) are substantially closer to the range fixed in the criteria established (maximum 1,7 $g.h^{-1}$ for sedimentation rate). As a result, a polymer concentration of 1 $g.L^{-1}$, a mixing time of 210 minutes in a bucket with 280mm diameter are the inputs with best results, presenting an initial density of 1,022 +/- 0,001 g/cm^3 and a final density, passed 24h, of 1,0053 +/- 0,001 g/cm^3. Since the experiments at different pH levels started before the test with run 10, all the runs tested in chapter 3.1.2 were conducted with a considered mixing time of 150 minutes.

The following graphic presents the results of density through time, considering different solution pH's at a polymer concentration of 1 $g.L^{-1}$.

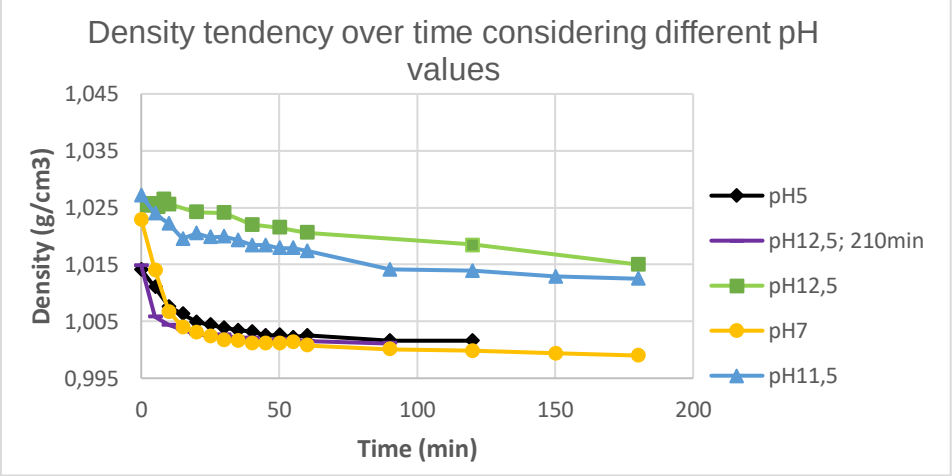

Figure 4.5-Density tendency over time considering different pH levels at a 1 $g.L^{-1}$ polymer concentration.

In figure Figure 4.5 is represented the runs tested at different pH values considering polymer 7156 at a concentration of 1 $g.L^{-1}$ and mixing time of 150 minutes. As it is visible, the runs executed at pH 12,5 and 11,5 start and end at the higher density values. For instance, at pH 12,5, the initial density value was 1,025 g/cm^3 and, passed 3h, the density value measured was 1,015 +/- 0,001 g/cm^3. For a pH of 11,5, the initial density value was 1,0271 +/- 0,001 g/cm^3 and, passed 3h, the final density value measured was 1,0125 +/- 0,001g/cm^3. At pH 7, the initial density value measured was 1,0229 +/- 0,001g/cm^3 however, passed 3h, the final density was 0,9990 +/- 0,001 g/cm^3. For pH 5, the initial density measured was 1,0141 +/- 0,001 g/cm^3 and the final density, passed 2h, was 0,9998 +/- 0,001g/cm^3. Finally, for pH 12,5 at a mixing time of 210 minutes, the initial density value measured was 1,0148 +/- 0,001g/cm^3 and a final density value 1,0011 +/- 0,001 g/cm^3. Thus, considering these results, it is noticeable that the results obtained at pH 12,5 and 11,5, for a mixing time of 150 minutes, are the ones with higher density values, 1,0254 +/-

0,001 g/cm^3 and 1,0271 +/- 0,001 g/cm^3 respectively. Despite both curves have a similar behaviour over time, tending to same value, passed 24h run 14 ends with a higher density value, as it is represented in the table below.

Table 4.4- Density values obtained passed 24h

Run	Mixing time (min)	pH	Density (+/- 0,001 g/cm^3)
5	150	12,5	1,0045
14	150	11,5	1,0056

Considering the results observed, the outputs values were analysed to identify the difference between run 5 and 14.

Table 4.5- Outputs achieved in each run

Run	pH	Gradient (%)	Density Conservation (%)	Sedimentation rate (g.h/L)
5	12,5	27	16	1,33
14	11,5	23	28	0,9

Besides, considering the outputs values obtained, displayed in Table 4.5, is distinct that run 14 provides the best results considering the criteria established initially. It has a smaller percentage for the gradient (23%), meaning a smaller difference between the density on top and on the bottom of the column, a higher value for density conservation (28%) and sedimentation rate lower than the established limit of 1,7 g.h/L (0,9 g.h/L). Therefore, this will be the pH value to consider in the next experiments.

These observations are in agreement to the bibliography which states that, with pH increase the association of particles is destroyed due to the increase in electrostatic repulsion, caused by the development of negative charges, surpassing the aggregation forces [68]. It is also reported that for some polyacrylamides a preferential pH range that does not goes above 12 [133], which justifies the values obtained when using a pH value of 12,5.

As mentioned above, the values obtained using a pH of 11,5 are due to the increase of repulsive interactions, causing dispersion to be promoted leading to a smaller sedimentation rate and a lower difference of densities along the column. However, it would be expected smaller values than those obtained with a pH of 12,5 therefore, despite the tendency, the results obtained contradict the information found in the bibliography. This may be related to the preferential pH range of the polyacrylamide. This may impose a limit of charges that make possible the electrostatic repulsion necessary to promote suspension.

Therefore, despite the achievement of some of the criteria established to understand how each variable affects the system, there is still a need to study the effect of more variables in the

sedimentation rate. With this, more information will be obtained to build a mathematical model able to predict sedimentation rates.

4.1.3 Polymer concentration in function of Soil fraction

In this chapter protocol explicit in chapter 3.1.3 was executed, performing a series of experiments combining the polymer concentration and the clay fraction in the solution in order to achieve a sedimentation rate less or equal to 1,7 g.h/L. For the execution of this protocol it was considered a 4L mixture with a mixing time of 210min in a 280mm diameter bucket, using different concentrations of 7156 and pH of 11,5, with the same criteria previously established.

At first, in order to corroborate the evidence that a clay mixing time of 210 minutes presents the best results, it was executed a test using 210 minutes of mixing time, pH 11,5, bucket diameter 280 mm and 400g of clay and it was compared with the run performed under the same conditions but with a mixing time of 150 minutes.

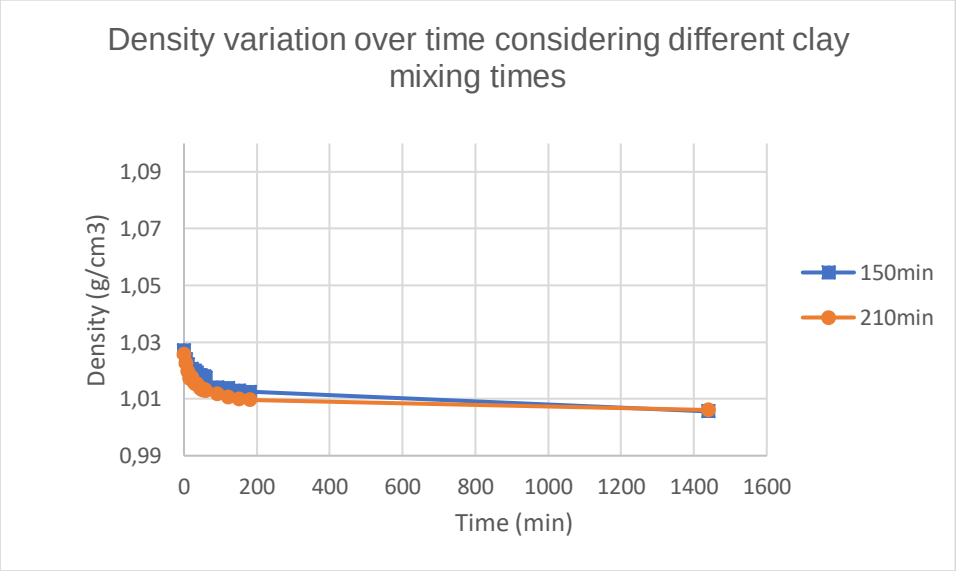

Figure 4.6- Density levels over time considering different clay mixing times.

As it is possible to notice from Figure 4.6, both curves (referring to a mixing time of 150min and 210min respectively) have a very similar behaviour (starting with an initial density of approximately 1,03 +/- 0,001 g/cm^3). However, passed 24h, the density value of the suspension obtained with a 210min mixing time is slightly superior to the one obtained with a 150 minute mixing time (1,0097 +/- 0,001 g/cm^3 and 1,0056 +/- 0,001 g/cm^3, respectively), even though it presents a more intense decrease in the density curve. Therefore, in order to accurately determine which of these runs presents the best results, it is required to analyse the outputs values obtained. The results are explicit in the table below.

Table 4.6-Outputs achieved in each run

Run	Mixing time (min)	Gradient (%)	Density Conservation (%)	Sedimentation rate (g.h/L)
14	150	23	28	0,9
20	210	14	32	0,82

Considering the outputs values obtained, represented in Table 4.6, run 20 (consisting in a mixing time of 210 minutes) has the best results since it has a lower gradient (14% comparing to 23% of run 14), a higher density conservation value (32% against 28% obtained in run14) and a lower sedimentation rate (0,82 g.h/L against 0,9 g.h/L obtained in run14). Therefore, this is the run whose characteristics will be used in the following experiments.

Once the optimum mixing time was determined, a series of experiments testing different soil concentrations were executed considering a 7156 concentration of 1 $g.L^{-1}$, pH 11,5 and a clay mixing time of 210 minutes.

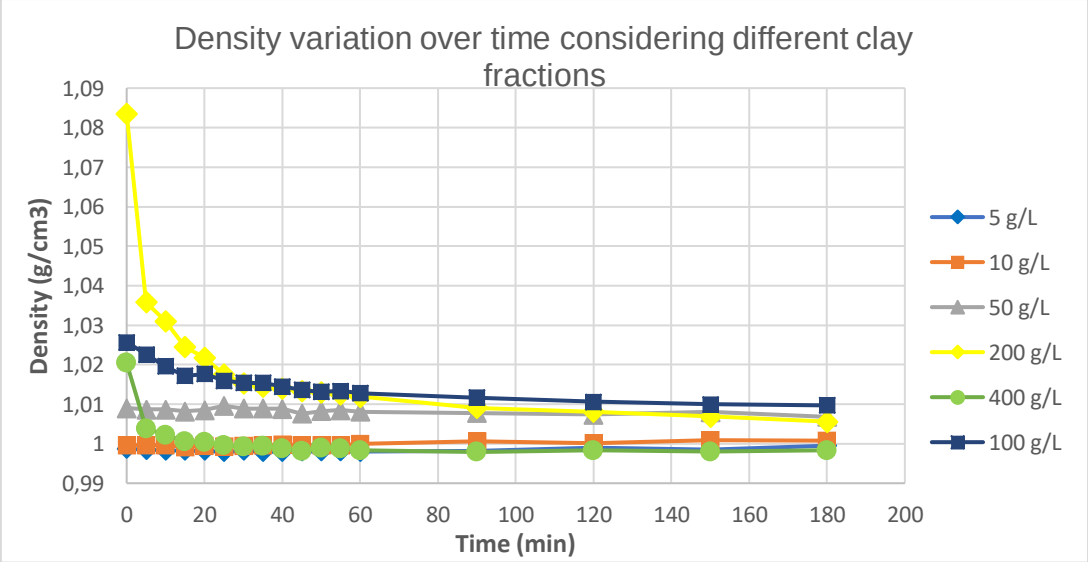

Figure 4.7- Density variation over time considering different clay fractions

As it is visible in Figure 4.7, there are different situations occurring. When using 200 $g.L^{-1}$ of clay, the initial density registered is manifestly superior (in approximately 0,055g/cm^3) to any other soil fraction. However, it experiments a sharp decrease over the 3h period studied (from 1,0800 +/- 0,001g/cm^3 to 1,0056 +/- 0,001g/cm^3). On the other hand, when considering 100 $g.L^{-1}$ of clay, the initial density value was 1,0257 +/- 0,001 g/cm^3 and, passed 3h, the final density value obtained was 1,0097 +/- 0,001 g/cm^3. For a clay concentration of 400 $g.L^{-1}$, the initial density value measured was 1,0204 +/- 0,001 g/cm^3, dropping to 0,9983 +/- 0,001 g/cm^3 passed a 3h period. For a clay concentration of 50 $g.L^{-1}$, the initial density value measured was 1,0090 +/- 0,001 g/cm^3

and, passed 3h, the density was 1,0081 +/- 0,001 g/cm^3. When testing a clay concentration of 10 g.L^{-1}, the initial density value measured was 0,9996 +/- 0,001 g/cm^3 and, passed 3h the value measured was 1,0008 +/- 0,001 g/cm^3. Finally, for a soil concentration of 5 g.L^{-1}, the initial density value measured was 0,9996 +/- 0,001 g/cm^3 and, passed a 3h period, the density value measured was 1,0008 +/- 0,001 g/cm^3.

From the graphic above it is possible to withdraw that 100 g.L^{-1} seems to be the optimum amount of clay to achieve the best density behaviour over time. It starts in a good value of initial density (1,0257 +/- 0,001g/cm^3) and maintains a relatively linear curve over time, while all the other runs experience a more significant decrease over time and/or start a much lower values of initial density. Thus, outputs values were evaluated to fully visualize the difference between each run.

Table 4.7- Outputs achieved in each run

Run	Clay fraction (g.L^{-1})	Gradient (%)	Density Conservation (%)	Sedimentation rate (g.h/L)
15	5	0	69	0,025
16	10	16	76	0
17	50	7	79	0,08
20	100	14	32	0,82
18	200	62	8	3,32
19	400	98	19	0,86

In Table 4.7 it is represented the outputs values achieved for each clay concentration. For run 15 it was observed a gradient value of 0%, a density conservation percentage of 69% and a sedimentation rate of 0,025 g.h/L. For run 16 it was obtained a gradient value of 16%, a density conservation percentage of 76% and a sedimentation rate of 0 g.h/L. For run 17 it was obtained a gradient of 7%, a density conservation percentage of 70% and a sedimentation rate of 0,08 g.h/L. For run 20, the gradient achieved was 14%, the density conservation percentage was 32% and the sedimentation rate obtained was 0,82 g.h/L. For run 18, the gradient percentage achieved was 62%, the density conservation percentage was 8% and the sedimentation rate obtained was 3,32 g.h/L. Finally, for run 19, it was achieved a gradient percentage 98%, a density conservation percentage of 19% and a sedimentation rate of 0,86 g.h/L.

From the results observed noticeable that run 20, using 100 g.L^{-1} of soil, presents output values that go according to the previously established limits that contribute to an optimum column homogeneity (with a gradient ≤ 30%) and sedimentation velocity (≤1,7 g.h/L), accordingly to the criteria previously established. It presents a 14% gradient value, 32% for density conservation

(starting with an initial density value over 1,02 +/-0,001g/cm^3) and sedimentation rate of 0,82 g.h/L.

Theoretically runs 15, 16 and 17 also presents outputs values inside the limits previously established. However, that is due to the fact that they contain such a small amount of clay (5, 10 and 50 g.L^{-1}, respectively), that 5the clay is easily completely incorporated in polymeric suspension. Despite that , not only those are not realistic clay concentration values when considering a construction environment but also, small clay concentrations translate into small initial density values (as seen in Figure 4.7), which compromises the stability of the hole.

Therefore, it is also important to analyse the viscosity variation in the solutions to understand the rheological modifications caused by the clay concentration used. The results are explicit in the following table.

Table 4.8- Runs and respective clay concentrations and initial and final Brookfield viscosity values.

Runs	**Clay concentration (g.L^{-1})**	**Brookfield viscosity $_{initial}$ (+/- 1% cP)**	**Brookfield viscosity $_{passed\ 24h}$ (+/- 1% cP)**
15	5	85,92	78,12
16	10	46,68	60,96
17	50	63,12	57,19
20	100	38,4	36,66
18	200	65,88	47,76
19	400	20,76	15,54

In Table 4.8 are represented the values of initial and final (passed 24h) Brookfield viscosity for each clay concentration tested. It is possible to notice that run 5 presented an initial viscosity of 85,92 +/- 1% cp and a final viscosity, passed 24h, of 78,12 +/- 1% cp. Run 16 presented an initial viscosity of 46,68 +/- 1% cp dropping to 60,96 +/- 1% cp passed 24h. In run 17, which considers a clay concentration of 50 g.L^{-1}, the initial viscosity measured was 63,12 cp and the final viscosity was 57,19 +/- 1%cp. For run 20, the variation was not significative, it presented an initial viscosity value of 38,4 +/- 1% cp and a final viscosity value of 36,66 +/- 1% cp. For run 18 the variation was more evident. It presented an initial viscosity value of 65,88 +/- 1% cp and a final value of 47,76 +/- 1% cp. Finally, for run 19 the initial viscosity value measured was 20,76 +/- 1% cp, and the final viscosity value was 15,54 +/- 1% cp.

According to the literature there is an optimum soil fraction to maintain and/or improve the solutions suspension capacity. In 2001, researchers developed a model for the viscosity of suspensions. According to it, at a high solid volume fraction, Φ>0,40, there is a decrease in the polymer suspensions capacity [57].

Therefore, accordingly to the experiments, a soil fraction of 100 g.L^{-1}, corresponding to a solid volume fraction of 0,1 (400g$_{clay}$/4000g$_{solution}$) is the maximum value we can have in order to achieve

and maintain a solutions suspensions capacity. Above this value there is a saturation of the solution, causing the solids to aggregate and sediment.

This may be a result of the saturation in the polymeric chain caused by the excess of soil in the mixture, which happens in runs 18 and 19 where the soil fractions are 0,2 and 0,4 respectively. As seen before, the variation of viscosity for run 18 is quite significative (from 65,88 cP to 47,76 cP passed 24h. this indicates a degradation in the polymeric chain caused by a saturation due to the excess of clay. For run 19 the initial viscosity value was already low (compared to the other runs) because the saturation of the polymeric chain happened immediately in the beginning of the process, instead of gradually.

The clay grains are composed of a series of cations (Al^{3+}, Fe^{3+}, Mg^{2+}, Fe^{2+} and Si^{4+}) that connect to the negative charges of the polyacrylamide chain. Thus, there is an interference in the PAM's rheological characteristics, causing it to experience a decrease in viscosity, leading it do degrade and lose its suspension capacity.

Therefore, despite the achievement of some of the criteria established in this chapter, there is still a need to analyse and understand how other factors and conditions affect the suspension in order to have a more diverse range of data to build the mathematical model in development in this project.

4.1.4 Comparison of different polymers

In this chapter, a series of experiments were performed, using different polymers and polymer concentration were tested in order to study their interference in the solutions density and sedimentation rate. For the execution of this protocol it was considered a 4L mixture with a mixing time of 210min in a 280mm diameter bucket, using different polymers and 100 $g.L^{-1}$ of clay, with the same criteria previously established.

The following table presents all the polymers tested as way to acess their effect in the solutions density and sedimentation rate

Table 4.9- Runs and respective polymer and polymer concentration

Run	Polymer (name)	[Polymer] ($g.L^{-1}$)
20	7156	1
21	-	0
22	9156+7156	0,5+0,5
23	9156	1
24	P400	0,5
25	P400	1
26	9698	0,245
27	9698	1

In Figure 4.8 is represented the densiy behaviour over time for the runs tested with different polymers.

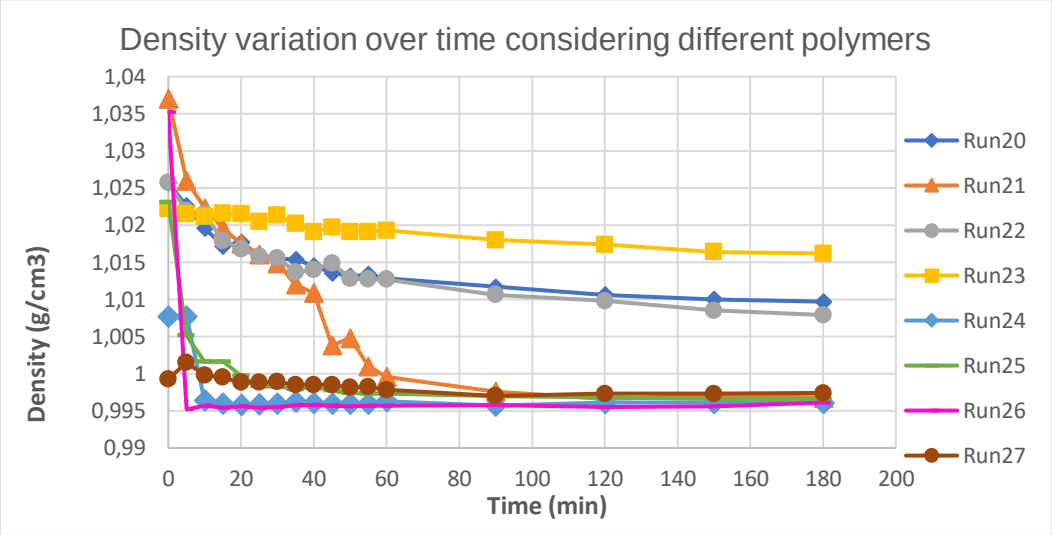

Figure 4.8- Density values over time considering different polymers

The graphic in Figure 4.8 represents the density tendency over time considering different polymers and different polymer concentrations, considering a pH of 11,5 and 100 $g.L^{-1}$ of clay. These runs were performed in order to determine the effect of polymers and polymer concentration in the suspension capacity of the solution.

As it is represented in Figure 4.8, run 23 starts a density value of 1,0231 +/- 0,001 g/cm^3, reaching a value of 1,016 +/- 0,001 g/cm3 passed the 3h period. Run 20 presents a similar behaviour starting at a density value of 1,0257 +/- 0,001 g/cm^3, however it drops to 1,0097 +/- 0,001 g/cm^3 passed 3h. Run 22 has a similar behaviour to run 20, starting at the same value, 1,0257 +/- 0,001 g/cm^3 and reaching a final density value of 1,0079 +/- 0,001 g/cm^3 passed 3h. run 21, performed with water, starts at a density value of 1,037 +/- 0,001 g/cm3 and it reaches a value of 0,9974 +/- 0,001 g/cm3 passed the 3h period. Run 26 starts with a density value of 1,0352 +/- 0,001 g/cm^3, however it suffers a deep and fast decrease through time, reaching the final density value of 0,9973 +/- 0,001 g/cm^3. Run 25 starts at a density value of 1,0220 +/- 0,001 g/cm^3 and, passed 3h the value registered was 0,9972 +/- 0,001g/cm^3. Run 24 has an initial density value of 1,0077 +/- 0,001 g/cm3 and a final density value of 0,9961 +/- 0,001 g/cm^3. Finally, run 27 presents a very linear density behaviour over time. It starts with 0,9993 +/- 0,001 g/cm^3 and, passed 3h the value measured was 0,9974 +/- 0,001 g/cm^3.

From the results observed, run 23 (performed with 9156) exhibit the best results regarding the density behaviour over time, maintaining a stable curve in the course of time (starting with a density value of 1,0231 +/- 0,001g/cm^3 and reaching a value of 1,016 g/cm^3 after 3h). The curves corresponding to runs 20 and 22 also present a similar behaviour however, passed 3h the density value measured is lower compared to run 23. On the other hand, it is also possible to notice that runs 24, 25, 26 and 27 present a much significant density decline over time compared with the

run executed just with water (run 21). This might indicate that the operational conditions used in these experiments are not the optimum for these polymers, causing them to lose density faster than expected. The polymer concentration used might also have influenced the density results, indicating that, for a pH of 11,5 and a mixing time of 210 minutes, these polymers need to be used in a higher concentration so they can have better results in conserving density over time.

The following table presents the outputs values obtained for each run.

Table 4.10- Outputs achieved in each run

Run	Polymer (name)	[Polymer] ($g.L^{-1}$)	Gradient (%)	Density Conservation (%)	Sedimentation rate (g.h/L)
21	-	0	99	1	1,7
22	9156+7156	0,5+0,5	20	26	0,88
23	9156	1	19	45	0,55
24	P400	0,5	100	11	0,48
25	P400	1	99	7	1,11
26	9698	0,245	20	1	1,62
27	9698	1	6	40	0,1

From Table 4.10, considering the limits previously established, it is noticeable that the run 23 (executed with the polymer 9156) presents the higher values for gradient (19%), density conservation (45%) and sedimentation rate (0,55 g.h/L), from all the ones tested, while the run executed with water presents the lower results comparting to the limits.

In order to fully comprehend the results obtained, it is important to analyse the characteristics of each polymer tested, as well as the rheological properties. For this reason, the following table exhibits the anionicity, molecular weight and Brookfield viscosity for each polymer.

Table 4.11- Runs and respective polymer characteristics and initial and final Brookfield viscosity value

Run	Polymer (name)	[Polymer] ($g.L^{-1}$)	Anionicity (%)	Molecular weight (MDa)	Brookfield viscosity $_{initial}$ (+/- 1% cP)	Brookfield viscosity $_{passed\ 24h}$ (+/- 1% cP)
21	-	0	-	-	2,52	1,38
22	9156+7156	0,5+0,5	30,08	15,95	42,54	38,88
23	9156	1	30	14,32	42,48	43,86
24	P400	0,5	21,2	19,2	17,76	17,04
25	P400	1	21,2	19,2	42,24	40,08
26	9698	0,245	34	31,08	6,06	5,52
27	9698	1	34	31,08	40,14	39,72

From Table 4.11 is possible to notice that the anionic polyacrylamide 9156, which presented the best results based on the previous analysis, has an anionicity of 30% and a molecular weight of 14,32 MDa. It is possible to notice that this polymer is able to maintain its viscosity practically

unaltered in a 24h period, indicating that it was able to maintain most of the material in suspension. From the literature it was observed that this anionicity value results in a high charge density in the molecule, due to the number of ionic groups. The molecular weight comes from the number of repeated group, leading to a longer molecule and therefore, a solution with higher viscosity [131]. Therefore, the results obtained with this polymer goes along with what is described in the bibliography.

Regarding runs 24, 25, 26 and 27, it is possible to notice that the polymers used in these experiments present high anionicity (21,2% for P400 and 34% for 9698) and high molecular weights (19,2 MDa for P400 and 31,08 MDa for 9698). When looking into the Brookfield viscosity values, it is clear that it remains almost unaltered through the 24h period. However, as seen before in graphic, the density value declines very expressively. This indicates that, even though these polymers are not able to retain all the material in suspension, they have the capacity to hold to a small amount for a period of 24h. Thus, the results obtained with these polymers might be due to the operational conditions, including the polymer concentration used.

Therefore, by executing these experiments, it was possible to collect data from very different scenarios and possibilities, which provide information to develop a mathematical model to predict sedimentation rates. Thus, to enrich the set of trends and information, additives were tested to evaluate their effect the soil suspension capacity.

4.1.5 Effect of the usage of additives

In this chapter, a series of experiments were performed using protocol explicit in chapter 3.1.4 where different polymers and additives were tested in order to study their influence in the solutions characteristics. For the execution of this protocol it was considered a 4L mixture with a mixing time of 210min in a 280mm diameter bucket, using different polymers and additives and 100 $g.L^{-1}$ of clay, with the same criteria previously established.

The table bellow presents the set of experiments performed and their respective conditions.

Table 4.12- Polymer and additive concentration for each run

Run	Polymer (name)	[Polymer] $g.L^{-1}$	Additive (name)	[Additive] $mL.L^{-1}$
28	PolyMud	1	Alfabond	1,4
29	PolyMud	1	HY5040	0,8
30	7156	1	Alfabond	1,4
31	7156	1	Hy5040	0,8
32	7156	1	Hy168	0,8

In Table 4.12 are represented the polymer/additives combinations testedand the respective polymer and additive concentrations.

The results obtained through this set of experiments are explicit in the figure bellow, presenting the demsity behviour over time for each combination of polymer/additive.

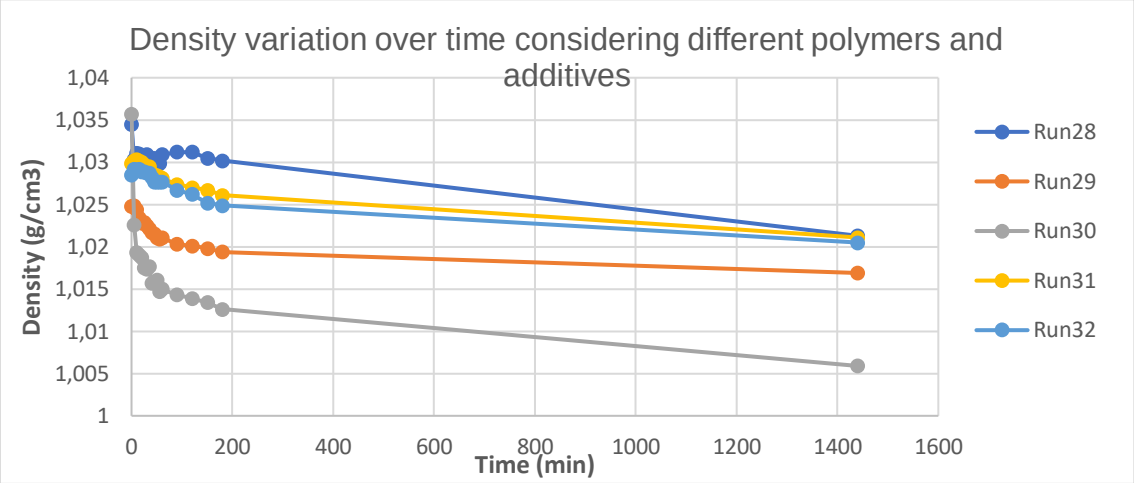

Figure 4.9- Density variation over time considering different polymers and additives

In the graphic in Figure 4.9 is represented the density behaviour of different solutions, achieved using different polymers and additives. For these experiments it was considered a polymer concentration of 1 $g.L^{-1}$, 5,6 mL of Alfabond and 3,2 mL of HY5040 and HY168.

As it noticeable, the run performed with 7156 and Alfabond, despite starting with a high-density value, experiences as accentuated decline over time. Similarly, the run using PolyMud and HY5040, even though it starts in a density value superior to 1,02 +/- 0,001 g/cm^3 also experiences a visible decline over time. On the other hand, the runs using PolyMud+Alfabond, PolyMud+HY168 and 7156+HY5040 have a similar behaviour, starting at a high-density value and conserving it over time.

Table 4.13- Outputs achieved in each run

Run	Polymer (name)	Additive (name)	Gradient (%)	Density Conservation (%)	Sedimentation rate (g.h/L)
28	PolyMud	Alfabond	43	72	0,55
29	PolyMud	HY5040	13	70	0,33
30	7156	Alfabond	31	31	1,24
31	7156	Hy5040	13	77	0,37
32	7156	Hy168	8	77	0,33

From Table 4.13 is possible to analyse the outputs values achieved for each run. As it was noticeable from Figure 4.9, run 28 (performed with PolyMud and Alfabond) presents the curve with the higher density values over time (starting at 1,0357 +/- 0,001 g/cm^3 and ending at 1,0205 +/- 0,001 g/cm^3 passed 24h) comparing to the other runs. It also presents the second higher value for density conservation (72% comparing to the 77% exhibit in runs 31 and 32) and a

sedimentation rate inferior limit to the value previously established (0,55 g.h/L comparing to 1,7 g.h/L). However, by analysing the outputs table, run 28 presents a gradient value of 43% (superior to the 30% limit established previously), which results in a significant difference between the top and the bottom of the column. Therefore, considering all the output values obtained, run 31 (executed with 7156 and HY5040) is the one with best results. It starts with a density value of 1,0302 +/- 0,001 g/cm^3 and passed 24h it had a density of 1,0205 +/- 0,001 g/cm^3. This resulted in high density conservation value (77%) which combined with a low gradient (13%) and a low sedimentation rate (0,37 g.h/L) provides us with more information to feed our mathematical model.

For the mathematical model a set of variables that condition the density values results (and as a result the sedimentation rate output) will be combined. Therefore, the results obtained when studying the variables polymer and additive concentration, pH and soil concentration provided an understanding on the trends experienced when manipulating these variables. However, all these preliminary studies were performed using one soil type (clay). Thus, it would have been important, considering the goals of this dissertation, to execute these experiments with other soil types, namely: sand and a mixture of sand and clay in different proportions.

4.2 R software modelling

Considering the tendencies observed in the previous chapters, in this chapter a set of experiments were performed to generate inputs for the R software, as specified in the protocol explained in 3.2.7. From the bibliography, a series of equations trying to describe the behaviour of a particle in a fluid were analysed. However, it was evident that it existed a gap when considering polymeric fluids and when trying to correlate that behaviour with the work field conditions. For this reason, R software was chosen to develop a new model, able to fulfil the requirements. Therefore, the first step consisted in performing a series of complementary runs with different initial conditions to feed the program. The operational conditions will be introduced in the following chapters. With the program, equations for initial and final density will be calculated. Through these two equations it will be obtained the expression to calculate the sedimentation rate. In order to achieve the highest accuracy possible, the model obtained is considered valid once the error for the sedimentation rate is ≤15%. Once that limit is achieved with a group of defined variables, another variable is added to obtain a final model with all the variables considered included. The errors for the initial density (Di), the final density (Df) and the sedimentation rate (Sed. rate) are calculated as shown:

Equation 4.4- Equation to calculate sedimentation rate in g.h/L

$$Sed.\,Rate_{Calculated/Experimental}(g.h/L) = \frac{|Di - Df|g/cm^3}{24h} * 1000\frac{cm^3}{L}$$

Equation 4.5- Sedimentation rate error

$$\%error\ Sed.Rate = \frac{|Sed.Rate\ Calculated\ value - Sed.Rate\ Experimental\ value|}{1} * 100\%$$

Equation 4.6- Initial density error

$$\%error\ Di = \frac{|Di_{calculated} - Di_{experimental}|}{0{,}025} * 100\%$$

Equation 4.7- Final density error

$$\%error\ Df \frac{|Df_{calculated} - Df_{experimental}|}{0{,}005} * 100\%$$

The coefficients 1 g.h/L, 0,025 g/cm^3 and 0,005 g/cm^3, for Sed.Rate, Di and Df, respectively, were assumed since they represent plausible values to calculate the errors.

Thus, the first step consisted in correlating polymer concentration in function of the solutions pH.

4.2.1 Polymer concentration and pH

The first stage of the strategy consisted in correlating polymer concentration and solution pH. Thus, tests were performed using polymer concentrations of 0, 0.4, 0.6, 0.8 and 1 g.L^{-1}, and pH values of 5, 7, 10, 11.5 and 12.5. Meanwhile, the soil concentration was maintained constant (100 g.L^{-1}), as well as polymer used (7156) and the mixing time (150min). All the data obtained can be seen in Appendix A, B, C and D.

For the data base, values of initial and final density were introduced as well as the correspondent values of polymer concentration and pH. In chapter 3.1.2 the effect of polymer concentration and pH in a solution's suspension capacity was studied. Thus, now a mathematical correlation will be obtained. Since, in this stage, the variables studied are polymer concentration and pH, the equations built will be in function of initial and final density since these are the variables that directly affect the average sedimentation rate. The data base is represented as follow:

Table 4.14- Database introduced in R software including run, polymer concentration, pH, initial and final densities measured

Run	[polymer] (g.L^{-1})	Initial pH	Di (+/- 0,001 g/cm^3)	Df (+/- 0,001 g/cm^3)
11	1	5,43	1,0141	1,0013
13	1	7	1,0229	0,9995
12	1	9,5	1,0148	1,0008
14	1	11,5	1,0271	1,0056
5	1	12,12	1,0365	1,0045
37	0,8	7	1,0036	0,9962
33	0,8	11,5	1,0297	1,0022

9	0,8	12,12	1,0305	1,0035
35	0,6	10	1,025	0,9976
8	0,6	12,12	1,0186	1,0034
58	0,5	5	0,998	0,9968
57	0,5	7	1,004	0,9966
59	0,5	11,5	1,0387	0,9973
36	0,4	7	1,0375	0,9973
38	0	5	1,038	0,9954
56	0	7	1,0413	0,9964
34	0	11,5	1,0514	0,9964

After introducing the data base into the R software, a series of equations were tested to find the one that best correlates the data introduced and provides the best approximations.

Table 4.15- Equations tested written in extend considering polymer concentration and pH

Equation Nr.	Equation
1	$Density = A + B * ([Polymer] + 1)^2 + C * ([Polymer] + 1) + D * pH$
2	$Density = A + B * ([Polymer] + 1)^2 + C * ([Polymer] + 1) + D * pH^2 + E * pH$
3	$Density = A + B * ([Polymer] + 1) + C * pH$
4	$Density = A + B * \ln([Polymer] + 1) + C * \ln(pH)$
5	$Density = A + B * log10([Polymer] + 1) + C * log10(pH)$

After testing all the equations expressed in Table 4.15 to achieve the calculated values for initial and final density, it was used Equation 4.1 to obtain the sedimentation rate values. After obtaining the values for initial density, final density and sedimentation rate, the respective errors were calculated through equations Equation 4.6, Equation 4.7 and Equation 4.5, respectively. Thus, the results obtained are expressed in the following table:

Table 4.16- Error percentages for initial density, final density and sedimentation rate

%error Di	%error Df	%error Sed.Rate
20,60	12,3	16

In Table 4.16 is represented the errors percentages obtained for Di, Df and Sed.Rate when applying equation number 2. As it is noticeable, the sedimentation rate error obtained is superior to the maximum limit established (15%) therefore, optimizations and data analysis were required in order to lower this percentage.

Thus, the first optimization alteration performed was using minute 5 after ending agitation as the initial density value. This hypothesis came from the fact that, when using the initial density value at minute 0, it is expected to achieve a non-accurate value due to measurements errors or a momentaneous dispersion of the medium resulting only from, agitation. When scaling up to a context of construction, not only using 0 or 5 minutes is not relevant, as it is not of interest that the initial density value is high if it suffers a decrease close to the value of water density passed such a short period of time.

In the following table there is a comparison between the average errors obtained when using the initial density value at minutes 0 and 5 after stopping the agitation.

Table 4.17-Errors comparison between minutes 0 and 5 after stopping agitation

Time after agitation (min)	**%error Di**	**%error Df**	**%error Sed.Rate**
0	20,60	12,3	16
5	15,7	12,3	15

From Table 4.17 it is possible to notice that at minute 0, the error for the initial value obtained was 20,6%, the error for final density was 12,3% and error for the sedimentation rate was 16%. On the other hand, when considering 5 minutes after agitation, the error for the initial density value was 15,7%, the error for final density value was 12,3% and the error for the sedimentation rate was 15%. As it is evident, when considering minute 0, the errors are higher when comparing to minute 5 for all the outputs obtained.

Thus, is possible to notice the improvement caused by this alteration in the initial density. For this reason, the initial density value considered to introduce in the program, is the value obtained at minute 5 after stopping agitation.

An additional optimization was required, causing to rearrange the polymer concentration scale so the software could give the necessary emphasis to this variable. When the program had to consider a polymer concentration of 0 $g.L^{-1}$ for the calculations, it was not possible to obtain results when using equations such as logarithmic and exponential. Therefore, in the equation, the polymer factor will be represented as [Polymer]+1.

Thus, considering all these criteria, the protocol present in chapter 3.2.7 was used to calculate a series of equations to be tested to achieve a mathematical model. These equations are represented in the table below:

Table 4.18- Errors and standard deviation of Di, Df and Sed.Rate for each equation tested considering polymer concentration and pH

Equation Nr.	Type of eq. for [Polymer]	Type of eq. for pH	%error Di	%Std. deviation Di	%error Df	%Std. deviation Df
1	Quad.	Linear	28,9	33	23,8	15
2	Quad.	Quad.	15,7	35	12,3	12
3	Linear	Linear	34,8	36	25,4	15
4	Ln	Ln	34,7	36	25,4	16
5	Log10	Log10	34,7	36	25,4	16

From Table 4.18 it is possible to notice that equation 1 presents an error percentage for initial density of 28,9% and an error percentage for final density of 23,8%. For equation 2, it was achieved an error for initial density of 15,7% and an error for final density of 12,3%. Equations 3, 4 and 5 have similar results presenting an error percentage for initial denisty of 34,8% and an error percentage forr final density of 25,4%. Thus, considering all these values, it is noticeable that equation 2, where both polymer concentration and pH are represented by a quadratic expression, is the one that presents lower error percentages for initial and final densities (15,7% and 12,3% respectively). Equation 1, where polymer concentration as a quadratic expression and pH a linear expression, has the second lower error percentages for initial and final densities (28,9% and 23,8%, respectively). This indicates that the quadratic expression is the one that best describes the behaviour of these variables and their influence in the initial and final density.

From the values of initial and final density previously calculated through the equations obtained, the sedimentation rate value will be calculated accordingly to Equation 4.4 and the sedimentation rate error will be calculated accordingly to Equation 4.5. Thus, it will be possible to corroborate and validate the set of equations selected, considering the maximum value established for the sedimentation rate error as 15%.

Table 4.19- Sedimentation rate error and standard deviation for each combination of equation

Equation	Type of eq. for [Polymer]	Type of eq. for pH	%Sed. Rate error	% Std. Deviation Sed. rate error
Di=A+B*([Polymer]+1)^2+C*([Polymer]+1)+D*pH^2+E*pH	Quad	Quad	15	32
Df=A+B*([Polymer]+1)^2+C*([Polymer]+1)+D*pH^2+E*pH	Quad	Quad		
Di=A+B*([Polymer]+1)^2+C*([Polymer]+1)+D*pH^2+E*pH	Quad	Quad	16	31
Df=A+B*([Polymer]+1)^2+C*([Polymer]+1)+D*pH	Quad	Linear		

From Table 4.19, it is noticeable that the selected combination of equations (equation number 2 for Di and Df) presents a sedimentation rate error of 15%. Therefore, it complies with the standard previously established, which was an average error percentage for the sedimentation rate ≤15%.

Therefore, the selected equations to correlate the effect of polymer concentration and solution pH are represented bellow:

$$Density_i = 1{,}0619 + 0{,}0184 * ([Polymer] + 1)^2 - 0{,}0423 * ([Polymer] + 1) + 0{,}0008 * pH^2 - 0{,}0124 * pH$$

Equation 4.8- Equation for initial density regarding a quadratic expression for polymer concentration and pH

$$Density_f = 1{,}0090 + 0{,}0042 * ([Polymer] + 1)^2 - 0{,}0069 * ([Polymer] + 1) + 0{,}0002 * pH^2 - 0{,}0032 * pH$$

Equation 4.9- Equation for final density regarding a quadratic expression for [polymer] and pH

In order to visualize the effect of the error percentages obtained for each of the outputs, graphics comparing the experimental values and the calculated values were designed. The following graphic presents this comparison for the initial density values.

Table 4.20- Runs and respective [polymer] and pH

Run	**11**	**13**	**12**	**14**	**5**	**37**	**33**	**9**	**35**
[Polymer]	1	1	1	1	1	0,8	0,8	0,8	0,6
pH	5	7	10	11,5	12,5	7	11,5	12,5	10

Run	**8**	**58**	**57**	**36**	**7**	**38**	**56**	**34**
[Polymer]	0,6	0,5	0,5	0,4	0,4	0	0	0
pH	12,5	5	7	7	12,5	5	7	11,5

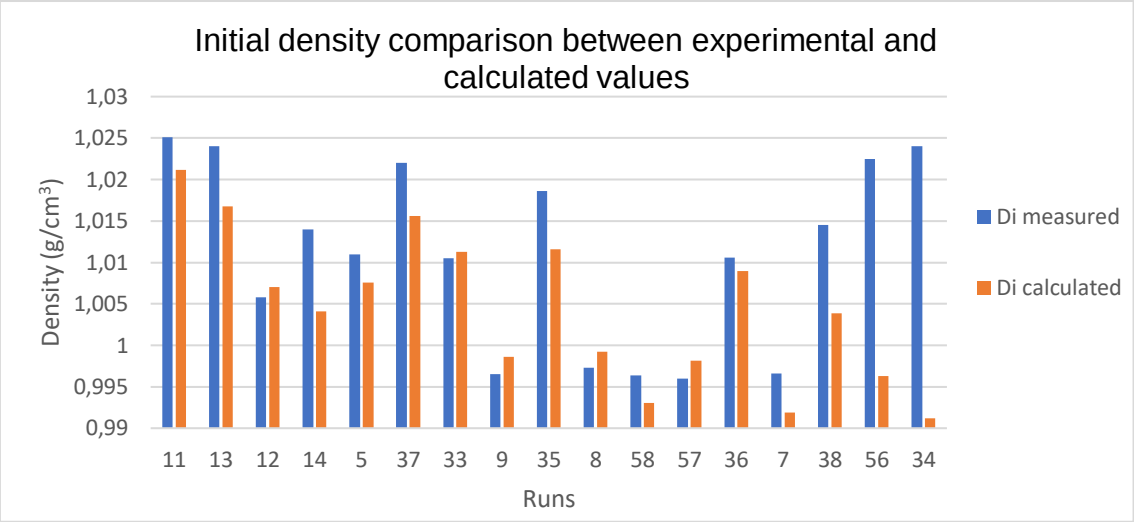

Figure 4.10- Comparison between experimental and calculated initial density regarding polymer concentration and pH.

In Figure 4.10 is represented the comparison between the initial density values obtained experimentally and the initial density values obtained through Equation 4.8.

As it is explicit in the figure, in a general way, the experimental values and the calculated values are quite approximated. For instance, for runs 12, 33 and 36 the difference between the experimental and the calculated are minimal, consisting in an initial density error of 5%, 3% and 7%, respectively. On the other hand, runs 56 and 34, present a very explicit difference between the experimental and the calculated, consisting in an initial density error 104,9% and 131,3% respectively.

Thus, the fit obtained through the Equation 4.8 is accurate, allowing to achieve values close to those obtained experimentally. This proves that a quadratic expression is the one that best defines the variables [polymer] and pH. However, the last runs, that correspond to the experiments conducted at polymer concentration 0 $g.l^{-1}$, present an average discrepancy between the measured and the calculated values of approximately 100%. This discrepancy results in a high error for the initial density, corresponding to 42,6%, 104,9% and 131,3% for the runs 38, 56 and 34, respectively. On the other hand, if these values are not considered, the average error for initial density obtained is 13,6%. Thus, the negative impact of these experiments in the general fit of the model becomes evident.

The difference obtained in runs 15, 16 and 17 is due to the fact that at 0 $g.L^{-1}$ the rheological characteristics of the suspension is very different from when there is polymer in the suspension. The following table makes that difference evident.

Table 4.21- Difference in Brookfield viscosity between suspensions with polymer and without polymer, in different pH's

Runs	[polymer] ($g.L^{-1}$)	pH	Brookfield viscosity (+/- 1% cP)
11	1	5	36,78

13	1	7	53,28
12	1	10	32,88
38	0	5	0,80
56	0	7	1,92
34	0	11,5	0,70

In Table 4.21 is represented the difference in Brookfield viscosity between suspensions with 1 $g.L^{-1}$ of polymer and suspensions without polymer. As it evident in the table, the runs composed of only water present very low viscosities (0,8 +/- 1% cP, 1,92 +/- 1% cP and 0,7 +/- 1% cP for runs 38, 56 and 34 respectively) when comparing with the experiments performed with a polymer concentration of 1 $g.L^{-1}$ (36,78 +/- 1% cP, 53,28 +/- 1% cP and 32,88 +/- 1% cP for runs 11, 13 and 12 respectively).

Thus, for the last 3 runs (38, 56 and 34), since the medium is only composed of water, there is no resistance to the movement of the soil particles, considering that the medium presents a low viscosity. However, this also implicates that after the agitation ends, all this solid in suspension will immediately begin to sediment. As seen in the state-of-the-art research, physical dispersive methods such as agitation are reversible [33] therefore, if the medium does not have suspension capacity, all the solids will begin to sediment. Therefore, in this set of experiments there are two different types of fluids composing the medium: a Newtonian fluid (water) and a non-Newtonian fluid (polymer). The first one, due to its low viscosity, does not have suspension capacity, while the second is able to maintain solids in suspension.

Therefore, even though the equation is generally able to predict the tendency of the density loss behaviour, it presents some difficulty in predicting the density value accurately when considering Newtonian fluids.

Regarding the final density, the following graphic presents the comparison between the experimental and the calculated values for final density.

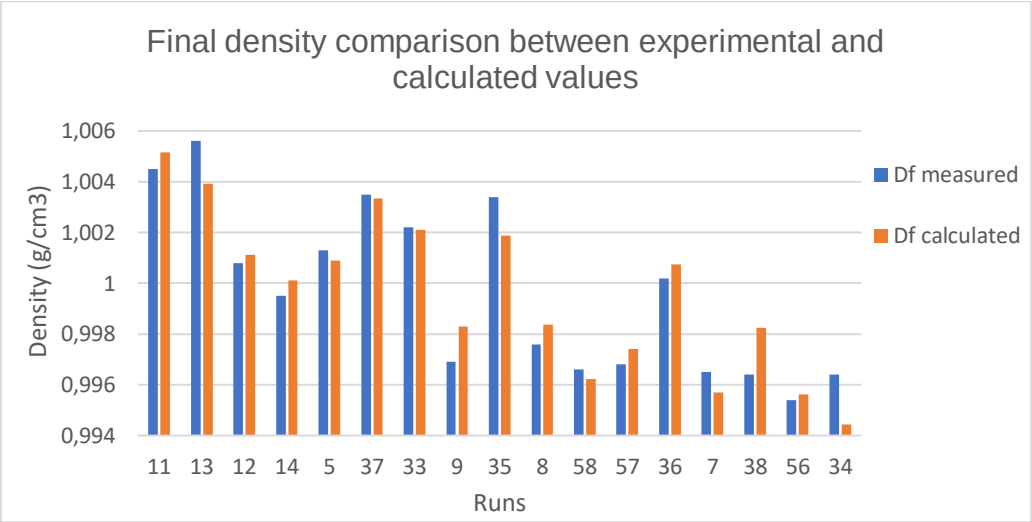

Figure 4.11- Comparison between experimental and calculated values of final density regarding polymer concentration and pH

Figure 4.11 represents a comparison between the final density values measured experimentally and the final density values obtained through Equation 4.9.

As it is explicit in the graphic, in a general way the values obtained experimentally are approximate to the values obtained through Equation 4.9. For instance, runs 5, 37 and 33 present the lower error percentages (8,19%, 3,17% and 1,68% respectively). On the other hand, the higher error percentage is 39%, obtained with run 34. This run corresponds to an experiment performed with a polymer concentration of 0 $g.L^{-1}$ and pH 7.

Comparing with Figure 4.10, corresponding to the initial density values, the fit here is more accurate (average error for Di- 15,7%, average error for Df- 12,3%). However, the major differences observed between the experimental and the calculated values occur (similarly to the initial density analysis) when there is no polymer in the medium. This corroborates the hypothesis that the model is trying to fit the equations to two different fluid types. Since the majority of the data corresponds to a non-Newtonian regiment, the runs corresponding to Newtonian fluids are not predicted with the same accuracy. Thus, these runs are acting toward increasing the average error percentage.

Despite that, the fit obtained through the Equation 4.9 is very accurate and close to the values obtained experimentally, with an average error of 12,3%, proving that a quadratic expression is the one that best defines these variables.

Sedimentation rate values result from a combination of initial and final density values and the validation of the model depends on the average error percentage obtained. The following graphic presents the comparison between the experimental and the calculated values for the sedimentation rate.

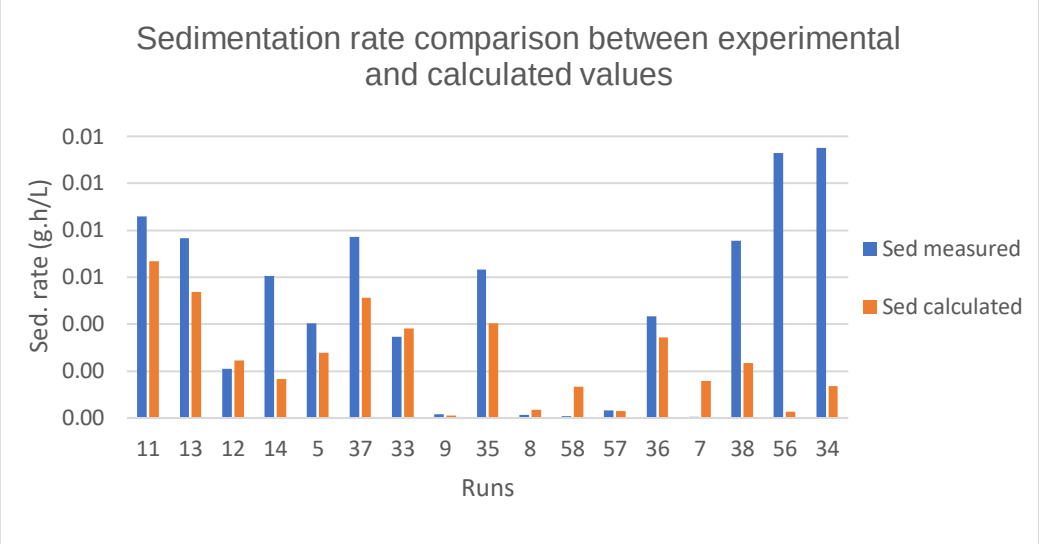

Figure 4.12- Comparison between experimental and calculated values for sedimentation rate regarding polymer concentration and pH.

Figure 4.12 represents a comparison between the sedimentation rate obtained experimentally and the sedimentation rate obtained through the calculated values of initial and final density.

As it is explicit in the graphic (and as it occurred for the initial and final density graphics), in a general way the values obtained experimentally are approximate to the values obtained through Equation 4.4. For instance, runs 12, 33 and 57 present the lower error percentages (4%, 3% and 0,4% respectively). On the other hand, runs 38, 56 and 34 present the higher error percentages (52%, 110% and 101%, respectively).

The tendency seen in the graphic goes along with what was expected considering that the sedimentation rate results from a combination of initial and final density. Therefore, as it was expected, Figure 4.12 reflects the trends observed in Figure 4.10 and Figure 4.11.

As presented in Figure 4.10, the runs with the highest error percentages correspond to the experiments performed with a polymer concentration of 0 g.L-1, exposing the limitations of the model when it comes to predict the behaviour of Newtonian fluids. However, when the suspension contains polymer in it the model obtained provides an accurate fit.

Therefore, it was already achieved an equation able to predict the sedimentation rate for a period of 24h considering 100 $g.L^{-1}$ of soil for the polymer 7156 (with an anionicity of 34% and molecular weight 13,39MDa), with a concentration between 0,4 and 1 $g.L^{-1}$, considering 1h30min of mixing time.

The equation is represented bellow:

Equation 4.10- Sed.Rate regarding polymer concentration and pH, for 100g.L-1 of soil and using the polymer 7156

$$Sed.Rate_{g.h/l} = \frac{Equation\ 4.8 - Equation\ 4.9}{24h} * 1000 \frac{cm^3}{L}$$

In conclusion, even though it was achieved an average sedimentation rate error <15%, as it was established in the beginning of this chapter, some optimizations could be conducted in order to lower the average sedimentation rate error value obtained. For instance, as seen before, the main differences observed between the measured and the calculated values occur when there is no polymer in the mixture. Thus, since the rheology of the suspension is very different accordingly to the presence or absence of polymer, a possible option could pass by developing different equations accordingly to the fluid type and nature. By doing this, the equations selected would properly define non-Newtonian fluids (polymeric suspensions) and new set of equation would be developed to better define Newtonian fluids (such as water).

It is important to notice that not all the subjects presented in the goals were approached. The model here obtained addresses a pH range between 5 and 12,5, using a fixed quantity of clay and considering a polymer (34% anionicity and 13,39 MDa molecular weight) with a concentration range between 0 and 1 $g.L^{-1}$. Therefore, it is still required to address a polymer and additive combination, as well as other soil types and quantities.

In conclusion, since there is a gap between the goal of the project and the model here obtained, the next step will consist in varying the clay concentration used.

4.2.2 Polymer concentration, pH and Soil concentration

Since a satisfactory equation was obtained considering the two variables polymer concentration and pH, the following step consists in adding one more factor. Thus, besides polymer concentration and solution pH the equation must consider the soil concentration present as well in the solution.

Besides being one of the goal variables, this is a very important factor to consider since it is directly influencing the values for initial and final density. As seen before in chapter 3.1.3 the tendency is the higher the soil concentration, the higher is the sedimentation rate. However, there are soil concentrations that provide a good correlation between Initial density value, density conservation and sedimentation rate. Thus, this variable had to be studied in more depth and correlated with the other goal variables.

For this, extra runs were performed using polymer concentrations of 0; 0,5 and 1 $g.L^{-1}$, pH of 5; 7 and 11,5 and soil concentrations of 25 $g.L^{-1}$, 100 $g.L^{-1}$ and 200 $g.L^{-1}$. The following table presents the results obtained for each equation tested. The equations built will be the initial and the final density in function of these variable. The equations tested are represented in the table below.

Table 4.22- Equations written in extend considering polymer concentration, pH and soil concentration

Equation Nr.	Equation
1	$Density = A + B * ([Polymer] + 1)^2 + C * ([Polymer] + 1) + D * pH^2 + E * pH + F * log10([Soil] * 4)$
2	$Density = A + B * ([Polymer] + 1)^2 + C * ([Polymer] + 1) + D * pH^2 + E * pH + F * (4 * [Soil]^2) + G * ([Soil] * 4)$
3	$Density = A + B * ([Polymer] + 1)^2 + C * ([Polymer] + 1) + D * pH^2 + E * pH + F * (4 * [Soil])$
4	$Density = A + B * ([Polymer] + 1)^2 + C * ([Polymer] + 1) + D * (pH) + E * log10([Soil] * 4)$
5	$Density = A + B * ([Polymer] + 1)^2 + C * ([Polymer] + 1) + D * pH + E * (4 * [Soil]^2) + F * (4 * [Soil])$
6	$Density = A + B * ([Polymer] + 1)^2 + C * ([Polymer] + 1) + D * (pH) + E * ([Soil] * 4)$

Table 4.23- Errors and standart deviation for Di, Df and Sed.Rate for each equation tested

Equation Nr.	Type of eq. for Polymer	Type of eq. for pH	Type of eq. for Soil	% error Di	%Std. deviation Di	% error Df	%Std. deviation Df
1	Quad	Quad	Log10	25	38	27902	33516
2	Quad	Quad	Quad	570822	921279	246083	4256662
3	Quad	Quad	Linear	57950	38724	30098	28046
4	Quad	Linear	Log10	43	57	22	21
5	Quad	Linear	Quad	564857	921190	2476064	4256537
6	Quad	Linear	Linear	51986	36524	29213	27961

From Table 4.23 is possible to notice that equation 1 presents an error percentage for initial density of 25% and an error percentage for final density of 27902%. For equation 4 it was achieved an error percentage for initial density of 43% and an error percentage for final density of 22%. Equations 2, 3, 5 and 6 have similar results presenting an error for initial density >50000% and an error for final density >29000%. Thus, considering all these values, it is possible to notice that equation 1, where [polymer] and pH have a quadratic expression and soil concentration has a logarithmic expression, is the one that presents the lowest error percentage for initial density (25%). On the other hand, equation 4, where polymer concentration has a quadratic expression, pH a linear expression and soil concentration a logarithmic expression, is the one that presents the lowest error percentage for final density (22%) and the second lowest error percentage for initial density (43%). This indicates that two different equations will be required to build the model

considering soil concentration. Equations 1 and 4 (present in Table 4.22) will be selected to define initial and final density, respectively.

From the values of initial and final density previously calculated through the equations obtained, the sedimentation rate value will be calculated accordingly to Equation 4.4 and the sedimentation rate error will be calculated accordingly to Equation 4.5. Thus, it will be possible to corroborate and validate the set of equations selected, considering the maximum value established for the sedimentation rate error as 15%.

Table 4.24- Sedimentation rate error and standard deviation

Equation Nr.	Type of eq. for [Polymer]	Type of eq. for pH	Type of eq. for [soil]	% error Sed	%Std. devition error Sed
1	Quad	Quad	log10	29	38
4	Quad	Linear	log10		

Considering that when using equations 1 and 4 for Di and Df, respectively, the values for initial density error percentage was 25%, and for final density it was 22%, from Table 4.24 it is possible to notice that the selected equation present a sedimentation error of 29%, therefore far superior to the maximum established limit of 15%. For this reason, it was necessary to look closely at the data to identify the cause of these high percentage errors.

In order to visualize the effect of the error percentages obtained for each of the outputs, graphics comparing the experimental values and the calculated values were designed. The following graphic presents this comparison for the initial density values.

Table 4.25- Runs and respective soil concentration ($g.L^{-1}$), pH and polymer concentration ($g.L^{-1}$)

Run	39	40	41	44	43	42	45	46	47	38	58	56	57
[Soil]	25	25	25	25	25	25	25	25	25	100	100	100	100
pH	5	5	5	7	7	7	11,5	11,5	11,5	5	5	7	7
[Polymer]	0	0,5	1	0	0,5	1	0	0,5	1	0	0,5	0	0,5

Run	13	34	59	14	5	12	11	9	33	37	8
[Soil]	100	100	100	100	100	100	100	100	100	100	100
pH	7	11,5	11,5	11,5	12,12	9,5	5,43	12,12	11,5	7	12,12
[Polymer]	1	0	0,5	1	1	1	1	0,8	0,8	0,8	0,6

Run	35	7	36	48	49	50	51	52	53	54	55	60
[Soil]	100	100	100	200	200	200	200	200	200	200	200	200
pH	10	12,12	7	5	5	5	7	7	7	11,5	11,5	11,5
[Polymer]	0,6	0,4	0,4	0	0,5	1	0	0,5	1	0	0,5	1

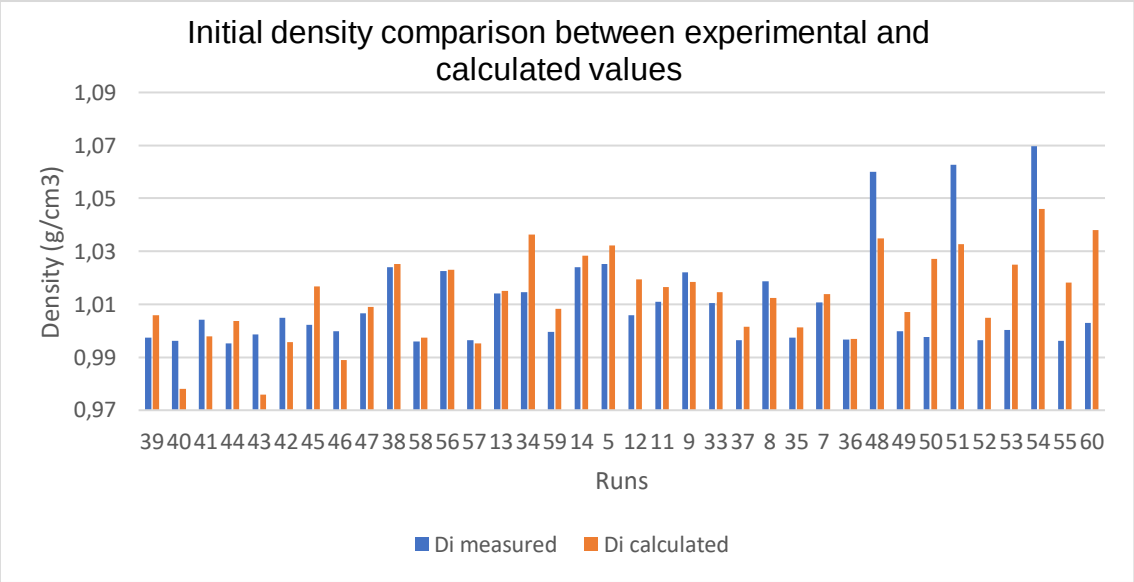

Figure 4.13- Comparison between experimental and calculated values of initial density regarding polymer concentration, pH and soil concentration.

In Figure 4.13 is represented the comparison between the initial density values obtained experimentally and the initial density values obtained through equation number 1 considering the variables soil concentration, pH and polymer concentration.

As it is explicit in the figure, in a general way, the experimental values and the calculated values are quite approximated. For instance, for runs 58, 56 and 57, the difference between the experimental and the calculated values are minimal, consisting in an initial density error of 5,5%, 2,3% and 4,8%, respectively. On the other hand, runs 55, 51, 54 and 60 present a more explicit difference between the experimental and calculated values, consisting in an initial density error of 113%, 122%, 105% and 130%, respectively.

Thus, despite some differences observed, equation 1 allows achieving close values to those obtained experimentally. This indicates that the quadratic expression is the one that best describes the variables polymer concentration and pH, and the logarithmic expression is the one that best describes the variable soil concentration. However, in the last runs, that correspond to the experiments conducted at a soil concentration of 200 g.L-1, present a more significant discrepancy, consisting in an average error of 96%. Thus, it becomes evident the difficulty of the model in predicting accurately the results obtained using this soil concentration.

In order to proper understand what might be causing these results, a rheological is required thus, the following table presents the Brookfield and Marsh viscosity values registered before and after the addition of clay to the polymeric suspension.

Table 4.26- Differences in Marsh and Brookfield viscosity before and after the addition of 200g.L-1 of clay for runs 5, 9, 53, 55, and 60

		Before Clay		After Clay	
Runs	**[Polymer] ($g.L^{-1}$)**	**Marsh Viscosity (+/- 2 s/quart)**	**Brookfield Viscosity (+/- 1% cP)**	**Marsh Viscosity (+/- 2 s/quart)**	**Brookfield Viscosity (+/- 1% cP)**
53	1	114	1166	51	13,86
55	0,5	51	21,36	49	10,08
60	1	84	81,36	79	31,32
9	0,8	61,56	31,44	56,69	32
5	1	82	33,84	65	63,24

From Table 4.26 is possible to notice the difference in Marsh and Brookfield viscosity before and after the addition of 200 $g.L^{-1}$ of clay (for runs 53, 55 and 60) and 100 $g.L^{-1}$ of clay (for runs 5 and 9). For runs 53, 55 and 60 it is evident that both Marsh and Brookfield viscosity suffer a decrease once clay in added. For instance, for run 53, before adding clay, the Marsh viscosity registered was 114 +/- 2 s/quart and the Brookfield viscosity was 1166 +/- 1% cP. On the other hand, after adding 200 $g.L^{-1}$ the value registered for Marsh viscosity was 51 s/quart and for Brookfield viscosity it was 13,86 +/- 1% cP. Therefore, there is a significant viscosity loss, resulting in a decrease of the polymer's capacity of maintaining the soil in suspension. On the other hand, for the runs executed with a soil concentration of 100 $g.L^{-1}$, regarding to Brookfield viscosity, there is an increase in the viscosity value after adding clay this indicates that the polymer was able to incorporate and suspend, at least, part of the soil added. The difference observed in Marsh viscosity is not significant.

The difference obtained in the final runs might be due to the fact that, when there is a high solid fraction in the polymeric suspension, a saturation of the polymeric chain occurs leading the fluid to suffer a decrease in viscosity, resulting in a fluid with similar properties as a Newtonian fluid. Thus, its ability to maintain the particles in suspension decreases as well. However, because the software is only able to evaluate and make predictions based on tendencies, it does not consider this effect in this soil concentration, since it is not able to predict the behaviour of Newtonian fluids. Therefore, the values obtained mathematically are generally superior to those obtained experimentally. In the following table are represented the viscosity values obtained before and after the addition of clay for some runs.

Therefore, even though the equation is generally able to predict the tendency of the density loss behaviour, it presents some difficulty in predicting the density value accurately when considering higher soil concentration.

Regarding the final density, the following graphic presents the comparison between the experimental and the calculated values for final density.

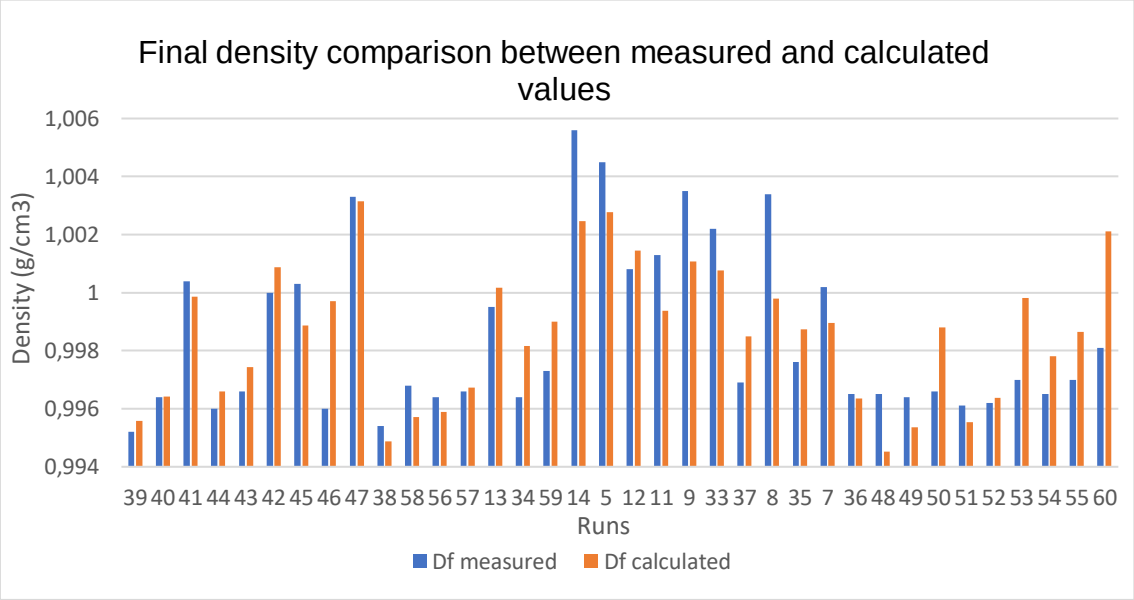

Figure 4.14- Comparison between measured and calculated values of final density regarding polymer concentration, pH and soil concentration.

Figure 4.14 represents a comparison between the final density values measured experimentally and the final density values obtained through equation 4.

As it is explicit in the graphic, in a general way the values obtained experimentally are quite approximated to the values obtained mathematically. For instance, runs 47, 57 and 36 present the lower error percentages (2,8%, 2,5% and 2,9%, respectively). On the other hand, runs 48, 53 and 60 present the higher error percentages (40%, 56% and 80%, respectively). These last runs correspond to the experiments executed with a soil concentration of 200 $g.L^{-1}$.

Comparing with Figure 4.13, corresponding to the initial density values, the major differences observed between the experimental and he calculated values, occur when the soil concentration of 200 $g.L^{-1}$. This corroborates the hypothesis that the model does not have the accuracy to predict the density loss behaviour precisely when a change in the fluid's nature occurs (passing from non-Newtonian to Newtonian). Thus, these runs are acting toward increasing the average error percentage of the model.

Despite that, the fit obtained with equation 4 (represented in Table 4.22) is generally accurate indicating that and close to the values obtained experimentally. This indicates that an equation with a quadratic expression for polymer concentration, linear expression for pH and logarithmic expression for soil concentration is the one that best describes these variables.

Sedimentation rate values resulting from a combination of initial and final density values was obtained. As seen in Table 4.24, it was obtained an average error percentage of 29%, therefore the model cannot be accepted. The following graphic exhibits a comparison between the experimental and the calculated values for sedimentation rate.

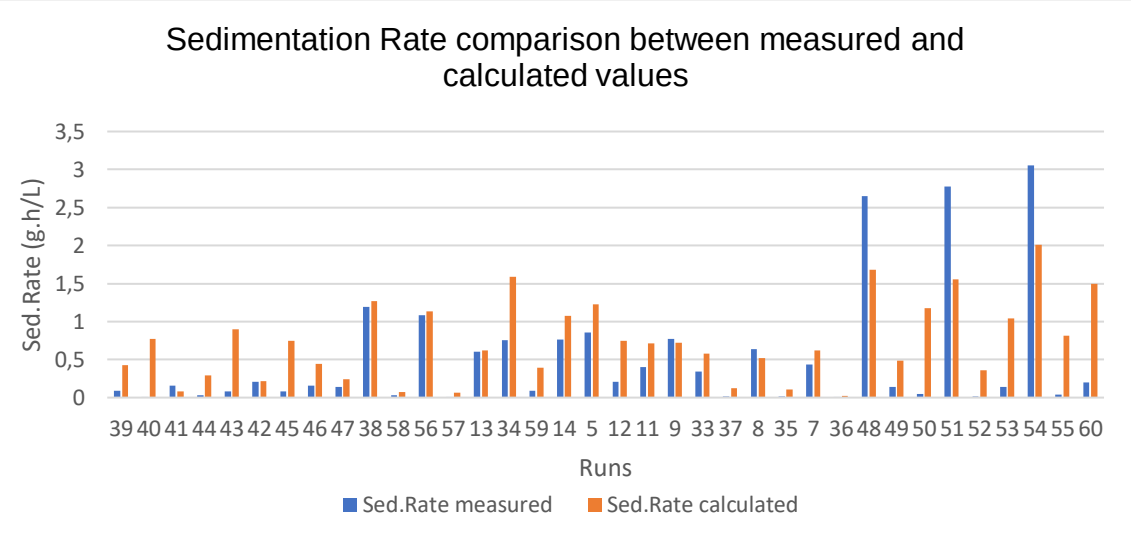

Figure 4.15- Comparison between measured and calculated values of sedimentation rate regarding polymer concentration, pH and soil concentration.

Figure 4.15 represents a comparison between the sedimentation rate obtained experimentally and the sedimentation rate obtained through the calculated values of initial and final density.

As it is explicit in the graphic (and as it occurred for the initial and final density graphics), in a general way the values obtained experimentally are approximate to the values obtained through Equation 4.4. For instance, runs 38, 58 and 56 present some of the lower error percentages (8%, 4% and 5% respectively). On the other hand, runs 40, 43, 55 ad 56 present some of the higher error percentages (76%, 82%, 77% and 130% respectively).

The tendency seen in the graphic goes along with what was expected considering that the sedimentation rate results from a combination of initial and final density. Therefore, as it was expected, Figure 4.15 reflects the trends observed in Figure 4.13 and Figure 4.14.

As presented in Figure 4.15, the runs with the higher error percentages correspond to the experiments performed with a clay concentration of 200 $g.L^{-1}$, exposing the limitations of the model when it comes to predicting the change in the fluid's nature that occurs when adding a certain soil quantity.

Thus, to solve this issue, the first hypothesis tested centred in removing the runs performed at a polymer concentration of 0 $g.L^{-1}$ since they correspond to the values that the model is not being able to predict. However, when testing the same equations for a data base without the 0 $g.L^{-1}$, an

error message appeared in the R software. The message indicated that the equation used could not provide a proper fit to the data introduced.

For this reason, a second strategy was used. It consisted in analysing the difference between the initial density value, and the density value passed 35 minutes. This strategy was based in the fact that in a construction context it is very important that the suspension can conserve its density for as long as possible. Therefore, if in the first 30 minutes after ending the agitation the difference to initial value is more than 60%, those runs are no longer valid.

After doing this analysis, we came across with two problematic runs:

Table 4.27- Comparison between density at minute 5 and minute 35for runs 51 and 54

Runs	[Soil] ($g.L^{-1}$)	[Polymer] ($g.L^{-1}$)	pH	Density at 5min (+/- 0,001 g/cm^3)	Density at 35min (+/- 0,001 g/cm^3)
51	200	0	7	1,0627	1,0282
54	200	0	11,5	1,0698	1,0334

Table 4.27 represents the difference in the density value measured at minute 5 and minute 35 after ending agitation. As it evident, in these two runs, the density loss over 35 minutes is very significant: from 1,0627 +/- 0,001 g/cm^3 to 1,0282 +/- 0,001 g/cm^3 in run 51, and from 1,0698 +/- 0,001 g/cm^3 to 1,0334 +/- 0,001 g/cm^3 in run 54. Considering that these runs were executed with a polymer concentration of 0 $g.L^{-1}$, this makes evident the difficulty of the model in predicting the behaviour of Newtonian fluids, particularly when there is a high solid fraction in suspension. For this reason, these runs may be influencing the results obtained in the modelling process. Thus, they were eliminated from the data base.

The equations tested in the R software for initial and final density were the ones selected as the best ones when the variable soil concentration was firstly introduced:

Equation 4.11- Initial density equation considering polymer concentration, pH and soil concentration

$$Di = A + B * ([Polymer] + 1)^2 + C * ([Polymer] + 1) + D * pH^2 + E * pH + F * log10(4 * [Soil])$$

Equation 4.12- Final density equation considering polymer concentration, pH and soil concentration

$$Df = A + B * ([Polymer] + 1)^2 + C * ([Polymer] + 1) + D * (pH) + E * log10(4 * [Soil])$$

Table 4.28- Error and standard deviation values for Di, Df and Sed. Rate considering Equation 4.11 and Equation 4.12

%error Di	%Std. deviation Di	%error Df	%Std deviation Df	%error Sed. rate	%Std. deviation Sed. Rate
15,6	18,2	23,9	21,7	15,0	17,0

From Table 4.28 is possible to conclude that, by eliminating those two values the model now fits the data and a sedimentation rate error between the limits previously established (≤15%).

In conclusion, it was already achieved an equation able to predict the sedimentation rate for a period of 24h considering 25, 100 and 200 g.L-1 of soil, with polymer 7156 (anionicity 34% and molecular weight 13,39 MDa) at a concentration range between 0 and 1 $g.L^{-1}$, and pH values between 5 and 12,5. The equations obtained are represented bellow:

Equation 4.13- Initial density equation considering a quadratic expression for polymer concentration and pH, and a logarithmic expression for soil concentration

$$Di = 1{,}1038 + 0{,}0400 * ([Polymer] + 1)^2 - 0{,}1216 * ([Polymer] + 1) + 0{,}0006 * pH^2 - 0{,}0084 * pH + 0{,}0059 * log10(4 * [Soil])$$

Equation 4.14- Final density equation considering a quadratic expression for polymer concentration, a linear expression for pH and a logarithmic expression for soil concentration

$$Df = 1{,}0008 + 0{,}0047 * ([Polymer] + 1)^2 - 0{,}0101 * ([Polymer] + 1) + 0{,}0006 * pH - 0{,}0014 * log10(4 * [Soil])$$

Despite the achievement of an average sedimentation rate error of 15%, it would be interesting if this value could be lowered even more in order to optimize the model here obtained. As it was discussed in this chapter, the main deviation between the measured and the calculated values occur in the runs with a clay concentration of 200 $g.L^{-1}$. However, the effect of the runs executed with a polymer concentration of 0 $g.L^{-1}$ is also felt. Therefore, one of the strategies to optimize the model could pass by developing a separate set of equations, designed uniquely for fluids with a Newtonian nature. Thus, it would be obtained equations designed for more specific fluid behaviours that would be able to provide more precise predictions.

Considering the goals of this project, there is still a need to address the usage of different soil compositions as well as a combination of different polymers and additives. Thus, this will be the following steps into obtaining a more complete mathematical model to predict sedimentation rates. Therefore, since the goal is to use anionic polyacrylamides, the way to differentiate them is through their anionic charge and molecular weight. As seen in chapter 4.1.4, these variables have a significant effect on the viscosity of the suspension values and, therefore, the densities obtained. Considering this, these parameters were varied in order to obtain a vaster set of experiments that include different polymer with different characteristics.

4.2.3 Polymer concentration, pH, Soil concentration, Anionicity and Molecular weight

These variables are going to be introduced and studied at the same time because, since they relate to a polymer and are dependent on each other, once one of these is altered a different polymer is obtained.

Besides being one of the goal variables, these are very important variables to consider since they are directly connected with all the other variables and, for this reason, have a direct effect in values for initial and final density. The tests performed in the previous runs were all executed with the same polymer, with an anionicity of 34% and a molecular weight of 13,39 MDa. Thus, for this polymer, it is already clear how it performs and affects the density values considering the other variables (polymer concentration, pH and soil concentration). However, there is still a need to study the effect of different anionicity percentages and molecular weights in the densities values obtained and, therefore in the sedimentation rate value.

For this, extra runs were performed using polymers with different value of anionicity and molecular weight. For this, it was considered two ranges of anionicity percentage: 0-16% and 16%-100%. Regarding to molecular weight four ranges were considered: 5-10Mda, 10-20Mda, 20-30Mda and 30-40Mda. Therefore, the polymers used resulted from a combination of these ranges of anionicity and molecular weight and are represented in the table below.

Table 4.29- Polymers and respective anionicity percentage and molecular weight

Polymer (name)	**Anionicity (%)**	**Molecular Weight (MDa)**
7136	6,4	10,5
7156	34	13,39
9698	34	31,08
A13	26	30,4
A35	32	29,5
A8	16	22,89
P9698	31,1	7,47
PP60	9	5,71

The following table exposes the results obtained for each equation tested. As before, the polymer concentration is represented in the equation formula as [Polymer]+1 and the initial density value is the one obtained at minute 5 after agitation. Density values were registered every 5 minutes for the first hour, after stopping agitation, and then for every 30 minutes for the next two hours. In this phase, values of pH, electrical conductivity, Marsh and Brookfield viscosity were registered as well. Passed 24 hours the final density value, as well as the other output values (pH, electrical conductivity, Marsh and Brookfield viscosity). For the data base, values of initial and final density were introduced as well as the correspondent values of polymer concentration, pH, soil

concentration, anionicity and molecular weight. The equations built will be initial and final density in function of these variable.

With the R software, a series of equations were tested to find the one that best correlates the data introduced and provides the best approximations. Since a satisfactory equation was obtained in the previous chapter considering the variables polymer concentration, pH and soil concentration, the new equation will be built over the previous one, testing different fits for the new variables introduced. In the following tale are represented in extend the equations tested.

Table 4.30- Equations written in extend considering polymer concentration, pH, soil concentration, anionicity and molecular weight.

Equation Nr.	Equation
1	$Density = A + B * ([Polymer] + 1)^2 + C * ([Polymer] + 1) + D * pH^2 + E * pH + F * log10([Soil] * 4) + G * Aniocity^2 + H * Aniocity + I * MW^2 + J * MW$
2	$Density = A + B * ([Polymer] + 1)^2 + C * ([Polymer] + 1) + D * pH + E * log10([Soil] * 4) + F * Aniocity^2 + G * Aniocity + H * pH^2 + I * pH$
3	$Density = A + B * ([Polymer] + 1)^2 + C * ([Polymer] + 1) + D * pH^2 + E * pH + F * log10([Soil] * 4) + G * log10(Aniocity) + H * log10(MW)$
4	$Density = A + B * ([Polymer] + 1)^2 + C * ([Polymer] + 1) + D * (pH) + E * log10([Soil] * 4) + F * log10(Aniocity) + G * log10(MW)$
5	$Density = A + B * ([Polymer] + 1)^2 + C * ([Polymer] + 1) + D * pH^2 + E * pH + F * log10([Soil] * 4) + G * Aniocity + H * MW^2 + I * MW$
6	$Density = A + B * ([Polymer] + 1)^2 + C * ([Polymer] + 1) + D * (pH) + E * log10([Soil] * 4) + F * Aniocity + G * MW^2 + H * MW$

Considering the set of equations mentioned in Table 4.30, the following table presents the error percentages for initial density, final density and sedimentation rate obtained for each equation, as well as the standard deviation of each error.

Table 4.31- Errors and standard deviations for Di, Df and Sed.Rate for each equation tested.

Equation Nr.	[Pol]+1	pH	[Soil]*4	Anionicity	MW	% error Di	%Std. deviation Di	% error Df	%Std. deviation Df
1	Quad	Quad	Log10	Quad	Quad	92578	47122	-	-
2	Quad	Linear	Log10	Quad	Quad	-	-	468786	226407
3	Quad	Quad	Log10	Log10	Log10	32	29	-	-
4	Quad	Linear	Log10	Log10	Log10	-	-	17	20
5	Quad	Quad	Log10	Linear	Quad	12791	22287	-	-
6	Quad	Linear	Log10	Linear	Quad	-	-	50454	59727

Table 4.31 presents the equations tested considering the variables polymer concentration, pH, soil concentration, anionicity and molecular weight. Regarding initial density values, as it possible to notice, equation 1 presents an error for initial density of 92578%. Equation 3 presents an error of 32% and equation 5 presents an error percentage of 12791%. Regarding final density, equation 2 presents an error for final density of 468786%, equation 4 presents an error for final density of 17% and equation 6 presents an error of 50454%.

Thus, considering these values, it is noticeable that equation 3, where both polymer concentration and pH have quadratic expression, soil concentration, anionicity and molecular weight have a logarithmic expression, is the one that present the lowest error percentage for initial density (32%). For final density, equation 4, where polymer concentration has a quadratic expression, pH has a linear expression, soil concentration, anionicity and molecular weight have a logarithmic expression, is the one that present the lowest error percentage (17%). This indicates that these types of equations are the ones that best describes the variables studied, therefore they were chosen to continue the development of the model.

From the values of initial and final density previously calculated through the equations obtained, the sedimentation rate value will be calculated accordingly to Equation 4.4 and the sedimentation rate error will be calculated accordingly to Equation 4.5. Thus, it will be possible to corroborate and validate the set of equations selected, considering the maximum value established for the sedimentation rate error as 15%.

Table 4.32- Sedimentation rate and standard deviation

Equation Nr.	Type of eq. for [Polymer]	Type of eq. for pH	Type of eq. for [Soil]	Type of eq. for Anionicity	Type of eq. for MW	% error Sed	%Std. deviation error Sed
3	Quad	Linear	Log10	Log10	Log10	31	29
4	Quad	Linear	Log10	Log10	Log10		

From Table 4.32 it is possible to see that the selected equations present a sedimentation error of 31%, therefore far superior to the maximum established limit of 15%. For this reason, it was necessary to look closely at the data in order to identify the cause of these high percentage errors. It is important to notice that the data base used in this analysis was built with all the runs executed so far, including those with a polymer concentration of 0 $g.L^{-1}$ and a soil concentration of 200 $g.L^{-1}$ which, as seen before, may interfere in the fit causing a bigger discrepancy between the values obtained experimentally and those calculated through the equations.

With this information in mind, the first strategy executed to solve the issue and lower the sedimentation rate value, consisted in separating the runs executed at a polymer concentration of 0 $g.L^{-1}$ from the others. However, an error message was generated in the R software, indicating that the equations could not provide a proper fit to the data introduced. To further develop this

strategy, it would be necessary to analyse the behaviour of these experiments and thus, create more accurate equations.

However, another strategy was tested. Considering that the experiments executed at a polymer concentration of 0 $g.L^{-1}$ were only executed once, the results obtained for these experiments were copied for all the polymers tested. Thus, there might be a high error propagation that is influencing the results obtained.

Therefore, as previously identified in chapter 4.2.2, runs 51 and 54 (executed at a polymer concentration of 0 $g.L^{-1}$, a soil concentration of 200 $g.L^{-1}$ and ate pH 7 and 11,5, respectively), were also eliminated here from all the polymer types considered. After that, the data base was updated, and the same equations were tested in R software.

Equation 4.15- Equation introduced and tested in R software for initial density

$$Di = A + B * ([Polymer] + 1)^2 + C * ([Polymer] + 1) + D * pH^2 + E * pH + F * log10(4 * [Soil]) + G * log10(Aniocity) + H * log10(MW)$$

Equation 4.16- Equation introduced and tested in R software for final density

$$Df = A + B * ([Polymer] + 1)^2 + C * ([Polymer] + 1) + D * (pH) + E * log10(4 * [Soil]) + F * log10(Aniocity) + G * log10(MW)$$

After updating the data base and obtaining the equations for initial and final density these equations were tested, and new average errors were obtained. The results are explicit in the following table.

Table 4.33- Errors and standard deviation for Di, Df and Sed. Rate (NC- Not considered)

Equation Nr.	%error Di	%Std. deviation Di	%error Df	%Std deviation Df	%error Sed. rate	%Std. deviation Sed. Rate
3	20	16	NC	NC	18	15
4	NC	NC	20	20		

From Table 4.33 is possible to conclude that, by eliminating those values the model now has a lower sedimentation rate error (18%) with a lower standard deviation (15%). The sedimentation rate error is now only 3% over the limit previously established (≤15%).

This was the lowest sedimentation rate error possible to obtain. In regard to the goals of the project, it considers different soil concentrations (25, 100 and 200 $g.L^{-1}$), achieved with different polymers with a polymer concentration between 0 and 1 $g.L^{-1}$ as well as a pH range between 5 and 12,5. The equation is represented bellow:

$$Sed.rate^3 = \frac{(Di - Df)}{24} * 1000$$

Equation 4.17- Final equation to predict initial density values considering polymer concentration, pH, soil concentration, anionicity and molecular weight

$$Density_i = 1{,}0479 + 0{,}0270 * ([Polymer] + 1)^2 - 0{,}0898 * ([Polymer] + 1) + 0{,}0002 * pH^2 - 0{,}0031 * pH + 0{,}0094 * log10(4 * [Soil]) + 0{,}0078 * log10(Aniocity) + 0{,}0009 * log10(MW)$$

Equation 4.18- Final equation to predict final density values (passed24h), considering polymer concentration, pH, soil concentration, anionicity and molecular weight

$$Density_f = 0{,}9933 + 0{,}0014 * ([Polymer] + 1)^2 - 0{,}0022 * ([Polymer] + 1) + 0{,}0003 * pH - 0{,}0005 * log10(4 * [Soil]) + 0{,}0018 * log10(Aniocity) + 0{,}0003 * log10(MW)$$

Sed.rate^3- Sedimentation rate considering different polymers and polymer concentrations, soil concentration of 25, 100 and 200 g.L^{-1} and 2h30min of agitation.

Although there was not enough time to optimize this value, which was the closest to the goal possible to obtain, this is the final model to consider so far.

To improve the error obtained and optimize the model achieved, it is important to analyse the variables here considered (namely anionicity percentage and molecular weight) and their influence in the outputs.

In the following table are represented values of initial and final density and Brookfield viscosity, considering different polymers at a concentration of 1 g.L^{-1}, pH 11,5 and soil concentration of 100 g.L^{-1}.

Table 4.34- Values of initial and final density and initial and final Brookfield viscosity, considering different polymers.

Polymer name	**Anionicity (%)**	**MW (MDa)**	**Di (+/- 0,001 g/cm^3)**	**Brookfield viscosity initial (+/- 1%cp)**	**Df (+/- 0,001 g/cm^3)**	**Brookfield viscosity final (+/- 1%cp)**
7136	6,4	10,50	0,9969	13,44	0,9969	19,08
7156	34,0	13,39	1,0240	69,84	1,0056	44,70
A13	26,0	30,40	1,0050	169,80	0,9993	90,24
A35	32,0	29,50	1,0062	69,00	0,9998	71,40
A8	16,0	22,89	0,9970	73,68	0,9970	76,20
P9698	31,1	7,47	1,0024	84,00	0,9988	84,24

PP60	9,0	5,71	0,9960	15,36	0,9960	14,04

In Table 4.34 are represented the initial and final values for density and Brookfield viscosity for different polymers under the same operational conditions. It is noticeable that polymer with higher anionicity percentage (7156, A13, A35 and P9698) present higher values of initial density (1,024 +/- 0,001 g/cm^3, 1,005 +/- 0,001 g/cm^3, 1,0062 +/- 0,001 g/cm^3, 1,0024 +/- 0,001g/cm^3, respectively) and initial viscosity (69,84 +/- 1% cp, 169,8 +/- 1% cp, 69 +/- 1% cp, 84 +/-1% cp, respectively). The same occurs for final values (passed 24h) of density and viscosity.

Thus, it goes along with what was seen in the state-of-the-art research, which says that polymers with a higher anionicity and molecular weight result in higher density values when mixed with clay, and are able to maintain more of the material in suspension. If, under the same operational conditions, one of these variables (anionicity or molecular weight) is in a lower range, the density values clearly decrease.

This behaviour is well represented through the model obtained, however there are clear differences between the measured and the calculated value for some polymers (7136, A8, P9698 and PP60). When looking into those polymers in more depth, it is noticeable that a low anionicity value is having a big impact in the results, since this is a characteristic that all these polymers have in common (except P9698). A low anionicity results in an inefficiency in maintaining solid particles in suspension. As seen in the state-of-the-art research, the polyacrylamide must have an anionic percentage of at least 20% to be considered efficient [131][130]. Therefore, the lower anionicity will provide these polymers different rheological characteristics that the model has difficulty predicting, as it happened in chapter 4.2.1 and 4.2.2 (with Newtonian fluids).

Thus, one alternative that could help solve this issue could pass by separating the data according ranges of anionicity percentage and molecular weight. And in R, developing equations specifically for the rheology of the suspension.

In a nutshell, a future work for this project will not only consider an optimization of the model obtained but will also have to address some of the goal variables that were not considered. Namely: usage of sand and mixture of sand/clay; effect of additives.

The final model here obtained considers pH (in a range between 5 and 12,5), polymer concentration (between 0 and 1 g.L^{-1}), clay concentrations (between 25 and 200 g.L^{-1}), anionicity percentage and molecular weight.

Due to the vast number of tests executed, as well as all the characterizations required, and the limited time of the project, it was not possible to address all the conditions explicit in the goal. Despite that, the model obtained is already an improvement regarding what was available until this day for this purpose. Therefore, the model here obtained is a good starting point to a further analysis and optimization in order to achieve the most accurate model able to predict sedimentation rates for a polymeric suspension.

4.2.4 Model validation

In order to access the model's efficiency different application limits were analysed. Through this study it was possible to conclude that when considering: 0 g/L ≤ [Polymer] ≤ 1 g/L; 5 ≤ pH ≤ 12,5; 25 g_{soil}/L ≤ [Soil] ≤ 200 g_{soil}/L; 6,4% ≤ Anionicity ≤ 34%; 5,7 MDa ≤ MW ≤ 31 MDa, 55% of the experiments presented an error percentage bellow or equal to 18%.

On the other hand, when altering the polymer concentration limit for 0,4 g/L ≤ [Polymer] ≤ 1 g/L, while maintaining the other conditions, 69% of the experiments executed presented an error percentage ≤ 18%. When altering the soil concentration to 25 g_{soil}/L ≤ [Soil] ≤ 100 g_{soil}/L, the percentage of experiments with an error ≤ 18% was 58%. Considering the solutions pH, when considering an alkaline range (9,5 ≤ pH ≤ 12,5) it was possible to achieve 64% of the experiments ≤ 18%.

Considering that all the alterations on the operations limits resulted in an improvement on the percentage of experiments with an error percentage ≤ 18%, a new set of limits was tested. Thus, when considering 0,4 g/L ≤ [Polymer] ≤ 1 g/L; 9,5 ≤ pH ≤ 12,5; 25 g_{soil}/L ≤ [Soil] ≤ 100 g_{soil}/L; 6,4% ≤ Anionicity ≤ 34%; 5,7 MDa ≤ MW ≤ 31 MDa, it was achieved a percentage of 81% of experiments with an error percentage ≤ 18%, proving that this is the best set of limits where the model can be used.

However, an optimization of the model is still required, and it would be interesting to evaluate the impact of the variable viscosity in order to assess its result in the output variables.

Despite requiring some optimizations, the model obtained is already able to predict, with an average 18% error, the sedimentation rate for a period of 24h.

5. Conclusions

The major breakthrough of this project was the development of a mathematical model able to predict average sedimentation rates for a period of 24h, with an error percentage of 18% and a standard deviation of 15%.

A series of variables were tested and correlated to analyse their effect in the fluid's suspension capacity. It was possible to withdraw that polymers with higher anionic percentages (between 20% and 40%), at a concentration of 1 $g.L^{-1}$, with a solution's pH of 11,5 and a clay concentration of 100 $g.L^{-1}$, contribute to the best density conservation through time, leading to the lowest sedimentation rates values. The usage of additives was also tested, concluding that it provides an efficient improvement to the sedimentation rates values

These preliminary results allowed to design the strategy to develop the mathematical model.

With the R modelling, it was achieved a final model, with an error of 18%. It considers polymer concentration (between 0 and 1 $g.L^{-1}$), solution's pH (between 5 and 12,5), soil concentration (between 25 and 200 $g.L^{-1}$) and also anionic percentage and molecular weight of a chosen polymer.

The final set of equations are represented as such:

$$Density_i = 1{,}0479 + 0{,}0270 * ([Polymer] + 1)^2 - 0{,}0898 * ([Polymer] + 1) + 0{,}0002 * pH^2 - 0{,}0031 * pH + 0{,}0094 * log10(4 * [Soil]) + 0{,}0078 * log10(Aniocity) + 0{,}0009 * log10(MW)$$

$$Density_f = 0{,}9933 + 0{,}0014 * ([Polymer] + 1)^2 - 0{,}0022 * ([Polymer] + 1) + 0{,}0003 * pH - 0{,}0005 * log10(4 * [Soil]) + 0{,}0018 * log10(Aniocity) + 0{,}0003 * log10(MW)$$

It was also achieved a mathematical model considering polymer concentration (between 0 and 1 g.L-1), and pH (between 5 and 12,5). The polymer used for this specific model was 7156, considering 100 $g.L^{-1}$ of clay. For this model, it was achieved an average error percentage for the sedimentation rate of 15%, with a standard deviation of 32%. By adding the variable soil concentration (between 25 and 200 $g.L^{-1}$) into the model, it achieved a model considering polymer concentration (between 0 and 1 $g.L^{-1}$), solution's pH (between 5 and 12,5) and soil concentration (between 25 and 200 $g.L^{-1}$), with an average error for the sedimentation rate of 15% as well, and a standard deviation of 17%.

In a nutshell, despite not comprising all the variables mentioned in the goal of the project and presenting an error percentage superior to 15%, the model obtained already provides a quite precise prevision for sedimentation rates, considering a wide variety of polymers, polymer and clay concentration and pH. Therefore, this set of equations are a good starting point in the development of a more optimized and precise model, able to include all the variables considered important, introducing for instance the variable viscosity, and with the smallest error percentage possible.

References

[1] R. Arshady, “Suspension, emulsion, and dispersion polymerization: A methodological survey,” *Colloid Polym. Sci.*, vol. 270, no. 8, pp. 717–732, 1992, doi: 10.1007/BF00776142.

[2] J. Daintith, Ed., *Oxford Dictionary of Chemistry*, 6ed ed. Oxford Uniiversity Press, 2008.

[3] D. N. Shaik, “What is a Suspension?,” 2020. [Online]. Available: https://www.toppr.com/guides/chemistry/is-matter-around-us-pure/what-is-a-suspension/.

[4] “Definition of a Suspension,” 2017. [Online]. Available: https://www.chemicool.com/definition/suspension.html.

[5] “Colloids,” in *Encyclopaedia Britannica*, 15th ed., 2020.

[6] L. L. Schramm, “Suspensions : Basic Principles,” pp. 3–44, 1996.

[7] P. J. Carreau and B. Vergnes, “Rheological Characterization of Fiber Suspensions and Nanocomposites,” *Rheol. Non-Spherical Part. Suspens.*, pp. 19–58, 2015, doi: 10.1016/B978-1-78548-036-2.50002-2.

[8] M. Reichert, “Hydrodynamic interactions : Theoretical concepts and simulation methods,” Universit¨at Konstanz, 2006.

[9] “Chapter 10 Dispersion of particles in liquids,” *Stud. Interface Sci.*, vol. 20, no. C, pp. 517–558, 2005, doi: 10.1016/S1383-7303(05)80011-0.

[10] “Dispersing Process.” [Online]. Available: http://www.inkline.gr/inkjet/newtech/tech/dispersion/. [Accessed: 16-Apr-2020].

[11] G. Imai, “Experimental studies on sedimentation mechanism and sediment formation of clay materials,” no. 43, p. 2091, 1981.

[12] A. J. S. Cuthbertson, O. Ibikunle, W. J. McCarter, and G. Starrs, “Monitoring and characterisation of sand-mud sedimentation processes,” *Ocean Dyn.*, vol. 66, no. 6–7, pp. 867–891, 2016, doi: 10.1007/s10236-016-0958-7.

[13] Flanders Marine Institute, “Sediment deposition and arosion processes,” 2019. [Online]. Available: http://www.coastalwiki.org/wiki/Sediment_deposition_and_erosion_processes.

[14] R. H. Müller, B. Herziger, F. Monsuur, and S. M. Pyo, *A novel amorphous delivery system to the skin for poorly soluble actives*, vol. 42, no. 6. RSCPublishing, 2008.

[15] H. Stechemesser and B. Dobiáš, “Coagulation and flocculation,” *Coagul. Flocculation, Second Ed.*, pp. 1–862, 2005, doi: 10.1680/bwtse.63341.061.

[16] A. W. College, “Flocculation,” 2017. [Online]. Available: https://www.youtube.com/watch?v=eST7k0lSICw.

[17] “Terminilogy and Symbols in colloidal and surface Chemistry Part I,” in *Pure and Applied Chemistry*, 1972, p. 609.

[18] T. Suopajarvi, “Functionalized nanocelluloses in wastewater treatment applications,” Universitatis Ouluensis, 2015.

[19] M. Chorom, P. Rengasamy, and R. S. Murray, “Clay dispersion as influenced by pH and net particle charge of sodic soils,” *Aust. J. Soil Res.*, vol. 32, no. 6, pp. 1243–1252, 1994, doi: 10.1071/SR9941243.

[20] K. Itami and H. Fujitani, “Charge characteristics and related dispersion/flocculation behavior of soil colloids as the cause of turbidity,” *Colloids Surfaces A Physicochem. Eng. Asp.*, vol. 265, no. 1–3, pp. 55–63, 2005, doi: 10.1016/j.colsurfa.2004.10.138.

[21] B. Alince and T. G. M. van de Ven, “Stability of clay suspensions-effect of pH and polyethylenimine,” *Journal of Colloid And Interface Science*, vol. 155, no. 2. pp. 465–470, 1993, doi: 10.1006/jcis.1993.1060.

[22] F. Rey, M. A. Ferreira, P. Facal, and A. A. S. C. Machado, “Effect of concentration, pH, and ionic strength on the viscosity of solutions of a soil fulvic acid,” *Can. J. Chem.*, vol. 74, no. 3, pp. 295–299, 1996, doi: 10.1139/v96-033.

[23] C. R. Evanko, R. F. Delisio, D. A. Dzombak, and J. W. Novak, “Influence of aqueous solution chemistry on the surface charge, viscosity and stability of concentrated alumina dispersions in water,” *Colloids Surfaces A Physicochem. Eng. Asp.*, vol. 125, no. 2–3, p. 104, 1997, doi: 10.1016/S0927-7757(96)03874-5.

[24] K. Hosseinzadeh, M. Ghayebzadeh, M. Shahi, and M. Babrzadeh, “Polymer Induced Flocculation for Treatment of a Tile Factory Wastewater using Polyacrylamide (PAM): Optimization by Response Surface Methodological Analysis,” vol. 3, no. 2, pp. 70–76, 2019, doi: 10.22034/mbt.2019.80849.1.

[25] I. Shainberg and G. J. Levy, “Flocculation and Dispersion,” *Encycl. Soils Environ.*, vol. 4, no. 1999, pp. 27–34, 2004, doi: 10.1016/B0-12-348530-4/00363-5.

[26] A. P. EDWARDS and J. M. BREMNER, “Dispersion of Soil Particles By Sonic Vibration,” *J. Soil Sci.*, vol. 18, no. 1, pp. 47–63, 1967, doi: 10.1111/j.1365-2389.1967.tb01487.x.

[27] H. S. Arora and N. T. Coleman, “The influence of electrolyte concentration on flocculation of clay suspensions,” *Soil Science*, vol. 127, no. 3. pp. 134–139, 1979, doi: 10.1097/00010694-197903000-00002.

[28] R. E. Cynthia, F. D. Robert, A. D. David, and W. N. J. John, “Influence of aqueous solution chemistry on the surface charge, viscosity and stability of concentrated alumina dispersions in water,” in *Colloids and Surfaces A: Physicochem. Eng. Aspects*, 125th ed., J. B. Li, Ed. Elsevier B.V., 1997, pp. 95–107.

[29] S. Shimabayashi, T. Uno, and M. Nakagaki, “Formation of a surface complex between polymer and surfactant and its effect on the dispersion of solid particles,” *Colloids Surfaces A Physicochem. Eng. Asp.*, vol. 123–124, pp. 283–295, 1997, doi: 10.1016/S0927-7757(96)03820-4.

[30] R. K. Schofield and H. R. Samson, “Flocculation of kaolinite due to the attraction of oppositely charged crystal faces,” *Discuss. Faraday Soc.*, vol. 18, pp. 135–145, 1954, doi: 10.1039/DF9541800135.

[31] G. Petzold, M. Mende, K. Lunkwitz, S. Schwarz, and H. M. Buchhammer, “Higher efficiency in the flocculation of clay suspensions by using combinations of oppositely charged polyelectrolytes,” *Colloids Surfaces A Physicochem. Eng. Asp.*, vol. 218, no. 1–3, pp. 47–57, 2003, doi: 10.1016/S0927-7757(02)00584-8.

[32] A. E. Domopoulou, K. H. Gudulas, E. S. Papastergiadis, and V. G. Karayannis, “Coagulation/flocculation/sedimentation applied to marble processing wastewater

treatment," *Mod. Appl. Sci.*, vol. 9, no. 6, pp. 137–144, 2015, doi: 10.5539/mas.v9n6p137.

[33] K. Borja, J. Mercado, and E. Combatt, "Métodos de dispersión mecánica en la determinación de fracciones granulométricas del suelo utilizando cuatro soluciones dispersantes," *Agron. Colomb.*, vol. 33, no. 2, pp. 253–260, 2015, doi: 10.15446/agron.colomb.v33n2.47236.

[34] E. M. and T. L. F. N. Ponnamperuma, "1966- Influence of redox potencial and partial pressure of Carbon dioxide on pH values and the suspension effect of flooded soils.pdf," in *Soil Science*, 1966, pp. 421–431.

[35] K. Miyahara, Y. Adachi, and K. Nakaishi, "The viscosity of a dilute suspension of sodium montmorillonite in an alkaline state," *Colloids Surfaces A Physicochem. Eng. Asp.*, vol. 131, no. 1–3, pp. 69–75, 1998, doi: 10.1016/S0927-7757(96)03961-1.

[36] H. Du Mas Des Bourboux *et al.*, "Baryon acoustic oscillations from the complete SDSS-III Ly α -quasar cross-correlation function at z = 2.4," *Astron. Astrophys.*, vol. 608, pp. 255–293, 2017, doi: 10.1051/0004-6361/201731731.

[37] H. J. Keh and W. T. Hsu, "Electric conductivity of a suspension of charge colloidal spheres with thin but polarized double layers," *Colloid Polym. Sci.*, vol. 280, no. 10, pp. 922–928, 2002, doi: 10.1007/s00396-002-0709-9.

[38] G. Petzold, H. M. Buchhammer, and K. Lunkwitz, "The use of oppositely charged polyelectrolytes as flocculants and retention aids," *Colloids Surfaces A Physicochem. Eng. Asp.*, vol. 119, no. 1, pp. 87–92, 1996, doi: 10.1016/S0927-7757(96)03740-5.

[39] Y. Otsubo, "Rheological behavior of suspensions flocculated by weak bridging of polymer coils," *J. Colloid Interface Sci.*, vol. 215, no. 1, pp. 99–105, 1999, doi: 10.1006/jcis.1999.6252.

[40] H. Schott, A. E. Royce, and U. S. A. Pa, "Effect of inorganic additives on solutions of nonionic surfactants." vol. 19, pp. 399–418, 1986.

[41] A. Alekseev, T. Alekseeva, Z. Sokołowska, and M. Hajnos, "Magnetic and mineralogical properties of different granulometric fractions in the soils of the Lublin Upland Region," *Int. Agrophysics*, vol. 16, no. 1, pp. 1–6, 2001.

[42] F. Del Giudice, G. D'Avino, F. Greco, P. A. Netti, and P. L. Maffettone, "Effect of fluid rheology on particle migration in a square-shaped microchannel," *Microfluid. Nanofluidics*, vol. 19, no. 1, pp. 95–104, 2015, doi: 10.1007/s10404-015-1552-x.

[43] S. M. Olhero and J. M. F. Ferreira, "Influence of particle size distribution on rheology and particle packing of silica-based suspensions," *Powder Technol.*, vol. 139, no. 1, pp. 69–75, 2004, doi: 10.1016/j.powtec.2003.10.004.

[44] L. J. Struble and X. Ji, "Rheology," in *Rheology. Handbook of analytical techniques in concrete science and technology*, 2001, pp. 333–367.

[45] H. A. Barnes, *Rheology: Principles, Measurements and Applications*, vol. 86, no. 3. Wiley-VCH, 1996.

[46] H. H. Winter and M. Mours, "Rheology of Polymers Near Liquid-Solid Transitions," *Adv. Polym. Sci.*, vol. 134, pp. 164–234, 1997, doi: 10.1007/3-540-68449-2_3.

[47] J. S. Chong, "Rheology of Concentrated Suspensions," in *Journal of appied polymer sciennce*, vol. 15, no. 1971, Salt Lake City: John Wiley & Sons, Inc, 1971, pp. 2007–2021.

[48] A. Otsuki, “Rheology of colloidal particle suspensions,” in *Rheology of Polymer Blends and Nanocomposites*, Vandoeuvre-le`s-Nancy: Elsevier Inc., 2020, pp. 49–71.

[49] S. L. M. Brito, D. Gouvêa, and R. Ganzella, “Principais fatores que influenciam o comportamento reológico de suspensões aquosas de um sistema varistor à base de zno,” *Congr. Bras. Cerâmica*, p. 7, 2004.

[50] M. Benna, N. Kbir-Ariguib, A. Magnin, and F. Bergaya, “Effect of pH on rheological properties of purified sodium bentonite suspensions,” *J. Colloid Interface Sci.*, vol. 218, no. 2, pp. 442–455, 1999, doi: 10.1006/jcis.1999.6420.

[51] V. C. Kelessidis, C. Tsamantaki, and P. Dalamarinis, “Effect of pH and electrolyte on the rheology of aqueous Wyoming bentonite dispersions,” *Appl. Clay Sci.*, vol. 38, no. 1–2, pp. 86–96, 2007, doi: 10.1016/j.clay.2007.01.011.

[52] A. Cerpa, M. T. García-González, C. J. Serna, and P. Tartaj, “Relationship between the colloidal and rheological properties of mineral suspensions,” *Can. J. Chem. Eng.*, vol. 79, no. 4, pp. 608–611, 2001, doi: 10.1002/cjce.5450790420.

[53] M. Van Den Tempel, “Rheology of concentrated suspensions,” *J. Colloid Interface Sci.*, vol. 71, no. 1, pp. 18–20, 1979, doi: 10.1016/0021-9797(79)90216-9.

[54] P. Del Gaudio, G. Ventura, and J. Taddeucci, “The effect of particle size on the rheology of liquid-solid mixtures with application to lava flows: Results from analogue experiments,” *Geochemistry, Geophys. Geosystems*, vol. 14, no. 8, pp. 2661–2669, 2013, doi: 10.1002/ggge.20172.

[55] M. Mooney, “The viscosity of a concentrated suspension of spherical particles,” no. August, pp. 162–170, 1950.

[56] E. H., “Kolloid-Z,” 1941.

[57] D. He and N. N. Ekere, “Viscosity of concentrated noncolloidal bidisperse suspensions,” *Rheol. Acta*, vol. 40, no. 6, pp. 591–598, 2001, doi: 10.1007/s003970100187.

[58] A. V. Bazilevsky, V. A. Kalinichenko, V. A. Plyashkevich, D. V. Badazhkov, and A. N. Rozhkov, “Sedimentation of particles in shear flows of viscoelastic fluids with fibers,” *Rheol. Acta*, vol. 45, no. 10, pp. 128–141, 2010, doi: 10.1007/s00397-017-1036-x.

[59] E. V.M and G. E.V, “Continuum Mechanical and its Applications in Gas and Oil Recovery,” in *Introduction to Continuum Mechanics*, Nedra, Moscow, 2008.

[60] N. M. Kovalchuk, I. Kuchin, V. Starov, and N. Uriev, “Aggregation in colloidal suspensions and its influence on the suspension viscosity,” *Colloid J.*, vol. 72, no. 3, pp. 379–388, 2010, doi: 10.1134/S1061933X10030117.

[61] D. Quemada and C. Berli, "Energy of interaction in colloids and its implications in rheological modeling", vol. 98, no. 1. 2002.

[62] Z. Neda, Y. Bre, L. Salvo, and M. Perez, “Computer Simulation of the Microstructure and,” *Acta Metall.*, vol. 48, pp. 3773–3782, 2000.

[63] C. yang Xu, Chun-li Wang, Chun-tian Zhang, Fei-nan Hu, Han-yi Liu, Tan-tan Zhou, Shi-wei Zhao, Zeng-chao Geng, “Aggregation of polydisperse soil colloidal particles: Dependence of Hamaker constant on particle size,” *Geoderma*, vol. 359, no. March 2019, p. 113999, 2020, doi: 10.1016/j.geoderma.2019.113999.

[64] S. P. Zamana, T. G. Fedorovsky, N. A. Golubkina, and A. V. Sokolov, “Compositional

change of solid and liquid phases of soil suspension depending on pH value," *IOP Conf. Ser. Earth Environ. Sci.*, vol. 350, no. 1, pp. 3–8, 2019, doi: 10.1088/1755-1315/350/1/012047.

[65] R. L. F. M. Saeed, "1977- relationship between suspension pH and zinc solubility in acid and calcerous soils.pdf." 1977.

[66] P. Sen M. Adhikari, B. Mandal, "1980- Interfacial phenomena of humic substances.pdf," *Soil Chem.*, pp. 603–607, 1980.

[67] S. Chen, G. Øye, and J. Sjöblom, "Effect of pH and salt on rheological properties of aerosil suspensions," *J. Dispers. Sci. Technol.*, vol. 28, no. 6, pp. 845–853, 2007, doi: 10.1080/01932690701345844.

[68] A. Finck, B. Preis, A. E. Foliar, and F. Proceedings, "Buchbesprechung," pp. 2–3, 1987.

[69] S. Goldberg and R. A. Glaubig, "Effect of saturating cation , ph , and aluminum and iron oxide on the flocculation of kaolinite and montmorillonite," vol. 35, no. 3, pp. 220–227, 1987.

[70] I. E. Melton and B. Rand, "Particle interactions in aqueous kaolinite suspensions. III. Sedimentation volumes," *J. Colloid Interface Sci.*, vol. 60, no. 2, pp. 331–336, 1977, doi: 10.1016/0021-9797(77)90292-2.

[71] J. Gustafsson, E. Nordenswan, and J. B. Rosenholm, "Effect of pH on the sedimentation, ζ-potential, and rheology of anatase suspensions," *Colloids Surfaces A Physicochem. Eng. Asp.*, vol. 212, no. 2–3, pp. 235–247, 2003, doi: 10.1016/S0927-7757(02)00332-1.

[72] W. J. Tseng and C. H. Wu, "Sedimentation, rheology and particle-packing structure of aqueous Al2O3 suspensions," *Ceram. Int.*, vol. 29, no. 7, pp. 821–828, 2003, doi: 10.1016/S0272-8842(03)00023-3.

[73] S. Kaufhold, R. Dohrmann, D. Koch, and G. Houben, "The pH of aqueous bentonite suspensions," *Clays Clay Miner.*, vol. 56, no. 3, pp. 338–343, 2008, doi: 10.1346/CCMN.2008.0560304.

[74] I. Nurdin, Ridwan, and Satriananda, "The effect of pH and time on the stability of superparamagnetic maghemite nanoparticle suspensions," *MATEC Web Conf.*, vol. 39, pp. 3–6, 2016, doi: 10.1051/matecconf/20163901001.

[75] D. L. Sparks *et al.*, "Charge Analysis of Soils and Anion Exchange," no. 5, pp. 1231–1253, 1996, doi: 10.2136/sssabookser5.3.c41.

[76] P. Rengasamy, E. Tavakkoli, and G. K. McDonald, "Exchangeable cations and clay dispersion: net dispersive charge, a new concept for dispersive soil," *Eur. J. Soil Sci.*, vol. 67, no. 5, pp. 659–665, 2016, doi: 10.1111/ejss.12369.

[77] J. B. C. Tianping Huang, "suspension of concentrated additives containing oil for fracturing and other fluids," US 7,543,646 B2, 2009.

[78] S. H. Piao, H. S. Chae, and H. J. Choi, "Carbonyl Iron Suspension With Core – Shell Structured," vol. 51, no. 11, pp. 2–5, 2015.

[79] G. Sen, S. Ghosh, U. Jha, and S. Pal, "Hydrolyzed polyacrylamide grafted carboxymethylstarch (Hyd . CMS-g-PAM): An efficient flocculant for the treatment of textile industry wastewater," *Chem. Eng. J.*, vol. 171, no. 2, pp. 495–501, 2011, doi: 10.1016/j.cej.2011.04.016.

[80] S. A. Visser and M. Caillier, “Observations on the dispersion and aggregation of clays by humic substances, I. Dispersive effects of humic acids,” *Geoderma*, vol. 42, no. 3–4, pp. 331–337, 1988, doi: 10.1016/0016-7061(88)90009-2.

[81] J. Tarchitzky and Y. Chen, “Polysaccharides and pH effects on sodium-mo ... polysaccharides and ph effects on sodium-montmorillonite ” *Soil Sci.*, vol. 167, no. December 2002, pp. 3–7, 2011, doi: 10.1097/01.ss.0000043035.84859.43.

[82] A. M. Wintermyer and E. B. Kinter, “Dispersing Agents for Particle-Size Analysis of Soils,” *Highw. Res. Board Bull.*, no. 95, pp. 1–14, 1955.

[83] A. Elsharief, “Effect of lime and Gypsum Additives on the Dispersive Characteristics of Two EFFECTS OF LIME AND GYPSUM ADDITIVES,” no. May, 2016.

[84] M. Gunaratne, “Design of driven piles and pile groups,” *Found. Eng. Handb.*, pp. 235–298, 2006, doi: 10.1201/9780203484418.

[85] G. Dugan, “Drilling foundation shafts, Control fluid loss,” 2018. [Online]. Available: https://www.nationaldriller.com/articles/91337-drilling-foundation-shafts-control-fluid-loss.

[86] R. D. Carico, “Suspension properties of polymer fluids used in drilling, workover, and completion operations,” *Soc. Pet. Eng. - SPE Calif. Reg. Meet. CRM 1976*, 1976, doi: 10.2523/5870-ms.

[87] A. Tehrani, “Behaviour of suspensions and emulsions in drilling fluids,” *Annu. Trans. Rheol. Soc.*, vol. 15, p. 17, 2007.

[88] S. qing Hao, “A study to optimize drilling fluids to improve borehole stability in natural gas hydrate frozen ground,” *J. Pet. Sci. Eng.*, vol. 76, no. 3–4, pp. 109–115, 2011, doi: 10.1016/j.petrol.2011.01.014.

[89] M. Negulescu, *Municipal waste water treatment.* New York, 1986.

[90] G. M, J. B, and J. S, “Aerobic MBRs for domestic wastewater treatment: a review with cost considerations,” *Sep. Purif. Technol.*, vol. 18, pp. 119–130, 2000.

[91] Z. Talip, M. Eral, and Ü. Hiçsönmez, “Adsorption of thorium from aqueous solutions by perlite,” *J. Environ. Radioact.*, vol. 100, no. 2, pp. 139–143, 2009, doi: 10.1016/j.jenvrad.2008.09.004.

[92] C. S. Lee, J. Robinson, and M. F. Chong, “A review on application of flocculants in wastewater treatment,” *Process Saf. Environ. Prot.*, vol. 92, no. 6, pp. 489–508, 2014, doi: 10.1016/j.psep.2014.04.010.

[93] F. Sekiou and A. Kellil, “Effect of organic and mineral matters on kinetic and performance of flocculation,” *Desalination*, vol. 249, no. 2, pp. 891–894, 2009, doi: 10.1016/j.desal.2009.09.019.

[94] L. Semerjian and G. M. Ayoub, “High-pH-magnesium coagulation-flocculation in wastewater treatment,” *Adv. Environ. Res.*, vol. 7, no. 2, pp. 389–403, 2003, doi: 10.1016/S1093-0191(02)00009-6.

[95] F. E. Aboussabiq, I. Kader Yettefti, J. Amine, M. del M. Socias-Viciana, and O. Assobhei, “Coagulation-flocculation of domestic wastewater by moroccan clays: Removal of organic matter and suspended solids,” *Carpathian J. Earth Environ. Sci.*, vol. 9, no. 1, pp. 33–42, 2014.

[96] N. Li, G. P. Sheng, Y. Z. Lu, R. J. Zeng, and H. Q. Yu, “Removal of antibiotic resistance genes from wastewater treatment plant effluent by coagulation,” *Water Res.*, vol. 111, pp. 204–212, 2017, doi: 10.1016/j.watres.2017.01.010.

[97] A. Joss, H. Andersen, T. Ternes, P. R. Richle, and H. Siegrist, “Removal of estrogens in municipal wastewater treatment under aerobic and anaerobic conditions: Consequences for plant optimization,” *Environ. Sci. Technol.*, vol. 38, no. 11, pp. 3047–3055, 2004, doi: 10.1021/es0351488.

[98] B. Ersoy, “Effect of pH and polymer charge density on settling rate and turbidity of natural stone suspensions,” *Int. J. Miner. Process.*, vol. 75, no. 3–4, pp. 207–216, 2005, doi: 10.1016/j.minpro.2004.08.011.

[99] M. I. Aguilar, J. Sáez, M. Lloréns, A. Soler, and J. F. Ortuño, “Nutrient removal and sludge production in the coagulation-flocculation process,” *Water Res.*, vol. 36, no. 11, pp. 2910–2919, 2002, doi: 10.1016/S0043-1354(01)00508-5.

[100] B. Ersoy, I. Tosun, A. Günay, and S. Dikmen, “Turbidity removal from wastewaters of natural stone processing by coagulation/flocculation methods,” *Clean - Soil, Air, Water*, vol. 37, no. 3, pp. 225–232, 2009, doi: 10.1002/clen.200800209.

[101] D. K. Bayel, Z. Karaca, V. Onen, and A. H. Deliormanli, “Abwasserklärung und Rückführung des aufbereiteten Wassers in Marmorverarbeitungsanlagen: Mineralische Trübe und Flockungsmittel,” *Mine Water Environ.*, vol. 35, no. 3, pp. 332–336, 2016, doi: 10.1007/s10230-015-0367-z.

[102] V. Onen, P. Beyazyuz, and E. Yel, “Removal of Turbidity from Travertine Processing Wastewaters by Coagulants, Flocculants and Natural Materials,” *Mine Water Environ.*, vol. 37, no. 3, pp. 482–492, 2018, doi: 10.1007/s10230-017-0499-4.

[103] F. Ozyonar and B. Karagozoglu, “Systematic assessment of electrocoagulation for the treatment of marble processing wastewater,” *Int. J. Environ. Sci. Technol.*, vol. 9, no. 4, pp. 637–646, 2012, doi: 10.1007/s13762-012-0093-z.

[104] H. K. Basaran and T. Tasdemir, “Determination of flocculation characteristics of natural stone powder suspensions in the presence of different polymers,” *Physicochem. Probl. Miner. Process.*, vol. 50, no. 1, pp. 169–184, 2014, doi: 10.5277/ppmp140115.

[105] M. Ehteshami, S. Maghsoodi, and E. Yaghoobnia, “Optimum turbidity removal by coagulation/flocculation methods from wastewaters of natural stone processing,” *Desalin. Water Treat.*, vol. 57, no. 44, pp. 20749–20757, 2016, doi: 10.1080/19443994.2015.1110725.

[106] B. T. Ribeiro, J. M. de Lima, N. Curi, and G. C. de Oliveira, “Aggregate breakdown and dispersion of soil samples amended with sugarcane vinasse,” *Sci. Agric.*, vol. 70, no. 6, pp. 435–441, 2013, doi: 10.1590/S0103-90162013000600009.

[107] M. Mohsen, N. Teong, and C. T. S. Y. Choong, “Desalination and Water Treatment October Optimization of flocculation process for cut-stone wastewater : effect of rapid mix parameters,” no. March 2013, pp. 37–41, 2013.

[108] American Petroleum Institute, *Glossary of Oilfield production terminilogy*, First edit., vol. 1, no. 2. Washington, 1988.

[109] R. Raymond, “Temperature Distribution in a Circulating,” *J. Pet. Technol.*, pp. 333–341, 1969.

[110] M. E. Baumert, E. N. Allouche, and I. D. Moore, “Drilling fluid considerations in design of engineered horizontal directional drilling installations,” *Int. J. Geomech.*, vol. 5, no. 4, pp. 339–349, 2005, doi: 10.1061/(ASCE)1532-3641(2005)5:4(339).

[111] A. Sanmi Apaleke, A. Al-Majed, and M. Enamul Hossain, “State of the art and future trend of drilling: An experimental study,” *SPE Lat. Am. Caribb. Pet. Eng. Conf. Proc.*, vol. 2, pp. 1728–1737, 2012, doi: 10.2118/153676-ms.

[112] Z. A. Zhou, O. Worku, L. X. Wang, Z. Xu, and J. H. Masliyah, “Viscosity of mixed clay suspensions,” *CIM J.*, vol. 3, no. 1, pp. 54–61, 2012.

[113] V. E. NASH, "*Role of Exchangeable Cations in Viscosity of Clay Suspensions*." Pergamon Press, 2013.

[114] O. B. Adeyinka, S. Samiei, Z. Xu, and J. H. Masliyah, “Effect of particle size on the rheology of athabasca clay suspensions,” *Can. J. Chem. Eng.*, vol. 87, no. 3, pp. 422–434, 2009, doi: 10.1002/cjce.20168.

[115] C. T. Y. and D. D. T, “Deflocculating Agents for Mechanical Analysis of Soils,” 1995.

[116] V. Sanz, A. Gozalbo, and V. Beltra, “Viscosity of concentrated clay suspensions : effects of solid volume fraction, shear stress , and deflocculant content,” vol. 101, no. 5, pp. 185–193, 2002.

[117] N. E. Education, “Soil Studies: Soil Particle Sizes.” .

[118] “Types of soils.” [Online]. Available: https://byjus.com/biology/types-of-soil/.

[119] I. Shainberg, J. D. Rhoades, and R. J. Prather, “Effect of Low Electrolyte Concentration on Clay Dispersion and Hydraulic Conductivity of a Sodic Soil,” pp. 273–277, 1980.

[120] R. J. Atkins, “Sediment Suspension by waves,” in *Encyclopedia of earth science series*, M. L. Schwartz, Ed. Springer, Dordrecht, 2005.

[121] D. B. Mengel, “Fundamentals of Soil Cation Exchange Capacity (CEC),” *Agronomy Guide*. [Online]. Available: https://www.extension.purdue.edu/extmedia/ay/ay-238.html.

[122] A. P.W. *et al.*, *Interactions at the Soil Colloid- Soil Solution Interface*. Springer-Science.

[123] W. G.N and Z. L.W, “Charge properties of soils colloids,” in *Soil physical chemistry*, S. D.L, Ed. Boca taron, FL: CRC Press, 1986, pp. 39–81.

[124] S. J. Anderson and G. Sposito, “Cesium-Adsorption Method for Measuring Accessible Structural Surface Charge,” *Soil Sci. Soc. Am. J.*, vol. 55, no. 6, pp. 1569–1576, 1991, doi: 10.2136/sssaj1991.03615995005500060011x.

[125] M. D. A. Bolland, A. M. Posner, and J. P. Quirk, “Surface charge on kaolinites in aqueous suspension,” *Aust. J. Soil Res.*, vol. 14, no. 2, pp. 197–216, 1976, doi: 10.1071/SR9760197.

[126] E. Tombácz and M. Szekeres, “Surface charge heterogeneity of kaolinite in aqueous suspension in comparison with montmorillonite,” *Appl. Clay Sci.*, vol. 34, no. 1–4, pp. 105–124, 2006, doi: 10.1016/j.clay.2006.05.009.

[127] O. J.D, S. I., and W. J. D., “American Soil Science Association,” 1980.

[128] H. Heller and R. Keren, “Anionic Polyacrylamide Polymers Effect on Rheological Behavior of Sodium-Montmorillonite Suspensions,” *Soil Sci. Soc. Am. J.*, vol. 66, no. 1, p. 19, 2002, doi: 10.2136/sssaj2002.0019.

[129] B. Gu and H. E. Doner, “Dispersion and Aggregation of Soils as Influenced by Organic and Inorganic Polymers and Inorganic Polymers,” *Soil Sci. Soc. Am. J.*, vol. 57, no. 3, pp. 709–716, 1993, doi: 10.2136/sssaj1993.03615995005700030014x.

[130] A. M. Helalia and J. Letey, “Polymer Type and Water Quality Effects on Soil Dispersion,” *Soil Sci. Soc. Am. J.*, vol. 52, no. 1, pp. 243–246, 1988, doi: 10.2136/sssaj1988.03615995005200010042x.

[131] C. A. Arnold and A. Wallace, “Polyacrylamide suspensions for soil conditioning” US 6,889,471 B2, 2005.

[132] A. I. Mamedov, L. E. Wagner, C. Huang, L. D. Norton, and G. J. Levy, “Polyacrylamide Effects on Aggregate and Structure Stability of Soils with Different Clay Mineralogy,” *Soil Sci. Soc. Am. J.*, vol. 74, no. 5, pp. 1720–1732, 2010, doi: 10.2136/sssaj2009.0279.

[133] A. D. Patel and K. McLaurine, “AQUEOUS BASED DRILLING FLUID,” 5,134,118, 1992.

[134] H. Heller and R. Keren, “ANIONIC POLYACRYLAMIDE POLYMER ADSORPTION BY,” *Clay Clay Miner.*, vol. 51, no. 3, pp. 334–339, 2003, doi: 10.1346/CCMN.2003.0510310.

[135] A. I. Mamedov and G. J. Levy, “Aggregate Stability as Affected by Polyacrylamide Molecular Weight , Soil Texture , and Water Quality,” vol. 71, no. 6, pp. 1909–1918, 2007, doi: 10.2136/sssaj2007.0096.

[136] H. Li, J. Long, Z. Xu, and J. H. Masliyah, “Effect of molecular weight and charge density on the performance of polyacrylamide in low-grade oil sand ore processing,” *Can. J. Chem. Eng.*, vol. 86, no. 2, pp. 177–185, 2008, doi: 10.1002/cjce.20029.

[137] R. A. Klein, “POLYMER HAVING A HYDROPHILIC BACKBONE AND HYDROPHOBIC MOIETIES AS SOL SUSPENDINGAGENT IN POWDER DETERGENTs,” USOO6498.136B2 (10), 2002.

[138] Y. Xu, L. Wang, T. Chu, and D. Liang, “Suspension mechanism and application of sand-suspended slurry for coalmine fire prevention,” *Int. J. Min. Sci. Technol.*, vol. 24, no. 5, pp. 649–656, 2014, doi: 10.1016/j.ijmst.2014.03.029.

[139] B. K. G. Theng and G. F. Walker, “Interactions of Clay Minerals with Organic Monomers,” *Isr. J. Chem.*, vol. 8, no. 3, pp. 417–424, 1970, doi: 10.1002/ijch.197000048.

[140] I. Chang, J. Im, and G. C. Cho, “Introduction of microbial biopolymers in soil treatment for future environmentally-friendly and sustainable geotechnical engineering,” *Sustain.*, vol. 8, no. 3, 2016, doi: 10.3390/su8030251.

[141] C. C. Georgios, F. L. William, and T. I. Arthur, “A mathematical model fo the dispersion of suspended sediments in coastal waters,” *Math. Model. Massachusets Bay*, pp. 1–146, 1974.

[142] H.-W. Fang and G.-Q. Wang, “THREE-DIMENSIONAL MATHEMATICAL MODEL OF SUSPENDED-SEDIMENT TRANSPORT,” *J. Hydraul. Eng. /*, pp. 578–592, 2000.

[143] Coulson and Richerdson, “Flow of Fluids through Granular Beds and Packed Columns,” in *CHEMICAL ENGINEERING*, 5th ed., 1830, pp. 190–243.

[144] S. H. K., “Development of industrial filtration,” in *The Chemical Engineer*, 1976.

[145] V. L. Lopes and L. J. Lane, “Modelling sedimentation processes in small watersheds,” *Model. Sediment. Process. small watersheds*, vol. 174, no. 497–508, 1988.

[146] Z. Suif, A. Fleifle, C. Yoshimura, and O. Saavedra, “Spatio-temporal patterns of soil erosion and suspended sediment dynamics in the Mekong River Basin,” *Sci. Total Environ.*, vol. 568, no. June, pp. 933–945, 2016, doi: 10.1016/j.scitotenv.2015.12.134.

[147] R. M. da Silva, C. A. G. Santos, and J. Y. G. dos Santos, “Evaluation and modeling of runoff and sediment yield for different land covers under simulated rain in a semiarid region of Brazil,” *Int. J. Sediment Res.*, vol. 33, no. 2, pp. 117–125, 2018, doi: 10.1016/j.ijsrc.2017.04.005.

[148] C. Kim, “Mathematical Model of Migration of Spherical Particles in Tube Mow Under the Influence of Inertia and Particle-particle Interaction,” *Korean J. Chem. Eng.*, vol. 21, no. 1, pp. 27–33, 2004, doi: 10.1007/BF02705377.

[149] H. Kourki and M. H. N. Famili, “Particle sedimentation: Effect of polymer concentration on particle-particle interaction,” *Powder Technol.*, vol. 221, no. December, pp. 137–143, 2012, doi: 10.1016/j.powtec.2011.12.050.

[150] M. Y. Wu and Y. Adachi, “Effects of electrolyte concentration and pH on the sedimentation rate of coagulated suspension of sodium montmorillonite,” *Colloids Surfaces A Physicochem. Eng. Asp.*, vol. 506, pp. 686–693, 2016, doi: 10.1016/j.colsurfa.2016.07.027.

[151] “Copasi.” [Online]. Available: http://copasi.org/.

[152] “Arena simulation software,” 2020. [Online]. Available: https://www.arenasimulation.com/what-is-simulation.

[153] “Microsoft excel.” [Online]. Available: https://www.microsoft.com/pt-pt/microsoft-365/excel.

[154] C. T. B. Sung, “Building mathematical models in Excel: A guide for agriculturists,” no. May, 2015.

[155] R. A. Fjeld, N. A. Eisenberg, and K. L. Compton, *Groundwater Transport*. 2006.

[156] “R framework.” [Online]. Available: https://www.r-project.org/about.html.

[157] “MathWorks.” [Online]. Available: https://www.mathworks.com/solutions/data-science.html.

[158] “Statistica.” [Online]. Available: https://statistica.software.informer.com/Download-grátis/.

Appendix A- Input variables and respective values introduced in each run.

Appendix A represents the inputs variables values (polymer name, additive name, polymer concentration, additive concentration, bucket diameter, mixing time, pH and clay concentration) for each run tested.

Appendix A.1- Part 1 of 4

Inputs								
Run	**Polymer (name)**	**[Polymer] (g/L)**	**Additive**	**[Additive] ($mL.L^{-1}$)**	**Bucket diameter (mm)**	**Mixing time (min)**	**pH**	**[Clay] ($g.L^{-1}$)**
1	7156	1,000	-	-	280	45	12,12	100
3	7156	1,000	-	-	280	90	12,12	100
5	7156	1,000	-	-	280	150	12,12	100
7	7156	0,400	-	-	280	150	12,50	100
8	7156	0,600	-	-	280	150	12,12	100
9	7156	0,800	-	-	280	150	12,12	100
10	7156	1,000	-	-	280	210	12,12	100
11	7156	1,000	-	-	280	150	5,43	100
12	7156	1,000	-	-	280	150	9,50	100
13	7156	1,000	-	-	280	150	7,00	100
14	7156	1,000	-	-	280	150	11,50	100
15	7156	1,000	-	-	280	210	11,63	5
16	7156	1,000	-	-	280	210	11,65	10
17	7156	1,000	-	-	280	210	11,65	50
18	7156	1,000	-	-	280	210	11,65	200
19	7156	1,000	-	-	280	210	11,65	400
20	7156	1,000	-	-	280	210	11,65	100
21	7156	0,000	-	-	280	210	11,80	100
22	7156+9156	1,000	-	-	280	210	11,65	100
23	9156	1,000	-	-	280	210	11,65	100
24	7156	0,500	-	-	280	210	11,65	100
25	p400	1,000	-	-	280	210	11,65	100
26	7156	0,245	-	-	280	210	11,65	100
27	9698	1,000	-	-	280	210	11,65	100
28	7156	1,000	Alfabond	1,4	280	210	11,65	100
29	7156	1,000	HY5040	0,8	280	210	11,65	100
30	7156	1,000	Alfabond	1,4	280	210	11,65	100
31	7156	1,000	HY5040	0,8	280	210	11,65	100
32	7156	1,000	HY168	0,8	280	210	11,65	100
33	7156	0,800	-	-	280	150	11,50	100

34	7156	0,000	-	-	280	150	11,50	100

Appendix A.1- Part 2 of 4

Inputs								
Run	**Polymer (name)**	**[Polymer] (g/L)**	**Additive**	**[Additive] ($mL.L^{-1}$)**	**Bucket diameter (mm)**	**Mixing time (min)**	**pH**	**[Clay] ($g.L^{-1}$)**
35	7156	0,600	-	-	280	150	10,00	100
36	7156	0,400	-	-	280	150	7,00	100
37	7156	0,800	-	-	280	150	7,00	100
38	7156	0,000	-	-	280	150	5,00	100
39	7156	0,000	-	-	280	150	5,00	25
40	7156	0,500	-	-	280	150	5,00	25
41	7156	1,000	-	-	280	150	5,00	25
42	7156	1,000	-	-	280	150	7,00	25
43	7156	0,500	-	-	280	150	7,00	25
44	7156	0,000	-	-	280	150	7,00	25
45	7156	0,000	-	-	280	150	11,50	25
46	7156	0,500	-	-	280	150	11,50	25
47	7156	1,000	-	-	280	150	11,50	25
48	7156	0,000	-	-	280	150	5,00	200
49	7156	0,500	-	-	280	150	5,00	200
50	7156	1,000	-	-	280	150	5,00	200
51	7156	0,000	-	-	280	150	7,00	200
52	7156	0,500	-	-	280	150	7,00	200
53	7156	1,000	-	-	280	150	7,00	200
54	7156	0,000	-	-	280	150	11,50	200
55	7156	0,500	-	-	280	150	11,50	200
56	7156	0,000	-	-	280	150	7,00	100
57	7156	0,500	-	-	280	150	7,00	100
58	7156	0,500	-	-	280	150	5,00	100
59	7156	0,500	-	-	280	150	11,50	100
60	7156	1,000	-	-	280	150	11,50	200
61	PP60	1,000	-	-	280	150	5,00	25
62	PP60	0,500	-	-	280	150	5,00	25
63	PP60	1,000	-	-	280	150	11,50	25
64	PP60	0,500	-	-	280	150	11,50	25
65	PP60	1,000	-	-	280	150	7,00	25
66	PP60	0,500	-	-	280	150	7,00	25
67	PP60	1,000	-	-	280	150	5,00	100
68	PP60	0,500	-	-	280	150	5,00	100
69	PP60	1,000	-	-	280	150	11,50	100
70	PP60	0,500	-	-	280	150	11,50	100
71	PP60	1,000	-	-	280	150	7,00	100
72	PP60	0,500	-	-	280	150	7,00	100
73	PP60	1,000	-	-	280	150	5,00	200
74	PP60	0,500	-	-	280	150	5,00	200
75	PP60	1,000	-	-	280	150	11,50	200

76	PP60	0,500	-	-	280	150	11,50	200

Appendix A.1- Part 3 of 4

Inputs								
Run	**Polymer (name)**	**[Polymer] (g/L)**	**Additive**	**[Additive] ($mL.L^{-1}$)**	**Bucket diameter (mm)**	**Mixing time (min)**	**pH**	**[Clay] ($g.L^{-1}$)**
77	P9698	1,000	-	-	280	150	5,00	25
78	P9698	0,500	-	-	280	150	5,00	25
79	P9698	1,000	-	-	280	150	11,50	25
80	P9698	0,500	-	-	280	150	11,50	25
81	P9698	1,000	-	-	280	150	5,00	100
82	P9698	0,500	-	-	280	150	5,00	100
83	7136	1,000	-	-	280	150	11,50	100
84	A35	1,000	-	-	280	150	11,50	100
85	A8	1,000	-	-	280	150	11,50	100
86	A13	1,000	-	-	280	150	11,50	100
87	9698	0,660	-	-	280	150	11,50	100
88	9698	0,330	-	-	280	150	11,50	100
89	A35	0,660	-	-	280	150	11,50	100
90	A13	0,660	-	-	280	150	11,50	100
91	A35	0,660	-	-	280	150	5,00	100
92	9698	0,660	-	-	280	150	5,00	100
93	A8	1,000	-	-	280	150	11,50	25
94	A8	1,000	-	-	280	150	5,00	100
95	P9698	1,000	-	-	280	150	11,50	100
96	P9698	0,500	-	-	280	150	11,50	100
97	P9698	1,000	-	-	280	150	11,50	200
98	P9698	1,000	-	-	280	150	7,00	200
99	PP60	1,000	-	-	280	150	7,00	200
100	P9698	1,000	-	-	280	150	7,00	100
101	P9698	0,500	-	-	280	150	7,00	100
102	P9698	0,500	-	-	280	150	11,50	200
103	7136	1,000	-	-	280	150	5,00	100
104	7136	1,000	-	-	280	150	7,00	100
105	7136	0,500	-	-	280	150	5,00	25
106	7136	0,500	-	-	280	150	7,00	25
107	7136	0,500	-	-	280	150	11,50	25
108	7136	1,000	-	-	280	150	5,00	25
109	7136	1,000	-	-	280	150	7,00	25
110	7136	1,000	-	-	280	150	11,50	25
111	7136	0,500	-	-	280	150	11,50	100
112	7136	0,500	-	-	280	150	7,00	100
113	7136	0,500	-	-	280	150	5,00	100
114	7136	0,500	-	-	280	150	5,00	200
115	7136	1,000	-	-	280	150	5,00	200
116	7136	1,000	-	-	280	150	7,00	200
117	7136	1,000	-	-	280	150	11,50	200

118	A8	1,000	-	-	280	150	11,50	200

Appendix A.1- Part 4 of 4

Inputs								
Run	**Polymer (name)**	**[Polymer] (g/L)**	**Additive**	**[Additive] ($mL.L^{-1}$)**	**Bucket diameter (mm)**	**Mixing time (min)**	**pH**	**[Clay] ($g.L^{-1}$)**
119	A35	1,000	-	-	280	150	11,50	25
120	A8	1,000	-	-	280	150	7,00	100
121	A8	1,000	-	-	280	150	5,00	200
122	A8	1,000	-	-	280	150	7,00	200
123	7136	0,800	-	-	280	150	12,50	125
124	9156	0,600	-	-	280	150	7,00	125
125	A13	0,750	-	-	280	150	10,00	75
126	A18	0,450	-	-	280	150	12,50	25

Appendix B- Output variables and respective values achieved after preparing a polymeric solution for each run

Appendix B represents the outputs variables values (Marsh viscosity, Brookfield viscosity, pH, Density and Electric conductivity) for each run tested.

Appendix B.1- Part 1 of 4

Polymer characterization						
Run	**Polymer (name)**	**Marsh viscosity (s/quart)**	**Brookfield viscosity (cP)**	**pH**	**Density (g/cm^3)**	**E.C (mS/cm)**
1	7156	76	34,08	11,95	0,9985	3,96
3	7156	77	35,88	12,01	0,9982	3,65
5	7156	82	33,84	11,91	0,9983	3,85
7	7156	62	11,22	12,13	0,9973	3,88
8	7156	67	18,36	12,04	0,9975	4,21
9	7156	62	31,44	11,60	0,9972	2,26
10	7156	74	34,56	12,01	0,9974	3,87
11	7156	157	2652,00	7,79	0,9958	21,90
12	7156	111	777,60	8,55	0,9957	34,80
13	7156	134	1680,00	7,75	0,9964	25,50
14	7156	86	47,46	11,53	0,9968	175,20
15	7156	105	92,88	11,49	0,9961	145,90
16	7156	83	60,84	11,62	0,9975	196,70
17	7156	87	61,20	11,76	0,9946	2,52
18	7156	73	64,68	11,62	0,9956	2,12
19	7156	88	69,00	11,81	0,9945	2,55

20	7156	88	44,88	11,81	0,9963	186,30
21	7156	28	1,14	11,80	0,9961	2,34

Appendix B.1- Part 2 of 4

Polymer characterization						
Run	**Polymer (name)**	**Marsh viscosity (s/quart)**	**Brookfield viscosity (cP)**	**pH**	**Density (g/cm^3)**	**E.C (mS/cm)**
22	7156+9156	101	78,60	11,97	0,9950	196,00
23	9156	91	80,52	11,70	0,9952	186,70
24	7156	77	19,44	11,70	0,9950	186,30
25	p400	92	93,72	11,50	0,9947	172,20
26	7156	56	8,82	11,73	0,9957	185,10
27	9698	120	92,88	11,50	0,9953	174,50
28	7156	81	69,48	11,52	0,9965	168,60
29	7156	65	63,36	11,58	0,9962	164,80
30	7156	100	81,00	11,53	0,9956	164,40
31	7156	93	82,80	11,49	0,9956	151,50
32	7156	85	73,08	11,55	0,9960	158,10
33	7156	61	31,56	11,99	0,9970	182,00
34	7156	27	0,57	11,57	0,9962	140,60
35	7156	79	92,40	9,61	0,9956	19,78
36	7156	68	64,44	7,44	0,9957	9,22
37	7156	131	285,60	7,58	0,9953	17,72
38	7156	27	1,06	6,51	0,9947	3,16
39	7156	26	1,20	6,93	0,9942	3,30
40	7156	72	80,40	7,41	0,9947	12,70
41	7156	131	-	7,68	0,9915	22,00
42	7156	127	4554,00	7,57	0,9938	21,70
43	7156	69	74,40	7,67	0,9950	13,45
44	7156	27	0,96	7,00	0,9937	4,63
45	7156	60	21,42	11,54	0,9948	150,80
46	7156	27	1,20	11,09	0,9946	79,90
47	7156	85	94,20	11,39	0,9969	107,20
48	7156	27	1,06	5,21	0,9957	1,22
49	7156	69	44,22	7,86	0,9946	12,34
50	7156	134	-	7,85	0,9948	21,30
51	7156	27	1,00	6,56	0,9959	4,17
52	7156	61	44,52	7,61	0,9957	13,87
53	7156	114	1166,00	7,94	0,9965	19,00
54	7156	27	1,06	11,55	0,9962	177,30
55	7156	51	21,36	11,51	0,9951	119,00
56	7156	26	0,57	6,56	0,9962	2,11
57	7156	64	88,56	7,45	0,9961	12,65
58	7156	68	31,26	7,66	0,9953	41,10
59	7156	54	22,14	11,43	0,9955	114,10

60	7156	84	81,36	11,50	0,9957	138,70
61	PP60	54	34,44	7,69	0,9945	86,00
62	PP60	31	7,92	7,44	0,9945	56,10

Appendix B.1- Part 3 of 4

Polymer characterization						
Run	**Polymer (name)**	**Marsh viscosity (s/quart)**	**Brookfield viscosity (cP)**	**pH**	**Density (g/cm^3)**	**E.C (mS/cm)**
63	PP60	69	29,40	11,53	0,9949	191,10
64	PP60	53	14,64	11,49	0,9947	171,60
65	PP60	60	39,48	7,82	0,9954	73,70
66	PP60	45	12,60	7,58	0,9950	50,30
67	PP60	54	32,28	7,32	0,9951	88,80
68	PP60	68	14,52	7,09	0,9940	48,30
69	PP60	57	22,32	11,74	0,9958	181,00
70	PP60	52	13,20	11,62	0,9958	177,30
71	PP60	59	23,22	7,40	0,9979	110,10
72	PP60	46	15,06	7,20	0,9976	53,00
73	PP60	70	25,56	7,38	0,9963	79,30
74	PP60	46	12,36	7,28	0,9955	46,10
75	PP60	56	17,28	11,52	0,9974	198,40
76	PP60	50	8,46	11,43	0,9970	175,50
77	P9698	230	-	7,54	9963,0000	22,30
78	P9698	100	-	6,90	0,9960	12,55
79	P9698	150	102,10	11,69	0,9969	145,30
80	P9698	57	40,20	11,37	0,9966	133,60
81	P9698	196	-	7,26	0,9965	19,80
82	P9698	110	662,40	6,92	0,9961	13,09
83	7136	62	17,10	11,59	0,9982	121,80
84	A35	240	98,40	11,31	-	132,80
85	A8	160	74,76	11,18	0,9968	175,20
86	A13	393	81,60	11,09	0,9972	125,70
87	9698	116	35,28	10,97	0,9978	123,50
88	9698	49	22,50	11,02	0,9977	123,00
89	A35	300	34,14	11,06	0,9973	126,20
90	A13	124	42, 54	11,02	0,9969	114,30
91	A35	230	47,28	6,97	0,9961	15,61
92	9698	101	42,66	7,20	0,9961	18,16
93	A8	145	32,76	11,12	0,9967	116,80
94	A8	190	50,16	6,85	0,9962	13,72
95	P9698	90	59,34	11,26	0,9978	136,70
96	P9698	66	37,02	11,13	0,9974	123,20
97	P9698	133	233,40	11,13	0,9968	119,70
98	P9698	261	-	7,08	0,9968	20,80
99	PP60	66	41,04	7,11	0,9975	72,90
100	P9698	140	3912,00	7,14	0,9946	20,70
101	P9698	112	573,60	7,05	0,9970	11,51

102	P9698	80	45,48	10,84	0,9971	90,90
103	7136	76	58,08	6,76	0,9976	6,85
104	7136	48	58,56	6,66	0,9976	6,68

Appendix B.1- Part 4 of 4

Polymer characterization						
Run	**Polymer (name)**	**Marsh viscosity (s/quart)**	**Brookfield viscosity (cP)**	**pH**	**Density (g/cm^3)**	**E.C (mS/cm)**
105	7136	50	29,76	6,65	0,9970	3,80
106	7136	47	34,92	6,44	0,9968	3,50
107	7136	46	10,56	10,99	0,9976	92,10
108	7136	76	58,32	6,75	0,9965	5,50
109	7136	50	69,36	6,45	0,9948	6,00
110	7136	32	8,40	10,77	0,9976	82,40
111	7136	43	8,52	11,14	0,9975	113,10
112	7136	45	24,24	7,00	0,9972	3,38
113	7136	46	21,48	6,70	0,9969	4,47
114	7136	44	40,80	6,30	0,9970	4,10
115	7136	66	57,24	6,65	0,9972	6,83
116	7136	55	61,20	6,88	0,9983	5,95
117	7136	60	21,72	11,08	0,9979	104,10
118	A8	124	81,36	11,08	0,9978	108,60
119	A35	367	112,70	11,22	0,9987	147,20
120	A8	228	-	6,72	0,9986	13,43
121	A8	186	787,20	6,81	0,9986	12,90
122	A8	213	1153,00	6,53	0,9985	11,77
123	7136	40	7,62	11,81	1,0004	3,99
124	9156	91	85,08	7,09	0,9988	12,15
125	A13	78	16,68	11,73	1,0000	3,05
126	A18	78	16,68	11,73	1,0000	3,05

Appendix C- Output variables and respective values achieved after adding clay to the polymeric mixture for each run

Appendix C represents the outputs variables values (Marsh viscosity, Brookfield viscosity, pH, Density, Density passed 5 minutes, Total density and Electric conductivity) for each run tested.

Appendix C.1- Part 1 of 6

After adding clay								
Run	**Polymer (name)**	**Marsh viscosity (s/quart)**	**Brookfield viscosity (cp)**	**pH**	**Density (g/cm^3)**	**Density at 5 min (g/cm^3)**	**E.C (mS/cm)**	**Total density (g/cm^3)**
1	7156	67	36,48	11,68	1,0392	1,0240	2,61	1,0278
3	7156	63	55,92	11,47	1,0167	1,0139	2,18	1,0495
5	7156	65	63,24	11,56	1,0365	1,0254	2,30	1,0564
7	7156	52	13,20	11,54	1,0106	1,0079	2,17	1,0178
8	7156	56	20,16	11,66	1,0186	1,0133	2,47	1,0459
9	7156	57	31,44	11,60	1,0305	1,0220	2,26	1,0450
10	7156	60	41,22	11,58	1,0221	1,0220	2,39	1,0386
11	7156	54	36,78	8,11	1,0141	1,0110	65,80	1,0668
12	7156	54	32,88	8,09	1,0148	1,0058	82,20	1,0741
13	7156	56	53,28	8,16	1,0229	1,0140	72,20	1,0452
14	7156	63	69,84	10,68	1,0271	1,0240	121,60	1,0518
15	7156	79	85,92	11,49	0,9987	0,9985	122,40	1,0158
16	7156	72	46,68	11,37	0,9996	0,9996	166,10	0,9763
17	7156	64	63,12	11,47	1,0090	1,0087	184,70	1,0115

Appendix C.1- Part 2 of 6

After adding clay								
Run	**Polymer (name)**	**Marsh viscosity (s/quart)**	**Brookfield viscosity (cp)**	**pH**	**Density (g/cm^3)**	**Density at 5 min (g/cm^3)**	**E.C (mS/cm)**	**Total density (g/cm^3)**
18	7156	66	65,88	10,16	1,0835	1,0358	140,80	1,0629
19	7156	62	20,76	9,55	1,0204	1,0038	185,20	1,1994
20	7156	60	38,40	10,43	1,0257	1,0226	128,10	1,0277
21	7156	29	2,52	10,53	1,0370	1,0260	115,40	1,0387
22	7156+9156	69	42,54	10,58	1,0257	1,0219	136,20	1,0669
23	9156	58	42,48	10,48	1,0222	1,0215	133,20	1,0516
24	7156	58	17,76	10,53	1,0077	1,0077	126,90	1,0584
25	p400	66	42,24	10,29	1,0231	1,0051	127,60	1,0398
26	7156	63	6,06	10,48	1,0352	0,9952	124,70	1,0256
27	9698	65	40,14	10,50	0,9993	1,0015	136,00	1,0689
28	7156	60	57,60	10,19	1,0345	1,0303	122,70	0,9946
29	7156	54	49,80	10,63	1,0248	1,0248	132,00	1,0549
30	7156	66	65,40	10,23	1,0357	1,0226	119,70	0,9700
31	7156	57	52,68	10,43	1,0299	1,0302	132,80	1,0509
32	7156	51	46,92	10,33	1,0285	1,0292	131,40	1,0292
33	7156	59	26,16	10,70	1,0297	1,0105	117,80	1,0304
34	7156	27	0,70	9,94	1,0514	1,0145	108,70	1,0111
35	7156	49	15,48	8,28	1,0250	0,9973	15,40	1,0213
36	7156	44	6,12	8,17	1,0375	0,9966	73,00	0,9972
37	7156	49	17,34	8,28	1,0036	0,9965	71,50	1,0181
38	7156	27	80,40	8,08	1,0380	1,0240	79,70	1,0527
39	7156	27	0,84	7,70	1,0020	0,9973	26,10	1,0051
40	7156	44	25,20	8,02	1,0105	0,9963	29,40	1,0147

Appendix C.1- Part 3 of 6

After adding clay								
Run	**Polymer (name)**	**Marsh viscosity (s/quart)**	**Brookfield viscosity (cp)**	**pH**	**Density (g/cm^3)**	**Density at 5 min (g/cm^3)**	**E.C (mS/cm)**	**Total density (g/cm^3)**
41	7156	64	90,00	8,63	1,0032	1,0032	37,70	1,1016
42	7156	60	89,76	8,68	1,0050	1,0047	37,50	1,0547
43	7156	46	18,06	8,08	1,0018	0,9986	32,60	1,0138
44	7156	27	1,32	7,69	1,0091	0,9953	26,80	1,0215
45	7156	50	26,88	11,12	1,0028	1,0023	118,00	1,0140
46	7156	27	1,20	10,04	1,0118	0,9998	66,30	1,0087
47	7156	66	54,42	10,88	1,0067	1,0067	87,60	0,9916
48	7156	27	4,38	8,11	1,1009	1,0600	109,20	1,0653
49	7156	87	5,34	8,09	0,9998	0,9955	120,20	0,9960
50	7156	70	15,30	8,26	1,0069	0,9977	114,30	1,0041
51	7156	44	5,22	8,13	1,0282	0,9962	117,30	1,0185
52	7156	27	-	8,17	1,0847	1,0627	103,90	1,0497
53	7156	51	13,86	8,20	1,0266	1,0003	110,30	1,0091
54	7156	30	2,82	9,74	1,1115	1,0698	120,90	1,0808
55	7156	49	10,08	9,68	1,0033	0,9961	127,90	1,0102
56	7156	28	1,92	8,03	1,0413	1,0225	63,50	1,0298
57	7156	44	18,30	8,02	1,0040	0,9964	68,50	1,0188
58	7156	48	8,16	8,19	0,9980	0,9960	98,10	1,0122
59	7156	58	13,80	10,19	1,0387	0,9995	91,70	1,0164
60	7156	79	31,32	9,81	1,1154	1,0029	129,00	1,0484
61	PP60	51	21,12	8,00	0,9950	0,9950	104,70	1,0172
62	PP60	29	2,88	7,91	0,9958	0,9951	73,30	1,0191
63	PP60	55	29,16	11,16	0,9980	0,9964	162,10	1,0354

Appendix C.1- Part 4 of 6

After adding clay								
Run	**Polymer (name)**	**Marsh viscosity (s/quart)**	**Brookfield viscosity (cp)**	**pH**	**Density (g/cm^3)**	**Density at 5 min (g/cm^3)**	**E.C (mS/cm)**	**Total density (g/cm^3)**
64	PP60	46	11,76	11,23	0,9960	0,9954	141,90	1,0071
65	PP60	54	23,40	8,02	0,9954	0,9950	102,10	1,0281
66	PP60	37	6,72	7,88	0,9950	0,9948	68,70	1,0105
67	PP60	61	12,72	8,02	0,9955	0,9951	149,40	1,0212
68	PP60	32	4,80	8,06	1,0014	0,9947	106,70	1,0286
69	PP60	55	15,36	10,23	0,9956	0,9956	181,00	1,0326
70	PP60	57	8,88	10,22	0,9973	0,9973	131,30	1,0137
71	PP60	56	9,12	7,91	0,9976	0,9974	150,90	1,0124
72	PP60	38	4,68	8,20	0,9969	0,9967	106,30	1,0050
73	PP60	45	6,84	7,73	0,9968	0,9968	194,80	1,0073
74	PP60	31	2,64	7,99	1,0040	0,9969	133,00	0,9967
75	PP60	54	7,74	9,43	0,9974	0,9974	198,90	1,0193
76	PP60	34	4,08	9,45	0,9990	0,9972	156,00	0,9975
77	P9698	98	112,20	8,45	0,9990	0,9985	35,10	1,0047
78	P9698	49	38,52	7,82	0,9978	0,9971	27,80	1,0378
79	P9698	112	99,48	11,05	1,0015	1,0015	105,90	0,9776
80	P9698	50	38,16	10,78	1,0049	1,0012	98,90	1,0259
81	P9698	55	47,85	7,91	0,9983	0,9973	71,80	0,9962
82	P9698	47	19,35	7,72	0,9980	0,9968	63,30	0,9931
83	7136	45	13,44	9,94	0,9969	0,9968	86,50	1,0196
84	A35	94	69,00	10,00	1,0090	1,0062	100,60	1,0484
85	A8	94	73,68	10,12	0,9970	0,9970	93,00	1,0062
86	A13	122	169,80	9,89	1,0062	1,0050	93,50	1,0458

Appendix C.1- Part 5 of 6

After adding clay								
Run	**Polymer (name)**	**Marsh viscosity (s/quart)**	**Brookfield viscosity (cp)**	**pH**	**Density (g/cm^3)**	**Density at 5 min (g/cm^3)**	**E.C (mS/cm)**	**Total density (g/cm^3)**
87	9698	69	25,32	9,84	1,0132	1,0032	92,00	1,0325
88	9698	48	9,48	9,91	1,0270	0,9978	84,90	1,0095
89	A35	60	48,36	10,06	1,0118	1,0047	88,80	1,0372
90	A13	80	48,72	9,93	1,0013	0,9998	94,50	0,9968
91	A35	53	0,66	7,74	0,9983	0,9972	61,50	1,0262
92	9698	56	-	7,74	1,0028	0,9970	65,50	0,9959
93	A8	120	10,06	10,71	0,9972	0,9971	94,20	0,9823
94	A8	71	10,63	7,67	0,9969	0,9968	65,40	1,0035
95	P9698	90	84,00	10,17	1,0031	1,0024	99,60	1,0081
96	P9698	59	43,32	10,00	1,0098	1,0002	84,80	1,0120
97	P9698	60	52,08	9,44	1,0150	0,9977	121,70	1,0219
98	P9698	64	52,98	7,83	0,9971	0,9971	116,70	1,0105
99	PP60	44	8,52	7,67	0,9984	0,9981	154,40	1,0060
100	P9698	62	31,68	7,88	1,0178	0,9989	67,70	1,0124
101	P9698	48	12,00	7,74	0,9978	0,9972	63,80	1,0094
102	P9698	55	11,16	9,24	0,9979	0,9977	110,00	0,9975
103	7136	39	10,80	7,45	0,9976	0,9975	63,50	1,0003
104	7136	39	9,96	7,48	0,9977	0,9973	61,10	0,9891
105	7136	39	10,08	7,07	0,9965	0,9965	20,10	0,9832
106	7136	40	9,84	7,00	0,9966	0,9965	19,40	0,9997
107	7136	42	8,40	10,39	0,9970	0,9970	64,80	1,0044
108	7136	64	26,40	6,88	0,9966	0,9966	20,90	1,0106
109	7136	55	25,80	6,74	0,9965	0,9964	19,72	1,0198

Appendix C.1- Part 6 of 6

After adding clay								
Run	**Polymer (name)**	**Marsh viscosity (s/quart)**	**Brookfield viscosity (cp)**	**pH**	**Density (g/cm^3)**	**Density at 5 min (g/cm^3)**	**E.C (mS/cm)**	**Total density (g/cm^3)**
110	7136	31	7,68	9,86	0,9997	0,9969	67,20	0,9996
111	7136	36	6,84	9,81	0,9972	0,9972	81,70	1,0020
112	7136	34	4,92	7,60	0,9972	0,9962	58,50	1,0071
113	7136	35	4,08	7,52	0,9970	0,9970	59,70	1,0074
114	7136	29	2,52	7,68	0,9999	0,9975	108,90	0,9755
115	7136	36	5,16	7,51	0,9988	0,9980	112,20	1,0148
116	7136	36	6,00	7,67	1,0110	0,9980	107,80	0,9990
117	7136	37	7,44	9,27	0,9985	0,9974	126,60	1,0001
118	A8	63	65,76	9,35	0,9977	0,9977	130,70	1,0059
119	A35	212	580,80	10,95	1,0026	1,0026	109,20	1,0533
120	A8	69	158,40	7,55	0,9985	0,9985	64,10	1,0400
121	A8	74	25,68	7,61	0,9981	0,9981	105,80	1,0255
122	A8	71	27,96	7,58	0,9983	0,9983	110,30	1,0352
123	7136	38	6,90	11,25	1,0038	1,0000	188,30	0,9963
124	9156	58	20,52	7,65	1,0001	1,0001	69,40	0,9948
125	A13	52	24,24	11,60	1,0033	1,0023	2,33	0,9895
126	A18	52	24,24	11,60	1,0033	1,0022	2,33	0,9895

Appendix D- Output variables and respective values achieved passed 24h in the top and the bottom of the column

Appendix D represents the outputs variables values (Marsh viscosity, Brookfield viscosity, pH, Density and Electric conductivity) for each run tested passed 24h in the top and the bottom of the column.

Appendix D.1- Part 1 of 6

			Top of the column					Bottom of the column				
Run	**Polymer**	**Density $_{24h}$ (g/cm^3) (surface)**	**Marsh Viscosity (s/quart)**	**Brookfield (mS/cm)**	**pH**	**Density (g/cm^3)**	**E.C (mS/cm)**	**Marsh (s/quart)**	**Brookfield (cp)**	**pH**	**Density (g/cm^3)**	**E.C (mS/cm)**
1	7156	1,0024	59	52,80	11,50	1,0026	2,45	56	48,60	11,62	1,0041	2,53
3	7156	1,0027	57	55,68	11,23	1,0033	2,07	62	53,40	11,38	1,0122	2,16
5	7156	1,0045	58	38,52	11,43	1,0043	2,22	59	37,08	11,54	1,0065	2,28
7	7156	1,0002	58	11,04	11,67	1,0012	2,20	58	10,32	11,55	1,0028	2,26
8	7156	1,0034	59	18,66	11,58	1,0035	2,38	55	17,82	11,61	1,0055	2,46
9	7156	1,0035	57	27,00	11,74	1,0027	2,13	50	25,68	11,58	1,0058	2,31
10	7156	1,0053	55	37,74	11,46	1,0053	2,23	56	37,68	11,54	1,0085	2,29
11	7156	1,0013	58	33,78	7,84	1,0010	68,10	56	32,16	7,88	1,0015	65,40
12	7156	1,0008	53	32,40	8,00	1,0008	82,00	58	30,66	8,05	1,0011	81,00
13	7156	0,9995	53	30,96	7,87	0,9997	80,70	54	29,82	7,77	1,0002	77,20
14	7156	1,0056	57	44,70	10,27	1,0053	121,30	57	44,04	10,39	1,0079	122,30
15	7156	0,9981	69	78,12	11,08	0,9979	108,20	71	79,20	11,08	0,9979	128,50
16	7156	0,9996	67	60,96	11,16	0,9991	161,10	66	64,56	11,29	0,9994	167,50
17	7156	1,0071	57	61,68	11,21	1,0060	175,50	58	56,52	11,27	1,0068	182,80

			Top of the column					Bottom of the column				
Run	**Polymer**	**Density $_{24h}$ (g/cm^3) (surface)**	**Marsh Viscosity (s/quart)**	**Brookfield (mS/cm)**	**pH**	**Density (g/cm^3)**	**E.C (mS/cm)**	**Marsh (s/quart)**	**Brookfield (cp)**	**pH**	**Density (g/cm^3)**	**E.C (mS/cm)**
18	7156	1,0039	54	47,76	9,89	1,0026	161,50	57	47,04	9,93	1,0140	156,70
19	7156	0,9997	46	15,54	9,13	0,9995	2,46	-	-	9,19	1,2732	189,90
20	7156	1,0061	53	36,66	10,30	1,0056	139,40	53	34,08	10,20	1,0071	132,80
21	7156	0,9978	28	1,38	10,16	0,9967	126,80	-	9,84	10,23	1,0804	120,20
22	7156+9156	1,0047	60	38,88	10,30	1,0031	138,20	54	37,92	10,37	1,0051	135,00
23	9156	1,0090	54	43,86	10,15	1,0074	128,80	55	44,22	10,25	1,0102	128,50
24	7156	0,9962	55	17,04	10,17	0,9964	127,90	-	-	10,13	1,3821	83,00
25	p400	0,9965	52	40,08	10,04	0,9966	121,40	-	-	9,93	1,2751	113,00
26	7156	0,9963	46	5,52	10,10	0,9960	128,90	45	5,22	10,06	0,9962	132,10
27	9698	0,9969	58	39,72	10,16	0,9969	140,70	62	38,40	10,33	0,9970	144,00
28	7156	1,0213	61	59,16	9,67	1,0237	131,60	68	91,44	9,70	1,0441	113,80
29	7156	1,0169	52	45,24	10,33	1,0162	136,20	52	44,88	10,38	1,0191	135,00
30	7156	1,0059	50	60,36	9,81	1,0082	120,20	52	64,20	9,91	1,0139	121,40
31	7156	1,0211	46	43,08	10,10	1,0220	134,00	48	46,80	10,16	1,0258	134,70
32	7156	1,0205	46	41,10	9,97	1,0210	143,60	49	39,12	10,04	1,0231	134,80
33	7156	1,0022	52	30,24	10,60	1,0020	120,70	53	28,26	10,50	1,0028	116,00
34	7156	0,9964	26	1,13	9,83	0,9963	122,60	-	846,00	9,68	1,2004	109,20
35	7156	0,9976	53	9,96	7,45	0,9973	82,20	53	11,34	7,46	0,9973	82,00
36	7156	0,9973	38	5,58	7,31	0,9967	78,50	37	5,82	7,37	0,9967	78,10
37	7156	0,9962	58	22,20	7,38	0,9959	87,20	57	23,40	7,33	0,9960	86,00
38	7156	0,9954	26	0,84	7,58	0,9955	80,30	26	0,84	7,63	0,9958	80,10
39	7156	0,9952	27	1,14	7,51	0,9949	28,70	28	1,20	7,41	0,9951	28,10

Appendix D.1- Part 3 of 6

			Top of the column					Bottom of the column				
Run	**Polymer**	**Density $_{24h}$ (g/cm^3) (surface)**	**Marsh Viscosity (s/quart)**	**Brookfield (mS/cm)**	**pH**	**Density (g/cm^3)**	**E.C (mS/cm)**	**Marsh (s/quart)**	**Brookfield (cp)**	**pH**	**Density (g/cm^3)**	**E.C (mS/cm)**
40	7156	0,9964	46	21,60	7,74	0,9960	31,70	46	26,64	7,79	0,9963	31,00
41	7156	1,0004	55	45,78	8,33	1,0004	45,70	54	55,56	8,06	1,0010	43,00
42	7156	1,0000	53	56,56	8,11	0,9997	43,90	54	85,80	8,36	1,0003	42,80
43	7156	0,9966	48	17,88	7,44	0,9967	35,50	48	16,98	7,57	0,9969	32,70
44	7156	0,9960	26	1,26	7,44	0,9957	28,80	26	1,26	7,44	0,9958	28,80
45	7156	1,0003	51	16,32	10,97	0,9999	112,00	50	19,86	11,07	1,0005	118,50
46	7156	0,9960	27	0,96	9,93	0,9966	68,40	27	0,97	9,97	0,9968	68,40
47	7156	1,0033	61	54,42	10,66	1,0031	84,40	58	54,96	10,69	1,0038	79,20
48	7156	0,9965	26	0,60	7,66	0,9966	128,90	28	4,92	8,00	1,0580	122,90
49	7156	0,9964	39	5,16	7,49	0,9962	135,50	36	5,16	9,00	0,9962	134,40
50	7156	0,9966	54	13,68	7,40	0,9966	136,40	59	15,36	7,40	0,9967	135,70
51	7156	0,9961	27	1,50	7,63	0,9958	130,30	28	3,06	8,02	1,0522	123,70
52	7156	0,9962	38	4,98	7,27	0,9961	130,50	36	4,98	7,37	0,9961	132,10
53	7156	0,9970	52	13,20	7,31	0,9970	144,80	47	13,68	7,30	0,9971	140,10
54	7156	0,9965	26	0,96	9,15	0,9965	141,10	28	12,00	9,36	1,0978	131,20
55	7156	0,9970	47	10,32	9,42	0,9968	151,80	47	9,96	9,37	0,9967	1,52
56	7156	0,9964	28	1,20	7,51	0,9956	73,40	28	0,96	7,69	0,9970	73,50
57	7156	0,9966	43	7,92	7,33	0,9959	75,60	43	8,34	7,30	0,9959	75,40
58	7156	0,9968	49	7,14	7,40	0,9962	104,90	49	7,92	7,35	0,9963	103,50
59	7156	0,9973	52	54,96	9,85	0,9971	103,70	51	13,92	9,94	0,9977	104,80
60	7156	0,9981	55	31,08	9,41	0,9978	154,70	61	35,76	9,45	0,9984	150,10
61	PP60	0,9960	52	21,60	7,54	0,9960	110,80	52	22,00	7,60	0,9960	111,00

Appendix D.1- Part 4 of 6

Appendix D.1- Part 4 of 6

			Top of the column					Bottom of the column				
Run	**Polymer**	**Density $_{24h}$ (g/cm^3) (surface)**	**Marsh Viscosity (s/quart)**	**Brookfield (mS/cm)**	**pH**	**Density (g/cm^3)**	**E.C (mS/cm)**	**Marsh (s/quart)**	**Brookfield (cp)**	**pH**	**Density (g/cm^3)**	**E.C (mS/cm)**
62	PP60	0,9958	28	4,56	7,39	0,9958	82,00	28	4,60	7,40	0,9958	81,50
63	PP60	0,9965	52	22,92	10,78	0,9965	149,20	48	23,00	10,81	0,9966	149,80
64	PP60	0,9963	50	13,20	10,88	0,9964	136,50	49	15,00	10,50	0,9964	136,00
65	PP60	0,9962	54	23,52	7,49	0,9960	104,30	53	23,40	7,33	0,9959	108,30
66	PP60	0,9959	33	6,24	7,24	0,9957	73,40	32	5,88	7,32	0,9957	73,50
67	PP60	0,9955	53	10,32	7,20	0,9954	159,60	53	10,92	7,30	0,9955	159,40
68	PP60	0,9962	29	4,08	7,35	0,9960	115,50	29	3,36	7,44	0,9960	114,30
69	PP60	0,9964	56	14,04	10,22	0,9961	187,20	55	13,80	10,08	0,9961	190,50
70	PP60	0,9963	40	8,52	10,11	0,9960	140,00	40	7,44	10,07	0,9960	139,20
71	PP60	0,9974	59	8,52	6,92	0,9973	157,90	58	9,00	6,92	0,9973	157,00
72	PP60	0,9971	36	4,44	6,93	0,9972	111,30	35	4,38	6,91	0,9972	110,00
73	PP60	0,9977	41	6,18	7,02	0,9977	193,50	44	6,36	7,03	0,9977	193,70
74	PP60	0,9976	29	2,52	7,09	0,9975	163,30	29	2,22	7,07	0,9975	163,30
75	PP60	0,9980	50	9,24	8,98	0,9979	0,22	47	18,48	9,03	0,9978	0,21
76	PP60	0,9977	31	4,32	9,05	0,9976	174,20	32	3,84	9,05	0,9975	173,20
77	P9698	0,9978	72	69,12	8,10	0,9978	39,80	75	123,90	8,03	0,9979	37,70
78	P9698	0,9969	45	36,15	7,02	0,9969	28,30	46	35,25	7,14	0,9969	28,40
79	P9698	0,9993	84	183,00	11,02	0,9990	107,20	80	101,50	11,31	1,0001	109,60
80	P9698	0,9979	47	62,10	10,67	0,9979	91,70	47	54,60	10,75	0,9981	97,70
81	P9698	0,9972	54	71,10	7,15	0,9975	78,90	52	75,60	6,97	0,9976	78,50
82	P9698	0,9969	51	25,80	6,89	0,9973	62,50	51	21,30	7,05	0,9973	66,30
83	7136	0,9969	43	19,08	9,49	0,9969	90,70	42	16,41	9,58	0,9969	90,40

			Top of the column					Bottom of the column				
Run	**Polymer**	**Density $_{24h}$ (g/cm^3) (surface)**	**Marsh Viscosity (s/quart)**	**Brookfield (mS/cm)**	**pH**	**Density (g/cm^3)**	**E.C (mS/cm)**	**Marsh (s/quart)**	**Brookfield (cp)**	**pH**	**Density (g/cm^3)**	**E.C (mS/cm)**
84	A35	0,9998	82	71,40	9,73	0,9992	102,00	90	84,00	9,81	1,0002	100,90
85	A8	0,9970	69	76,20	9,75	0,9972	94,60	70	76,80	9,86	0,9973	93,50
86	A13	0,9993	91	90,24	9,65	0,9986	96,80	99	93,60	9,73	0,9995	95,50
87	9698	0,9982	50	5,67	9,87	0,9979	97,80	55	5,91	9,65	0,9985	98,40
88	9698	0,9976	50	0,68	9,63	0,9973	95,90	50	0,70	9,80	0,9973	96,50
89	A35	0,9986	64	8,33	9,86	0,9994	97,10	57	9,67	9,78	0,9994	95,50
90	A13	0,9978	64	9,54	9,69	0,9976	93,90	67	9,42	9,74	0,9978	97,50
91	A35	0,9974	55	36,36	6,90	0,9971	69,50	53	37,00	6,63	0,9972	70,10
92	9698	0,9974	53	28,80	6,75	0,9970	74,10	52	30,00	6,63	0,9972	73,80
93	A8	0,9972	77	90,96	10,37	0,9972	86,60	74	92,00	10,62	0,9973	87,10
94	A8	0,9968	58	65,28	7,29	0,9968	61,80	57	67,10	7,32	0,9969	62,10
95	P9698	0,9988	68	84,24	10,14	0,9985	85,80	73	84,60	10,04	0,9990	95,50
96	P9698	0,9980	51	42,60	9,81	0,9977	86,60	49	39,72	9,84	0,9979	88,30
97	P9698	0,9977	56	50,16	9,20	0,9980	135,90	60	53,16	9,25	0,9981	136,50
98	P9698	0,9971	67	40,44	6,91	0,9980	120,80	59	39,48	6,86	0,9980	120,60
99	PP60	0,9981	53	10,20	6,87	0,9981	179,10	43	8,64	6,92	0,9987	178,50
100	P9698	0,9979	49	32,52	7,01	0,9979	74,10	49	39,36	6,99	0,9979	73,10
101	P9698	0,9972	52	14,04	6,93	0,9972	68,10	50	12,36	7,02	0,9972	67,60
102	P9698	0,9976	51	11,04	8,96	0,9976	125,00	49	10,92	8,97	0,9976	125,30
103	7136	0,9974	38	9,96	7,01	0,9974	67,10	38	10,56	6,90	0,9974	66,80
104	7136	0,9973	36	9,48	6,88	0,9973	64,40	35	9,24	6,91	0,9974	64,40
105	7136	0,9965	39	9,36	6,81	0,9965	20,90	38	9,48	6,74	0,9965	20,80

			Top of the column					Bottom of the column				
Run	**Polymer**	**Density $_{24h}$ (g/cm^3) (surface)**	**Marsh Viscosity (s/quart)**	**Brookfield (mS/cm)**	**pH**	**Density (g/cm^3)**	**E.C (mS/cm)**	**Marsh (s/quart)**	**Brookfield (cp)**	**pH**	**Density (g/cm^3)**	**E.C (mS/cm)**
106	7136	0,9965	37	9,36	6,67	0,9965	19,80	37	9,24	6,67	0,9965	19,80
107	7136	0,9968	40	9,36	10,03	0,9968	64,20	40	9,50	10,03	0,9969	65,00
108	7136	0,9965	56	21,72	6,63	0,9965	22,60	57	22,00	6,65	0,9965	22,90
109	7136	0,9963	51	25,56	6,38	0,9963	20,60	52	26,00	6,39	0,9963	21,00
110	7136	0,9970	30	9,00	9,62	0,9970	70,20	30	9,07	9,65	0,9972	70,90
111	7136	0,9972	34	5,88	9,57	0,9972	85,40	34	6,00	9,60	0,9973	86,00
112	7136	0,9972	32	4,08	7,16	0,9972	61,40	32	4,10	7,17	0,9973	61,50
113	7136	0,9970	33	3,72	7,07	0,9970	61,70	33	4,20	7,10	0,9970	61,90
114	7136	0,9975	27	2,16	7,16	0,9975	111,30	27	3,00	7,30	0,9976	111,50
115	7136	0,9980	35	5,28	6,84	0,9980	120,00	36	5,76	6,90	0,9980	119,00
116	7136	0,9980	33	5,52	7,00	0,9980	116,10	35	5,40	7,05	0,9980	115,80
117	7136	0,9975	37	7,08	8,96	0,9974	131,50	35	6,84	8,98	0,9975	131,60
118	A8	0,9978	64	30,24	9,16	0,9977	132,20	62	38,40	9,12	0,9978	133,40
119	A35	1,0090	134	621,60	10,72	1,0011	82,00	127	726,00	10,81	1,0012	108,20
120	A8	0,9982	79	196,80	6,87	0,9983	65,70	78	197,00	6,90	0,9983	66,00
121	A8	0,9982	61	110,40	6,78	0,9982	113,60	60	114,00	6,70	0,9983	113,80
122	A8	0,9982	62	72,00	6,82	0,9982	111,20	61	73,00	7,01	0,9983	111,30
123	7136	1,0005	35	9,18	11,46	1,0001	179,70	35	6,78	11,44	1,0001	179,60
124	9156	0,9997	57	14,58	7,87	0,9993	73,10	57	12,90	7,81	0,9993	73,40
125	A13	1,0000	63	33,90	9,25	0,9999	60,00	63	34,26	9,46	1,0000	65,10
126	A18	1,0005	54	17,10	11,90	1,0002	198,80	54	18,60	11,88	1,0004	2,14